"TRANS-PACIFIC RADIO INTERFEROMETER OBSERVATIONS OF QUASI-STELLAR OBJECTS"

by

Jacob Samuel Gubbay, B.Sc., (W.A.)
Department of Physics

A thesis
presented for the degree of
Doctor of Philosophy
in the
University of Adelaide
February 1970

TABLE OF CONTENTS

SUMMARY

This thesis discusses observations on a number of radio sources using widely separated radio telescopes as interferometer pairs to study the small scale angular structure of quasi-stellar objects which are less than one thousandth of a second of arc across at 2,300 MHz, and their secular variations. One radio telescope in Australia and at least one radio telescope in California, U.S.A. were employed in making simultaneous observations during each experimental run. The telescopes and associated facilities belong to the Deep Space Network of the Jet Propulsion Laboratories. Of the two JPL radio telescopes in Australia and the three in California, each has participated in at least one of three experiments. The team of five experimenters who carried out the investigations came from the University of Adelaide, the Ownes Valley Radio Observatory, the Jet Propulsion Laboratories and the Australian Department of Supply.

In June 1967 the two Australian radio telescopes were successfully operated as an interferometer pair using the Hanbury Brown technique. However, when the same technique and mode of operation were applied in a trans-Pacific experimental assay in September of that year, the sensitivity achieved was found to be inadequate for the smaller components.

The first experiment using the Michelson technique took place on the 2nd and 3rd November 1967 and employed the radio telescope at the Island Lagoon station in South Australia and two radio telescopes in California separated by a distance of a few miles. Data were recorded on magnetic tape at each station and dispatched to the University of Adelaide for data reduction on the CDC 6400. In the reduction process, the data are correlated, due allowance being made for a difference in the timing standards at the two stations, and then the spectrum about the predicted doppler frequency is examined for significant correlation. A separate search for actual clock difference was made when this was in doubt, accepting the predicted doppler frequency for the correlated data, or a constant error in this predicted frequency.

The sources were known and also shown to be totally unresolved for the Californian baseline and therefore the results for this baseline were suitable for calibrating the correlation peaks observed using the trans-Pacific baseline in terms of their correlated flux densities. However no correlations were observed for the trans-Pacific baseline at this time.

On May 30, 1968 a second experiment was performed. This time the Pioneer VIII spacecraft and pulsar CP1133 were included in the list of sources to serve as controls. The spacecraft was observed in order to obtain a correlation

peak in the frequency domain to indicate the discrepancy between actual and predicted values of the doppler difference frequency for the two stations. The pulsar data were used in order to confirm the value of the clock difference between the stations across the Pacific. The data reduction programme was refined and 16 minutes of recorded data on each pair of tapes were reduced at the University of Adelaide Computing Centre. Correlated flux was observed by the trans-Pacific pair of stations for a number of sources known to be variable.

The long baseline data taken in November 1967 were then processed, taking into account the difference between the predicted and actual doppler frequency indicated by the Pioneer spacecraft result, and unresolved components were observed for at least two sources. Four separate observations on 3C 273 had been made on the occasion of the first experiment and the results were internally consistent. They also corresponded in flux density with the observations in May 1968 when two separate observations on this source were obtained. Two such independent sets of records were obtained on the first occasion for 3C 279 and it was evident that the correlated flux density had increased markedly over the intervening period. P 1510 showed a more moderate increase in component flux density. A statistical evaluation of the results is included in this work.

A further experiment was performed on the 9th June 1969.

On this occasion only one station in California collaborated with the station in Australia. There was again no significant variation in the intensity of the 3C 273 component whereas the intensities of the components for 3C 279 and P 1510 had continued to increase. The history of the component intensities for the three sources was compared with the history of their total intensities observed at the same operating frequency by G.D. Nicolson using a sister radio telescope of the Deep Space Network near Johannesburg. From the comparison of the secular values of total and component flux densities, it appears that the variation in the flux density of the unresolved component of 3C 279 is wholly responsible for the variation in total flux density for this source. 3C 273 and P 1510 do not show a correspondence of this nature. Over a period of 19 months the flux density of the variable component in 3C 279 had increased by about 250%.

The implications of the results as they bear on various models for quasar variations and on the location hypotheses are discussed.

PREFACE

This thesis contains no material that has been accepted for the award of any other degree or diploma in any University, and to the best of the candidate's knowledge and belief contains no material previously published or written by another person, except where due reference is made in the text of the thesis.

Jacob Samuel Gubbay

ACKNOWLEDGEMENTS

A proposal to conduct trans-Pacific interferometer experiments on quasi-stellar sources, in 1967, using the NASA-JPL Deep Space Network of satellite tracking stations was favourably received by the Jet Propulsion Laboratory who appointed the project Manager, Mr. Justin R. Hall to oversee preparations for the experiments. Mr. H. Spitzmesser assumed this function for the third experiment. Station personnel assisted the experimenters in the conduct of the three experiments which followed, and included the two Australian-based Deep Space Stations DSS 41 at Island Lagoon and DSS 42 in Tidbinbilla as well as DSS 14, DSS 11 and DSS 12, three Deep Space Stations near Goldstone in the Majove Valley, California, U.S.A.

The co-experimenters conducting the experiments were Dr. D. S. Robertson and Mr. A.J. Legg, both of the Australian Defence Scientific Service, and Dr. A. T. Moffet of Owens Valley Radio Observatory, California Institute of Technology, Mr. B. Seidel of the Jet Propulsion Laboratory, California Institute of Technology and the writer. Dr. R. Ekers of the Owens Valley Radio Observatory, California Institute of Technology joined the experimental group for the third experiment.

Dr. D.S. Robertson and Dr. A.T. Moffet were primarily responsible for the conduct of the experiments at the

Australian and American stations respectively. Mr. A.J. Legg, the Systems Analyst at DSS 41, was concerned with data collection. The main responsibilities of the writer were the scheduling of the observations and data reduction. The areas of responsibility, however, overlapped and the success of the experiments was due to the close working association between the experimenters. The interpretation of results was achieved by consultation between Dr. D.S. Robertson and the writer on the one hand and Dr. A.T. Moffet on the other.

Dr. G.D. Nicolson of DSS 51 near Johannesburg let us have his unpublished results on the total intensities of sources which appear in table 8.1 and figure 8.2.

The writer was in tenure of a scholarship awarded by the Board of the Australian Public Service while at the University of Adelaide where he had the privilege of discussing this work with Professor K. G. McCracken and receiving his constant support in these investigations.

The reduction programme was translated from the IBM 7090 version for use on the CDC 6400 at the University of Adelaide Computing Centre with the assistance of Mr. J. Weadon and Dr. Barbara Kidman of the Computing Science Department, and Mr. E. Williams of the Physics Department, University of Adelaide.

The figures were drawn by Miss H. Fleming and Mrs. M.

King.

Credit is also due to my charming daughters Ingrid and Frances for minimizing my domestic obligations.

CHAPTER 1

REVIEW

In the two decades that have passed since the identification of the first galactic radio sources a number of different classes of extragalactic radio objects have been observed over the spectral region limited by the presence of the neutral and ionized constituents of the earth's atmospheric mantle.

The identification of some of these extragalactic radio objects with optical objects has allowed new developments in the description of galactic energetic processes but little is yet known about the formation of galaxies.

The identification of the radio source 3C 273 was made possible by the development and employment of the occultation technique by Hazard, Mackay and Shimmins, 1963 to obtain a precise determination of its position. The emission spectrum of the associated optical object in 3C 273 was interpreted as the Balmer series of hydrogen by Maarten Schmidt in 1963 at a red shift displacement of 0.158. This value of the red shift was anomalously high and close inspection of the source since that time has uncovered other unexpected characteristics. A subsequent search for sources of similar characteristics led to the discovery of the class of sources known as quasi-stellar objects which manifest emission line red shifts from 0.158 for 3C 273 to 2.380 for 5C 2.56.

Radio astronomers generally use the term quasi-stellar source, or the fore-shortened forms quasar or QSS to refer to these bodies. However, the category includes sources which exhibit radio spectra characteristic of quasi-stellar objects but which have not as yet been identified.

The impact of the observations of quasi-stellar sources on the fundamental concepts of astronomy in the first four years, and the contending hypothesis relating to their location, their nature and their cosmological implications are reviewed in Appendix 4. We shall concern ourselves here with developments since 1967 which have some bearing on observed variations in the centimetre and millimetre radiation from quasi-stellar sources. The short time scale of these variations appeared to provide cogent argument against the interpretation of their associated red shift as due to the effect of Hubble expansion of the universe which would place them at distances commensurate with the limits of the observable universe.

A comprehensive account of the problems posed by the quasi-stellar source is given in relatively recent reviews. Hunter, Sofia and Fletcher, 1966 represent the case for the view that the QSS's are no further than the galaxies in our immediate neighbourhood rather than at the cosmological distance indicated when their large spectral red shift is interpreted in terms of Hubble expansion. The 1966 Christmas address given by Dr. Sciama 1967 to the British Astronomical Association marks an important turning point as the author,

who claims to have been a fervent admirer and supporter of the 'Steady State' theory which requires that the location of QSS's be local, considers cummulative evidence from distributions of various classes of radio sources and background black-body radiation and concludes that the 'Steady State' theory is almost certainly wrong. Maran and Cameron 1967 reviewed the proceedings of the 'Texas Symposium' on Relativistic Astrophysics held in New York in January 1967 where widely divergent views on QSS models and their location was discussed. It is noteworthy that Hoyle and Fowler who are among the principal proponents of the 'Steady State' theory suggested that quasars lie at middle distances ~ 100 megaparsecs of ~ 320 light years and ascribed their red shift as partly due to the effect of gravitation. This represents a modification of the orthodox 'Steady State' theory.

In general, the stage which investigations had reached at the time of the conference may be summarized by a statement due to Sandage, himself a supporter of the cosmological location hypothesis for QSS's, demonstrating the quandary in which the observationalist found himself, to the effect that no crucial experiment had yet been performed to distinguish between the rival location hypotheses.

The energetics of QSS's and thus their essential nature devolves on measurement of their angular size and their distance. The main problems relating to location, energetics and evolution of QSS's and radio galaxies are reviewed by

Longair, 1967. Difficulties were encountered in developing an evolutionary sequence as it was assumed that the dimensions of variable components could not exceed the light travel time across the component. The extremely high photon energy-density that would follow as a result would require that the relativistic electrons lose their energy through inverse-Compton scattering of light photons, so that energy is radiated in the form of X-rays and γ-rays. Longair concludes that models of QSS's in which radio and optical emission originate from the same volumes and are produced by the synchrotron process, are therefore not self-consistent. However, the assumption that the light travel time must determine the upper limit on the metric size of a variable component is shown to be invalid by Rees, 1967 and as a result of the present work, as discussed in Chapter 8. Rees, 1967, Rees and Simon, 1968, Morrisson and Sartori, 1968, and Ozernoy and Sazonov, 1968 demonstrated that where a component expands at an ultrarelativistic velocity, the metric extension of the source can be several orders higher than indicated by the light travel time. To illustrate the basic argument, let us consider a spherically symmetrical disturbance which begins to expand from some central point at a velocity close to the velocity of light, and a remote observer at rest with respect to the origin of the disturbance. An event A at the intersection of the expanding shell with the line of sight from a remote observer to the origin of the disturbance is followed by an event B at the intersection at a later time. The

proper time for the two events is t_A and t_B respectively so that an observer travelling with the point on the expanding sphere at which the two events take place measures the interval between the two events as $t_B - t_A$. However the time between the two events $t'_B - t'_A$, seen by the remote observer must approach zero as the radial velocity of the disturbance approaches the velocity of light, as subsequent events take place at progressively closer distances from the remote observer. Hence $t'_B - t_B < t'_A - t_A$ and therefore $t'_B - t'_A < t_B - t_A$. The argument for events at points moving transverse to the line of sight is more complex but it has been shown that observed time intervals can be many times shorter than the corresponding interval in proper time. The upper limit to the metric size of an expanding shell is indeed determined by the light travel time where the time refers to the age of the source in the reference frame of a point on the expanding envelope.

Kellermann and Pauliny-Toth, 1968 reviewed the observed variations in the centimetre and millimetre spectrum of two Seyfert galaxies and a number of QSS's, and concluded that in every instance the variations conformed with the synchrotron source model and the light travel time restriction on the metric size derived from the frequency of the maximum flux density of the variable component. Here the light travel time referred to the age of the source as seen by a remote observer at the earth, which is calculated from the rate of change of intensity at the observing frequency after the

manner of Sklovsky, 1961, Sklovsky, 1965 and Van der Laan, 1966.

Andrew, Locke and Medd, 1969 monitored the 2.8 cm and 4.8 cm emission from 50 sources in their variable source observational programme. Three of these sources, P1510-08, P0736+01 and NRAO 512 showed behaviour which did not conform to the model of a uniform and spherical cloud of electrons expanding adiabatically with its magnetic field and radiating through a process of magnetic bremsstrahlung, as described by Van der Laan, 1966. These anomalous results may be due to geometrical departures from the model and may be more amenable to the rigorous relativistic treatment of secular variations for ultra relativistic expansion rates. The mid-1967 burst associated with P1510 is further complicated by the apparent protracted injection of particles into the radio emission zone.

McCrea, 1967 suggested that the rapid fluctuations in the intensity of light from some quasars was due to the successive occultations of the bright central core of a galaxy by a number of its protostars. Appenzeller and Hiltner, 1967 and Viovanathan, 1968 have observed polarization in the visible region for several quasi-stellar objects and Kinman claims that of five sources studied, two have shown variable polarization. Appenzeller and Hiltner conclude from their work that a degree of polarization as high as that obtained for 3C 279 is infrequent at 4200Å, the observing wavelength, and that a high degree of polarization may be characteristic of certain

"active" stages in the evolution of quasi-stellar objects. This suggestion seems to stand on better ground than the occultation model of McCrea which sets an upper limit to the luminosity of the source which should be apparent at the termination of each occultation. Variations in the optical brightness and polarization of the quasi-stellar source 3C 345 reported by Kinman et al 1968 would place grave restrictions on the model.

Optical variations have also been detected in two N-galaxies. Oke, 1967 observed 3C 371 to change in brightness by one magnitude in two years. This N-galaxy has a very bright concentrated nucleus producing non-thermal radiation, as has a Seyfert galaxy. The N-galaxy 3C 390.3 was seen to vary by Cannon, Penston and Penston, 1968 who suggest that quasi-stellar objects are in fact N-galaxies at such great distances that only the core of these objects remains visible.

Earlier, Dent 1966 had drawn a similar conclusion from his observation of a sharp increase in the flux density from the quasi-stellar source 3C 273 at 8 GHz and by comparing its behaviour with the Seyfert galaxy NGC 1275 at the same observing frequency.

The clustering of red shift about certain values which show a periodicity, as first noted by Burbridge and Burbridge, 1967 is not yet well understood. Burbridge and Burbridge, 1969 find that this evidence and the tendency of the red shift of absorption lines to cluster about the value of 1.95

irrespective of the corresponding emission line red shift point either to remarkable cosmological effects or to the conclusion that intrinsic red shift components are important. Quasi-stellar sources may indeed have been ejected from larger primordial bodies to form galactic clusters as proposed by Bell, 1969. This view which divides the observed red shift into a larger positive component due to Hubble expansion and a positive or negative component of smaller absolute value due to an intrinsic velocity, cannot easily be discounted. However lack of absorption shortward of Lyman α inthe spectrum of the quasi-stellar object, short term optical and radio variations and the extreme amounts of energy involved in such short apparent time scales, pose serious problems which must be understood before any view can become established

Some progress in the field of quasar energetics has been made in the present work. New evidence on the expansion velocities of variable components obtained in the course of our observations is discussed in Chapter 8, as it bears on the predictions of Rees, 1967 and of Rees and Simon, 1968. Some of the ramifications of ultra-relativistic expansion velocities of the variable components of quasi-stellar sources are explored.

CHAPTER 2.

AIMS OF THE EXPERIMENTAL INVESTIGATION

An interferometer experiment, using two satellite tracking stations of the NASA-JPL Deep Space Network, was performed by Gubbay and Robertson in June, 1967 following a proposal which appears here as Appendix 4. The Hanbury-Brown post detection technique was adopted, as discussed in section 3.1 as it called for minimal modifications to the standard tracking station configuration. The results indicated that baselines of greater than ten million wavelengths would be required to determine the small scale angular structure in 3C 273 (see Appendix 1).

The importance of these measurements of angular diameter had become widely recognised as theoretical predictions of the angular dimensions of variable quasi-stellar sources based on the time scale of these variations differed widely from predictions resting on the assumption that these sources radiated through synchrotron action and were at cosmological distances. In the Northern Hemisphere, two other groups, Broten et al, 1967a, 1967b, in Canada and Bare et al, 1967, in the U.S.A., one using digital and the other using analogue data recording and reduction techniques, had conducted similar experiments and at about the same time as those in Australia. The resolving powers in both cases were of the same order of magnitude and the results also showed that interferometer baselines would have to be extended in order

to test whether the cosmological location hypothesis was viable in view of the observed variable behaviour of some sources. Interferometric observations were carried out over increasing baselines in North America by Clark et al, 1967, 1968 and by Moran et al, 1968. The experiments have been reviewed by Cohen, Jauncey, Kellermann and Clark, 1968 and Bernard Burke, 1969. In common with the Australian experiment the respective operating frequencies were derived from rubidium frequency standards. However, each group worked independently and conducted measurements at different observing frequencies.

The measurement of angular dimensions of the components of a quasi-stellar source is tied to many questions of the day in astrophysics. In particular the optical line spectrum of quasi-stellar sources or "quasars" manifest a large red shift. If the red shift is interpreted as Hubble expansion, quasars would appear to be the furthermost objects of our physical universe, their distance being greater than that of other objects seen hitherto by about 1 order of magnitude. Their brightness would then appear to exceed that for known galaxies by about 2 orders of magnitude. The temperature of the source is proportional to the cube of its distance and therefore, in consequence of temperature, luminosity and light time consideration, quasars would be extremely large and expending vast amounts of energy. On the other hand, temporal variations which have been observed in the radio region at centimetre and millimetre wavelengths, argue

against anomalously large dimensions if the value of the velocity of light is a constant for the physical universe.

Some independent measurement of the distance and size of the quasar would assist in resolving the apparent contradiction. If this hiatus were to persist in the light of further evidence then we would appear to be seeing objects over fifteen light years across, varying as much as three fold in intensity in the space of a few months, or otherwise, objects measuring a few light days across would all be seen to be moving away from us at abnormally high velocities; yet of all such objects none has been found to be approaching us. The first alternative was considered to require modifications to the fundamental assumption that the velocity of light is independent of space and time, while the other suggests the improbable egocentric view that these objects were expelled from our galaxy and from no other galaxy (within our neighbourhood at least). The only viable model in such a case was the one expounded by Rees, 1967 and later by Ozernoy and Sazonov, 1968 which appears to successfully explain the observed red shift as well as the time scale of source variations on the basis of an ultra-relativistic expansion of source components at distances indicated by their emission line red shift in the optical region of the spectrum. This model is a development of the quasi-stationary synchrotron model treated by Le Roux, 1961 and the model of the variable source expounded by Sklovsky, 1960, 1965 and Van der Laan, 1966.

The angular diameter of a source is related to both its physical diameter and its distance from the observer. A measurement of angular diameter thus provides a constraint on these physical quantities. The synchrotron model of the radio source relates physical dimension to spectral shape or temporal variation, both of these latter being directly observable. Where the physical diameter has been deduced in this manner, the measurement of angular diameter leads directly to a determination of range albeit inprecise, which will, however, adjudicate between the rival quasar location hypotheses. The "cosmological" hypothesis places these sources between 10^9 and 10^{10} light years away while the "local" hypothesis views these sources as objects originating at the galactic centre and which, as the result of an explosion some 10^7 years ago, were propelled outwards. They would now appear to be receding in the intermediate distance, about 10^7 light years away, at relativistic velocities. In order to obtain a determination of quasar location, the statistical relation between angular dimension and red shift, and between angular dimension and temporal variation of these sources should be described. If, for instance, none of these sources can be resolved with a 10,000 km baseline interferometer operating at S-band, this indicates that the upper limit of physical size is no more than light months or perhaps a few light years. In this case, the "cosmological" view can no longer be held as "incompatible" with the intensity variation phenomena.

The dependence of flux density on the metric diameter of a spherically symmetrical synchrotron source in which the magnetic field is randomized and isotropic is described by equations 93-105 of Le Roux, 1961. Values of the diameter of well known simple non-thermal sources obtained with this model are in fair agreement with observation. The model was further developed independently by Slish, 1963 and Williams, 1963. Thus a measure of the distance of simple sources may be obtained.

Variable sources however appear to be complex and in general the smallest components can be expected to vary most rapidly. The age of a variable component may be calculated from the observed rate of change in flux density from the source, as demonstrated by Van der Laan, 1966. The rate of change of the frequency at which the varying constituent of flux density is a maximum and the rate of change in flux density at the spectral peak as it moves toward lower frequencies are dependent on the radius and the rate of expansion of an electron gas, cooling adiabatically as it expands with its frozen-in magnetic field.

The immediate objectives of the present work may therefore be enumerated as follows.

(a) Extension of the visibility function of a population of quasi-stellar sources in order to determine their small-scale angular structure and thus to compare the values obtained against the predictions based on local and cosmological location hypotheses.

(b) Classification of sources with small components and identification of associated characteristics of this class, such as observed secular variations.

(c) Determination of the rate of expansion of components associated with bursts in the wavelength region shortward of 13 cm. Some information on the strength of the magnetic field and the electron densities and temperatures obtaining in the expanding components might be derived when sufficient data on a number of sources becomes available.

(d) Confirmation that the co-ordinates of the observing stations participating in the interferometer experiments were correct to about 200 metres.

The results of the investigations are listed in Chapter 7 and observed variations in the contribution of unresolved components to the flux density of some of these sources are discussed in Chapter 8.

In Chapter 6, the effect of an error on the position of each station is considered and a highly significant error in one of the station co-ordinates originally provided, is indicated.

CHAPTER 3.

DESCRIPTION OF THE EXPERIMENTS

In the course of the investigation five stations of the J.P.L. Deep Space Network participated on at least one occasion. Two of these stations are located in Australia, one at Island Lagoon (DSS 41), in South Australia and the other at Tidbinbilla (DSS 42), in the Australian Capital Territory some 1,200 kilometers away. The other three stations are within fifteen kilometers of each other at Goldstone in California, U.S.A. and are designated Mars (DSS 14), Echo (DSS 12), and Pioneer (DSS 11). The Mars station is equipped with a 210 foot primary reflector on an X - Y mount whereas each of the other stations has an 85 foot primary reflector on a polar mount. The hyperbolic sub-reflector of the Cassegranian system focusses the beam into the feed horn in the Cassegranain cone. A maser immersed in liquid helium acts as a selective amplifier and is centred at about 2295 MHz, corresponding to a receiving wavelength of about 13cms.

The operational facilities at each station are described in section 4 of this chapter. Each station complex has identical basic facilities and this feature together with the ease of intercommunication during the experiments have simplified the operational procedures.

3.1 Experiments Using the Post- Detection Technique

In June 1967, Gubbay and Robertson conducted a series

of interferometric observations on 3C 273 using the Australian Based stations DSS 41 and DSS 42. The published report of this work appears here as Appendix 1.

The output of each receiver was passed through a mixer amplifier, detector and filter and then recorded on magnetic tape. The data recorded at each station were correlated using the IBM 7090 at Salisbury, South Australia. This technique is primarily due to Hanbury Brown and Twiss, 1954 and was employed by Jennison and Das Gupta, 1956a, 1956b to describe the structure of Cygnus A and Casseiopeia. Phase information is lost as the signal passes through the detector but the technique is more sensitive where S/N power is greater than unity than the pre-detection method and was originally devised to overcome the difficulty of providing phase stable transmission of data over long distances. The demands on the frequency and timing standards are easily met and would only require crystal clocks accurate to one part in 10^7.

The observations indicated that 3C 273 was only partially resolved with a baseline of 1200 km or 9 million wavelengths. Consequently Gubbay, Legg, Robertson, Moffet and Seidel collaborated in a trans-Pacific interferometer experiment using the post-detection technique, in September 1967. Time correlation of DSS 41 and DSS 14 standards was obtained through the use of a ranging transponder on one of the lunar orbiting spacecraft. A pre-detection or Michelson interferometer experiment had already been scheduled for November 1967 but

as the post-detection technique required little modification to station configuration and had already been employed successfully it appeared that the use of the 210 ft. antenna at DSS 14 with the 85 ft. antenna at DSS 41 would provide useful preliminary information. It was found that the correlated flux density of all sources observed was below the system threshold of 5 flux units. The list of sources included 3C 273, 3C 279, 3C 286 as well as the Crab Nebula. It was evident that the correlation threshold had to be improved. This was achieved by employing the Michelson mode of operation and by increasing the 3db bandwidth of the recorded data from 400 Hz to 1 kHz.

3.2 Calculation of the Differential Doppler Frequency

Two stations on the surface of the earth, in general, undergo differential motion with respect to a celestial object. The spectrum of the object seen at one station is displaced by the differential doppler frequency with respect to the other station. The value of this frequency is obtained by expressing the difference of the station component velocities along the line of sight to the object in terms of the wavelength corresponding to the operating receiver frequency. If the displacement of the spectrum of the object is greater than the bandwidth of the data, the only correlations that might be perceived are correlations between different parts of the spectrum of the object. The differential doppler frequency was calculated prior to the experiment as the

doppler difference was known to be several times greater than the bandwidth and necessitated a relative shift in receiver frequencies in order to view the same spectral range of the source at each station.

The differential doppler frequency is identical to the fringe or fringing frequency but the treatment deals with each station separately and differential phase is simply obtained by integrating the differential frequency. However cross-terms between station doppler frequencies appear when the object is within the solar system where, in non-relativistic terms, proper motion, aberration and parallax have an effect. The relativistic treatment as given by Pauli, 1958 does not distinguish between these effects.

The frame of reference used is the N.A.S.A. 1966 earth model ellipsoid, which has a semi-major axis of 6378.165 km and a flattening ratio of 1/298.3.

3.2.1 Sources Outside the Solar System

The problem can be expressed in terms of three vectors, $\underline{\omega}$, the angular velocity of the earth, $\underline{l}$, the unit vector along the line of sight which, in the case being considered, is identical for each station, and $\underline{R}_{12}$, the vertical distance between the two stations, which rotates about $\underline{\omega}$ (see diagram).

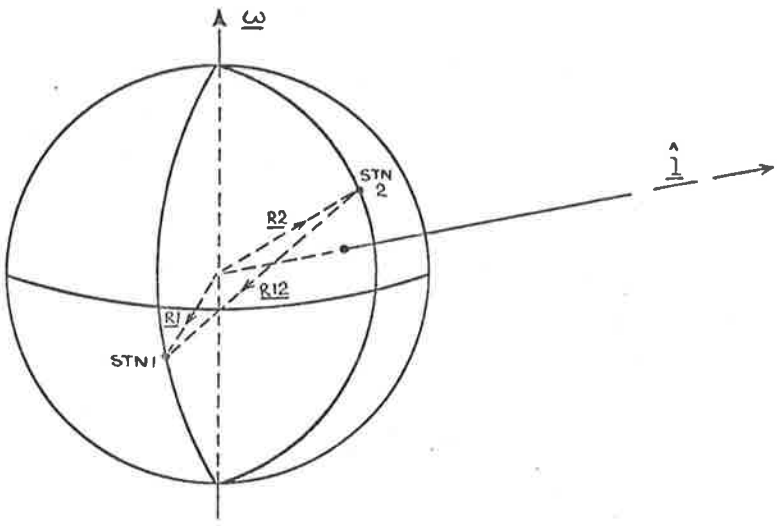

$$\underline{v} = \underline{\omega} \times \underline{R}$$

where $\underline{v}$ is the velocity of the station at any instant with respect to the axis of the earth, and $\underline{R}$ is the radius vector to any point on the earth. The component of the velocity of station 1 along the line of sight can then be written

$$\underline{v}_{11} = (\underline{\omega} \times \underline{R}_1) \cdot \hat{\underline{l}}$$

and the differential velocity

$$\underline{v}_{11} - \underline{v}_{21} = \hat{\underline{l}} \times \underline{\omega} \cdot (\underline{R}_1 - \underline{R}_2)$$

may be expressed in terms of wavelength of the signal to obtain the differential doppler frequency ν_D, thus

$$\nu_D = \Delta f = \hat{\underline{l}} \times \underline{\omega} \cdot (\underline{R}_1 - \underline{R}_2) * \frac{f}{c}$$

where c is the velocity of light and f is the receiving frequency. This equation reduces to

$$\nu_D = \frac{\omega}{c} \cos(\text{DECQ}) \; (AX_1 * f_1 * \sin(\text{DLNG31}) - AX_2 * f_2 * \sin(\text{DLNG32}))$$

where

DECQ = declination of the quasar

AX_1 = distance of station 1 from the axis of rotation

AX_2 = distance of station 2 from the axis of rotation

f_1 = receiving frequency at station 1

f_2 = receiving frequency at station 2

DLNG31= longitude of the sub-quasar point - longitude of station 1

DLNG32= longitude of the sub-quasar point - longitude of station 2.

The relative phase is then obtained by integrating ν_D with respect to time.

$$\text{PHASE} = \frac{1}{c} * \cos(\text{DECQ}) * (AX_1 * f_1 * \cos(\text{DLNG31}) - AX_2 * f_2 * \cos(\text{DLNG32}))$$

3.2.2 Sources Within the Solar System

For a source within the solar system the unit line of sight vectors from each station cannot be considered to be parallel. Further the effects of proper motion are, in general, not negligible. The case of a satellite transmitting at the Deep Space Network frequency has practical application. In particular, the strong signals from Pioneer VIII some 30 million kilometers distant was used as an experimental control (see section 3.4). Satellite tracking by two stations operating as an interferometer can also provide useful geodetic data (see Chapter 6).

Let $\underline{v}_s$ be the velocity of the spacecraft with respect

to the centre of the earth. The doppler difference frequency between two stations operating at closely matching receiving frequencies, now involves an additional term which reduces to zero when $\underline{l}_1 = \underline{l}_2$, where $\underline{l}_1$ and $\underline{l}_2$ are the unit vectors along the line of sight from the respective stations to the spacecraft. This term, ν_d, is due to the difference in the components of the velocity of the spacecraft with respect to the two stations and may be expressed:-

$$\nu_d = - \underline{v}_s \cdot (\hat{\underline{l}}_1 - \hat{\underline{l}}_2) * \frac{f}{c}$$

$$= - \underline{v}_s \cdot \left(\frac{\underline{l}_1}{l_1} - \frac{\underline{l}_2}{l_2} \right) * \frac{f}{c}$$

$$= \left\{ - \frac{\underline{v}_s}{l_1} \cdot (\underline{l}_1 - \underline{l}_2) + \frac{\underline{v}_s \cdot \hat{\underline{l}}_2}{l_1} (l_1 - l_2) \right\} * \frac{f}{c}$$

The first term appearing in the brackets on the right hand side can be rewritten as

$$\frac{\underline{v}_s}{l_1} \cdot \underline{R}_{12}$$

and thus appears as a component of the angular velocity of the spacecraft along the interferometer baseline. The second term appears when the spacecraft to station distances are unequal. The value of the various terms are given here for a typical case when Pioneer VIII was observed at which time ν_D had almost obtained its maximum value and viewing conditions from DSS 42 and DSS 14 were similar.

$$\nu_D = 4221.15 \text{ Hz}$$

$$\nu_d = -4.36 \text{ Hz} + 0.48 \text{ Hz} = -3.88 \text{ Hz}$$

Whereas ν_D was increasing at the rate of about 3 Hz/min., ν_d decreased only by about 0.02 Hz over 10 min.

In practice however the total doppler difference frequency, was calculated from the equation:

$$\nu(\text{spacecraft}) = \frac{f_1}{c} (\underline{\omega} \times \underline{R}_1) \cdot \hat{\underline{l}}_1 - \frac{f_2}{c} (\underline{\omega} \times \underline{R}_2) \cdot \hat{\underline{l}}_2$$

which represents the difference between two determinants of the form

$$\frac{f\omega}{c} \begin{vmatrix} 0 & 0 & 1 \\ \frac{XL_1}{L_1} & \frac{YL_1}{L_1} & \frac{ZL_1}{L_1} \\ X_1 & Y_1 & Z_1 \end{vmatrix}$$

where the rows represent the components of the vectors $\underline{\omega}$, $\underline{l}_1$ and $\underline{R}_1$ respectively, along the X, Y, and Z directions in space centered at the earth. The X and Y directions of the reference frame lie in the equatorial plane and in the direction of zero right ascension and 6 hours in right ascension respectively. The z axis is coincident with the axis of the earth and of the same sense as the radius vector to the North pole. The values of the components of the vectorial distance and of the velocity of the spacecraft with respect to the centre of the earth, in this frame of

reference, were supplied by the Jet Propulsion Laboratory.

3.2.3 Assessment of the Effect of the Tracking Motion of the Antenna

The tracking arm of the antenna will rotate in some manner depending on the design of the mount in the course of an observation. The station position represented by the vector $\underline{R}$ may be expressed by two component vectors $\underline{R}_s$ and $\underline{R}_1$ where $\underline{R}_s$ represents the position of a fixed point F along the moving arm or the extension of the moving arm, with respect to the center of rotation, and $\underline{R}_1$ is the vectorial distance of the antenna from this fixed point (see diagram).

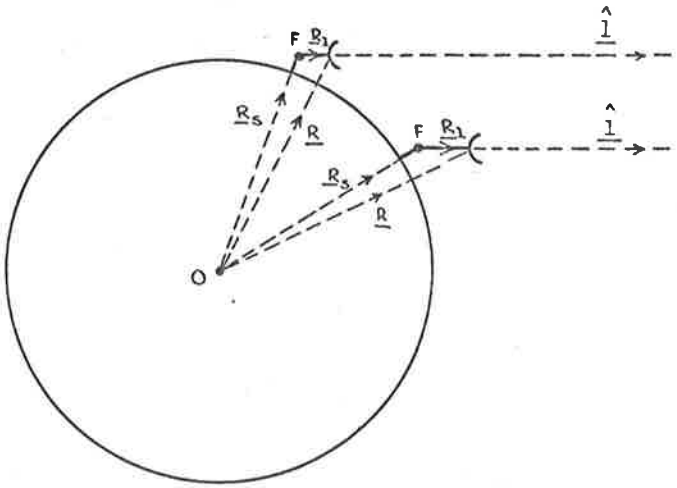

From above (section 3.2.1)

$$\nu_D = \frac{f}{c} (\underline{\omega} \times \underline{R}) \cdot \hat{\underline{l}}$$

$$= \frac{f}{c} [(\underline{\omega} \times \underline{R}_s) \cdot \hat{\underline{l}} + (\underline{\omega} \times \underline{R}_1) \cdot \hat{\underline{l}}]$$

The second term is identically zero by virtue of the fact that $\underline{R}_1$ is always parallel to $\hat{\underline{l}}$. Geodetic experiments

will therefore refer to the location of the point F which should be accurately determined with respect to the centre of the base of the antenna. For the X - Y mount of the 210 foot antenna at Goldstone the point F is independent of the declination of the source but for the polar mounts which support the 85 foot antenna of the Deep Space Network the position of F is a function of the declination of the source. However the locus of F as source declination is varied lies along the polar axis of the mount which is set parallel to the axis of the earth. Consequently $\underline{\omega} \times \underline{R}_s$ is independent of source declination and ν_D is unaffected.

3.2.4 Refraction

At the receiving frequency of the Deep Space Stations, i.e. 2300 MHz, refraction occurs principally in the troposphere. Refraction in the solar plasma and in the ionosphere is negligible and the treatment of refraction in the troposphere would apply equally for these media.

The effects of refraction are two-fold. The path of the ray suffers a deviation at the boundary of two media of differing refractive indices according to Snell's law

$$\mu = \frac{\sin i}{\sin r}$$

where μ is the ratio of the refractive indices of the media, i and r are the angles between the vertical at the point

where the ray undergoes refraction and the pathos of the incident and the refracted rays respectively. For the troposphere μ is given by

$$\mu = \frac{76.6}{T*10^6}\left(p + \frac{4800e}{T}\right)$$

provided the operating frequency $\leq$ 30 GHz.

Here T ~ 320°K, the temperature of the troposphere

p ~ 1000mb, at the base of the troposphere

e ~ 20mb, the partial pressure of water vapour in the troposphere.

From above, the doppler shift at an observing station ν_D can be expressed

$$\nu_D = \frac{f}{c}(\underline{\omega} \times \underline{R}) \cdot \hat{\underline{1}}$$

$$= \frac{fR}{c}\,\underline{\omega} \cdot (\underline{R} \times \hat{\underline{1}})$$

The scalar value of the quantity in brackets is sin i where $\hat{\underline{1}}$ refers to the path of the incident ray. If $\hat{\underline{1}}$ refers to the path of the refracted ray the scalar value becomes sin r. The direction of the resultant vector however remains unchanged as R_1, the path of the incident ray and the path of the refracted ray are coplanar. Thus the effect of the quantity in brackets alone would alter the value of ν_D by the factor sin r/sin i. Now the value of c, the phase velocity of light is modified by the same factor and consequently the

nett effect of refraction on the doppler frequency shift is identically zero.

The computer software which drives the antenna when tracking a celestial source takes account of refraction corrections so that no calculations for this effect were necessary when producing predictions for antenna pointing. During the experiments its value fell within the range 0.015° to 0.035°. The angle between the electrical axis of the antenna and the 3db point is about 0.200° for the 85 foot antenna and 0.060° for the 210 ft. antenna.

3.2.5 Scattering and Scintillation

Radiation from celestial sources received at the earth has passed through the solar plasma. The plasma acts as a scattering medium so that, to an observer at the earth, a part of the total radiation flux from the source appears to come from a halo about the source. The power scattered into the halo and its angular extent increases with the electron density of the plasma and therefore with the distance of the line of sight, at the point of closest approach, to the sun, as shown by Cohen, Gundermann and Harris 1967. An assessment of the magnitude of this effect by Dr. Little, Dr. Cohen at Cal. Tech. and by Dr. Denniso n at the University of Adelaide indicate that at 13 cm, the DSS receiving frequency, we would be in a regime of weak scattering at any distance from the sun greater than a few solar radii.

When the optical path is 100 R. from the sun at its point of closest approach, a point source would still look like a point but would be surrounded by a halo of diameter ~ 0.002 containing about 1 per cent of the flux. Closer in, the proportion of the flux in the halo increases. A minimum distance of 10° from the sun was adopted as a criterion in our selection of sources so that a maximum of ~5% of the flux density from a point source would be lost from the unresolved component seen with the trans-pacific interferometer.

The effect of scintillation due to irregularities in the solar plasma in the line of sight is to introduce a secular variation in the apparent position and brightness of the source. The bandwidth of the spectrum of these variations is up to about 10 Hz. Secular variation in position at frequencies above 0.05 Hz and an amplitude greater than about 0.01° would have resulted in fluctuations and broadening of the correlation peaks due to jitter in the doppler difference frequency when the data streams were correlated coherently over 100 seconds. However, the observed fluctuations in the correlation peaks observed appear to agree closely with the theoretical noise statistics for the data reduction system (see Chapter 5) and in any case, instabilities in the Rubidium atomic standard would tend to disguise scintillation effects if these were present. Brightness fluctuations are smoothed over the period of integration.

The presence of electrons in the solar cavity increases the value of c, the phase velocity of light, by a factor of $\sim (1 + 10^{-12})$ resulting in a correction to predicted frequency of the order of 10^{-8} Hz which is negligible.

3.2.6 Rotation of the Earth About the Sun, Moon and Planets

The rotation of the centre of gravity of the earth about the other bodies of the solar system does not directly affect the value of the differential doppler frequency except insofar as the interaction with such bodies result in precession and nutation of the axis of the earth. The rate of change of displacement in the direction of the axis does not exceed about 0.5" per day. The correction to the differential doppler frequency due to the motion is << 0.001 Hz.

A further correction arises indirectly through the differential signal arrival times for the two observing stations. The velocity of the centre of mass of the earth alters over the differential time interval. The earth's orbital velocity therefore cannot be common to both stations when the differential time 0. However, for a differential time of 10ms the correction to the doppler difference frequency would not exceed $\sim 5*10^{-4}$ Hz.

3.2.7 Apparent Angular Motion of Source Due to Precession of the Earth's Axis

The apparent angular motion of a source due to precession of the axis of the earth results in a correction term in the formula for the differential doppler frequency in the manner dealt with in section 3.2.2.

The correction term can be expressed approximately as follows:-

$$\Delta\nu = \underline{\dot{\theta}} \cdot \frac{\underline{R}_2 - \underline{R}_1}{c} f$$

where $\underline{\dot{\theta}}$ represents the apparent angular velocity of the source about the centre of the earth. For the trans-Pacific baseline experiments,

$$\frac{\underline{R}_2 - \underline{R}_1}{c} f = \frac{R_{12}}{\lambda} \sim 80 \times 10^6$$

and as $\dot{\theta}$ does not exceed about 3×10^{-11} radians/sec,

$$|\Delta\nu| \nmid 0.003 \text{ Hz}$$

3.2.8 Relativistic Effects

Let us consider a source at a great distance moving at a speed v with respect to a point on the axis of the earth and transmitting a signal at frequency f_o in the source reference frame. The relative velocity w of a station on the surface of the rotating earth with respect to the source is

$$w = \frac{u + v}{1 + \frac{uv}{c^2}}$$

where u is the component of the instantaneous velocity of the station relative to the point, along the direction of the line of sight to the source. We obtain

$$\frac{dw}{du} = \frac{1 - \frac{v^2}{c^2}}{\left(1 + \frac{uv}{c^2}\right)^2}$$

The signal frequency f′ in the station reference frame is

$$f' = f_o \frac{1 - \frac{w}{c}}{\sqrt{1 - \frac{w^2}{c^2}}}$$

and by logarithmic differentiation with respect to u, Δf′ is expressed in terms of Δu

$$\Delta f' = - \frac{\Delta u}{c} f' \frac{1}{1 - \frac{w^2}{c^2}} \frac{dw}{du}$$

or from above,

$$\Delta f' = \frac{\frac{\Delta u}{c}}{1 - \left(\frac{u}{c}\right)^2} f'$$

The relativistic logarithmic increment Δf′/f′ is independent of the radial velocity of the source, i.e. independent of the value of the red-shift for the source.

Integrating the expression for Δf′/f′ from a time t_1 to

t_2 to obtain the signal frequency f, in the station reference frame,

$$\left[\log f\right]_{t_1}^{t_2} = \tfrac{1}{2}\left[\log \frac{1 - \frac{u}{c}}{1 + \frac{u}{c}}\right]_{t_1}^{t_2} + \log g$$

where g is a constant of integration. We can thus obtain the expression

$$f' = \left(\frac{1 - \frac{u}{c}}{1 + \frac{u}{c}}\right)^{\frac{1}{2}} g$$

When $u = 0$, $f' = f'_A$, where f'_A is the frequency observed on the axis of the earth, but from above $f' = g$ when $u = 0$, so that we have

$$f' = \left(\frac{1 - \frac{u}{c}}{1 + \frac{u}{c}}\right)^{\frac{1}{2}} f'_A$$

The differential doppler frequency for two stations on the geoid becomes

$$f'_{(STN1)} - f'_{(STN2)} = \left\{\left(\frac{1 - \frac{u_1}{c}}{1 + \frac{u_1}{c}}\right)^{\frac{1}{2}} - \left(\frac{1 - \frac{u_2}{c}}{1 + \frac{u_2}{c}}\right)^{\frac{1}{2}}\right\} f'_A$$

neglecting second order terms

$$f'_{(STN1)} - f'_{(STN2)} = -(u_1 - u_2)\, f'_A / c$$

in agreement with the non-relativistic treatment. It should be noted however that the frequency in the frame at rest

with respect to the point on the axis appears here and not the respective station operating frequencies. In practice f'_A is approximated for the trans-Pacific geometrical configuration where $u_1 \simeq -u_2$ by averaging the frequencies in the observing band at each station

$$f'_A \simeq \left\{ (f_1 + \tfrac{1}{2}b) + (f_2 + \tfrac{1}{2}b) \right\} / 2$$

where b is the common effective bandwidth of the signal.

The relativistic treatment by Pauli 1958, page 19 and on P49 of the Explanatory Supplement to the Astronomical Ephemeris, includes the effect of planetary aberration which will therefore not be considered separately.

The correction required by special relativity to the doppler frequency at either station where

$$\left|\frac{u}{c}\right| \sim 10^{-6}$$

is less than $0.5\ (f - f)\ 10^{-12}$ i.e. less than 2×10^{-9} Hz.

As the earth rotates about its axis, each station will appear to describe the section of a right circular cone, as seen from the other station. This transverse motion results in a differential transverse doppler shift of the signal for the two stations. The effect for the experiments considered is negligible.

For two stations on the earth at different gravity

potential levels the general theory of relativity states that a signal at frequency ν at the station of higher potential appears at a frequency $\nu + \Delta\nu$ at the other station where

$$\frac{\Delta\nu}{\nu} = \frac{M_e G h}{R_e^2 c^2}$$

where G the gravitational constant = 6.67×10^{-9} $m^2/Kg\ sec^2$

M_e the mass of the earth = 6.25×10^{24} Kg

R_e the radius of the earth = 6.4×10^6 m

c the velocity of light = 3×10^8 m/sec

and here h is assumed to be the difference in height above sea level in metres for the two DSS stations.

$$\Delta\nu < 2 \times 10^{-3} \text{ Hz}$$

as the value of h does not exceed 1000 metres.

3.2.9 Calculation of Parameters for the Geometrical Configuration of the Observations

The calculations above of the doppler difference frequency for any two observing stations is simplified by the use of vector methods rather than co-ordinate geometry. In the following the technique is extended to the calculation of the baseline, the differential time of arrival of the signal waveform at the two stations, the angle θ between the line of sight to the source and the direction of the baseline and finally the orientation angle ϕ between the direction of the

measured dimension of the source and the axis of the earth.

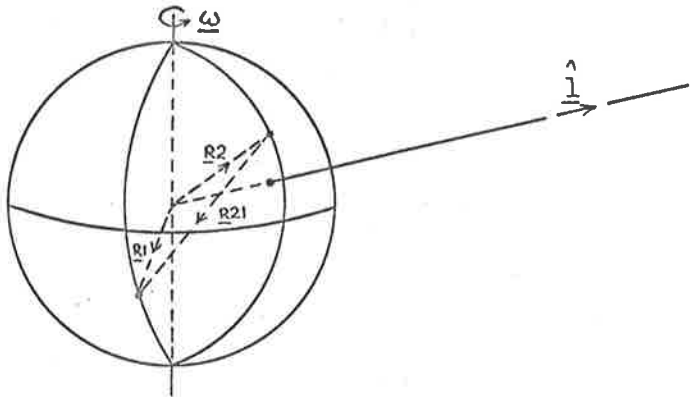

The baseline $\underline{B}$ is then simply expressed as

$$\underline{B} = \underline{R}_2 - \underline{R}_1 = \underline{R}_{21}$$

and

$$B(\lambda) = \frac{f}{c} R_{21}$$

where $B(\lambda)$ is the baseline distance in wavelength units. The effective baseline is $\underline{R}_{21} \times \hat{\underline{l}}$ and the resolving power, RP, of the baseline is equal to $c/\pi f |\underline{R}_{21} \times \hat{\underline{l}}|$.

The differential time of arrival of corresponding features of the waveform, LAG, becomes

$$LAG = \frac{1}{c} (\underline{R}_2 - \underline{R}_1) \cdot \hat{\underline{l}} = \frac{1}{c} \underline{R}_{21} \cdot \hat{\underline{l}}$$

where c is the wave group velocity. If θ is the angle between the line of sight vector and the direction of the baseline,

$$\sin\theta = \hat{\underline{l}} \times \hat{\underline{R}}_{21} \quad \text{and} \quad \cos\theta = \hat{\underline{l}} \cdot \hat{\underline{R}}_{21}$$

and if ϕ is the orientation of the measured dimension

$$\cos\phi = (\hat{\underline{l}} \times \hat{R}_{2\,1}) \times \hat{\underline{l}} \cdot \hat{\underline{\omega}}$$

$$= \hat{\underline{R}}_{2\,1} \cdot \hat{\underline{\omega}} - \hat{\underline{l}} \cdot \hat{\underline{\omega}} \, (\hat{\underline{R}}_{2\,1} \cdot \hat{\underline{l}})$$

$$= \frac{Z_{2\,1}}{R_{2\,1}} - \sin(\text{declination of source}) * \frac{\text{LAG} * c}{R_{2\,1}}$$

where $Z_{2\,1}$ is the component of $R_{2\,1}$ in the direction of the axis, $\hat{\underline{\omega}}$.

For long baselines where the common sky is limited to a few hours of right ascension, ϕ is principally dependent on the declination of the source. When the stations are disposed so that the common sky covers many hours in right ascension both ϕ and the effective baseline and therefore the resolving power of the geometrical configuration, vary over a wide range. The effect of a change in the orientation of the measured dimension can be studied separately by employing different station pairs as interferometers.

3.3 The Intermediate Interferometer

Section 3.1 dealt with the reasons for the transition from the post-detection to the pre-detection mode of interferometer operation. For reasons discussed in section 4.3 the transition was not complete.

The pure Michelson or predetection technique would have required detection subsequent to coherent integration of all the data, whereas the post detection of Hanbury Brown technique can be represented as the limiting case of the

Michelson treatment where detection occurs after correlation of each data sample pair so that frequency and phase information is lost. Detection took place in the reduction programme after each 10 second block of data had been coherently integrated. The two streams of data were slipped relatively in time as required by the differential in signal arrival times at the two stations and then coherently integrated over a period of 10 seconds and a fourier search about the predicted doppler frequency was effected before detection. The results of each block of 10 seconds were added for corresponding points of the fourier array.

For a given total observation time T, the threshold of the system reduces as the length of the coherent block of samples, t, increases in accordance with the relation

$$\frac{S}{N} \propto \sqrt{tT} \quad B \left(\frac{S}{N}\right)_1 \left(\frac{S}{N}\right)_2$$

approximately that given by Clark 1968 for low values of $\left(\frac{S}{N}\right)$, where B is the data bandwidth and $\left(\frac{S}{N}\right)_1$ and $\left(\frac{S}{N}\right)_2$ are the signal to noise ratios at the respective stations.

The effect of t and T on the statistics of the calculated correlation coefficient is dealt with in Chapter 5. For a given value of T, the total number of independent samples, the value of t must be optimized with regard to:-

(a) The phase stability of the primary frequency standards at the stations.

(b) The threshold required for the sources under study.

(c) The information sought, i.e. the visibility function of the source or the secular variation in flux density of the source. In the latter case statistical errors have to be constrained at the expense of system threshold (see Chapter 5).

The visibility function is the fourier transform of the spatial frequency composition of the source. Information on the shape of the source, the relative intensities of the shell structure or of the components in a dumbell or double source structure can be obtained from the visibility function.

3.4 Design of the Experiments

After the interferometer experiment of June 1967 (see section 3.1) was completed, Dr. Robertson of W.R.E. suggested that other stations of the Deep Space Network could operate jointly in a similar manner to extend and diversify the working baseline. In particular, an experiment employing stations in Australia and in California would be required to adjudicate against the local and cosmological location of quasars as the proponents of the rival views had predicted quasar angular dimensions which were at variance and a trans-Pacific baseline experiment could discriminate between the respective values for angular size (see Chapter 2).

A meeting was called by Justin R. Hall of J.P.L. and took place on 12 September, 1967. The receiver and data

recording configuration adopted at this meeting is shown in figure 3.1. Data reduction was the responsibility of J.S. Gubbay.

An experiment having the following objectives were planned for November, 1967:-

(a) To test the feasibility of a Michelson phase-sensitive interferometer over longer baselines than had previously been used.

(b) To place upper limits on the diameters of a number of quasi-stellar radio sources. The Michelson interferometer offered two orders of magnitude greater sensitivity than the post-detection correlation interferometer, tried between DSS 41 and DSS 14 in September, 1967. Thus many fainter sources could be observed in a given amount of antenna time.

(c) To examine the feasibility of the long-baseline interferometer for checking the time difference between two station clocks. The initial experiment offered the possibility of synchronization to within about 20μs. Possible extensions of the technique using wider recording bandwidth to reduce synchronization errors to less than 1μs had been suggested by Gubbay and Robertson, 1967 (see Appendix 1).

(d) Sources to be observed included 3C 273, 3C 279, 3C 286, 3C 287, 3C 298, NRAO 530, among others.

The actual source list (see Chapter 7) for the experiment which took place on the 2 and 3 of November 1967 did not however include 3C 286 and 3C 287 as they did not appear to vary and were located in a region of high galactic background.

3.4.1 Selection of Sources

The sources selected for immediate study fell into one or more of the following categories:-

(a) Sources that had exhibited an unresolved component when observed by

(i) Gubbay and Robertson 1967, using the two stations in Australia DSS 41 and DSS 42 at a baseline distance of about 9 million wavelengths,

(ii) The Canadian group, Broten et al. 1967, observing with a baseline of $4\frac{1}{2}$ million wavelengths,

(iii) NRAO group, Bare et al. 1967, observing across a baseline distance of 20 million wavelengths.

(b) Sources with a high red shift, i.e. Q.S.O.'s.

(c) Sources that exhibited scintillation when viewed close to the sun by Cohen, Gundermann and Harris, 1967.

(d) Sources which had been observed to vary in flux density (at short wavelengths) by Dent, 1965 Epstein, 1965 and Low, 1965, as discussed in Chapter 1.

(e) And those sources whose spectral flux maxima lay at relatively high frequencies.

For practical reasons a right ascension bracket of 4 to 5 hours containing the most interesting group was defined. All of these sources lay within the declination limits of the common viewing limits for the participating radio telescopes i.e. $\pm 40^{o}$, and exceeded 1 flux unit in total flux density.

3.4.2 Calibration of the strength of the Unresolved Component

In order to avoid systematic errors in the measurement of the flux density of the unresolved component the source was viewed simultaneously across a short baseline and across the trans-Pacific baseline.

The short baseline station pair comprised an 85 foot antenna and a 210 foot antenna at a baseline separation of about 12 kilometers or 5 kilometers acoording to whether DSS 12 or DSS 11 respectively were assisting in the observations with DSS 14. All the sources were known to be

unresolved at this distance and consequently the correlated flux provided a measure of the total strength of the source. The zero distance value for the visibility function of the source could then be directly compared with the correlated flux density for a baseline separation of 80 million wavelengths. The telescope pair making the trans-Pacific observations was equivalent to the short baseline pair in that:

(a) The station in Australia assisting in the observations, DSS 41 or DSS 42 possessed the same standard 85 foot antenna and receiving system as did DSS 12 and DSS 11. The receiver noise temperature was closely similar for these four stations.

(b) The 210 foot antenna and equipment at the Mars site, DSS 14, were common to both the long and short baseline station pairs.

Thus the sensitivity of both station pairs could be considered to match closely. The height of the correlation peaks for the long and short baseline were considered in arbitrary units in the first instance although the peaks for the short baseline agreed closely with the anticipated values calculated from the total source strength, effective antenna area and system noise temperature. The flux of the component seen with the trans-Pacific pair was quite simply obtained from the catalogued values of total flux density at various wavelengths to provide information on the spectral

curve at 13 cm, and the ratio of the peak heights for the short and long baselines.

The short baseline correlation peak heights were later plotted against the total strength of a number of sources in figure 1 of Gubbay, Robertson, Moffet and Seidel, 1969 (see Appendix 2 and Chapter 7). The source strengths were obtained by interpolation of source strengths observed at various frequencies. A linear relationship between the logarithm of total strength and the square of the correlation peak is required and the degree to which this condition is fulfilled is an indication of the validity of the reduction process and the accuracy of the measurement of the correlation flux. However an assessment based on this criterion must be pessimistic as factors such as source strength interpolation errors and possible secular variations of total source strengths contribute to the scatter of points about the calibration line adopted, particularly for the weaker sources. A detailed assessment of statistical errors is given in Chapter 5.

When no zero baseline measurement is made, as was provided in this instance by the two DSN stations in California, the calibration of the correlation peaks is a somewhat more complex process. The source itself may contribute significantly to the background noise. The system noise temperature at DSS 14 is about 20°K and this contribution does at times raise the apparent system noise temperature as much as 10°K. The correlation coefficient

obtained will relate to the enhanced noise temperature. It is therefore essential to obtain noise temperature measurements while observing each source. Where a concurrent zero baseline measurement is obtained this effect is accounted for in the calibration curve thus obtained.

3.4.3 Determination of Viewing Parameters

The observation of each source was timed to fulfill the following conditions as closely as possible:-

(a) The contribution to background noise rose rapidly for antenna elevation below about 15°. In all cases except for 3C 345 where the maximum elevation at the Australian station lies somewhat below this figure, observations were scheduled so that viewing elevations were above 20° (see figure 7.2 to 7.5).

(b) For the 1967 and 1968 experiments observations were scheduled (except for 3C 345) for those times when the relative doppler difference frequency was at or close to its maximum value (see figure 7.2). In 1967 the trans-Pacific baseline was the longest in terms of metric distance and in terms of wavelengths and therefore the fringing frequency was unprecedently high and errors in data reduction would arise from errors in predicted frequency. As the differential of frequency with respect to time approaches zero, the difference between predicted frequency

and actual frequency due to the least accurately known parameters in the geometrical configuration, e.g. declination of the source, approached a constant value thus minimizing 'walking' of the peak due to change in the difference between the actual and the predicted doppler difference frequency. However although such divergences in the actual frequency did exist, it was found that for the standard mode of data reduction, (coherent integration of 10 second blocks of data, see Chapter 4), walking was imperceptable even when the fringing frequency was decreasing rapidly as was the case for 3C 345.

For the 1969 experiment emphasis was placed on optimum viewing elevations at the stations to minimize the effect of ground reflections, rather than maintaining quasi-stationary fringing frequencies. The fringing frequency for all observations were well in excess of 1 kHz, the bandwidth of the data recorded, and the respective station synthesizers were set so that the doppler difference frequency was diminished to a value between 30 Hz and 60 Hz where possible.

The contours of resolution are mapped for the trans-Pacific baseline over the area of common sky (see fig. 7.3). The orientation of the measured dimension is defined as the angle between the projection of the baseline on the plane normal to the line of sight and the North Pole, measured in

a clockwise direction. Contours of orientation are displayed in Chapter 7.

Computer listings of the elevation and hour angle at the respective stations, baseline distance in kilometers and wavelength, angle of line of sight to the baseline, orientation of measured dimension, fringing frequency, and differential time of arrival for the station pair against UT as argument, were on hand during the experiment. They were employed in scheduling the observations and re-scheduling them during the experiment when problems with equipment made this necessary. When an unlisted source was included during the experiment, scheduling and synthesizer setting were chosen by reference to the contour map for elevation and fringing frequency.

3.4.4 Experimental Controls

The simultaneous observation across a short baseline and the trans-Pacific baseline with similar standard or common equipment to calibrate the correlated flux of the unresolved component directly against the correlated flux from the whole source was described in section 3.4.2. It also provided a means of indirectly calibrating the long baseline correlation peaks in terms of flux density independently of a knowledge of system sensitivity.

The short baseline correlation peaks were easily seen but as it was possible that no correlation peaks would be

observed for the trans-Pacific baseline it was necessary to include two other experimental controls to ascertain the correct functioning of the remote (Australian station) in that event. Thus the following ancillary experiments were performed in the course of the observations on quasars on the 30th May, 1968:-

(a) The Pioneer VIII space craft which at that time was at a distance of 30 million kilometers, was observed using the quasar observation configuration. The very strong short baseline and trans-Pacific baseline correlation peaks were equal (as required) and appeared at the predicted frequency within an acceptable tolerance (see Chapter 6).

(b) During the experiment on the 2nd November, 1967 the settings for Universal Time were accidentally tampered with and uncertainty in the setting for UT extended the search for correlation flux. In order to reduce the uncertainty in station clock settings to ± 1 ms, well within range of the programme searching in the time domain (see Chapter 4), pulsars CP 0950 and CP 1133 were observed in the course of the observations of 30th May, 1968. The relative clock displacements between DSS 14 and DSS 42 were about 700 μs away from the displacement determined by the Moonbounce equipment (see Chapter 4). The system configuration was altered to the

post detection mode for collection of the pulsar data. The relative clock displacement was determined from the position of the intensity correlation peaks with respect to UT at DSS 42. This determination of relative clock displacement was carried out by Dr. D.G. Singleton at W.R.E. in South Australia.

The determination of relative clock displacement by the Moonbounce procedure was found to correspond with the displacement required by the correlation peaks for quasars. The agreement was better than 50 μs as no divergence could be detected from the Moonbounce and later quasar determination, the noise equivalent bandwidth of the data (see Chapter 5) being about 1250 Hz.

3.4.5 Mode of Station Operation

Dr. D. Robertson, A. Legg, and J. Gubbay conducted the interferometer experiments at the Australian end and Dr. A. Moffet and Dr. R. Ekers conducted the experiments at the American based station. All participating stations were in voice contact throughout the period of the experiment.

The antennae were driven by computer in "star track mode" using only the source coordinates as input. Antenna polarizers were switched to right circular, and the maser front end operated at a frequency between 2295 MHz and 2298.333333 MHz. The Rubidium frequency standard drove a synthesizer. The synchronized frequency was multiplied by

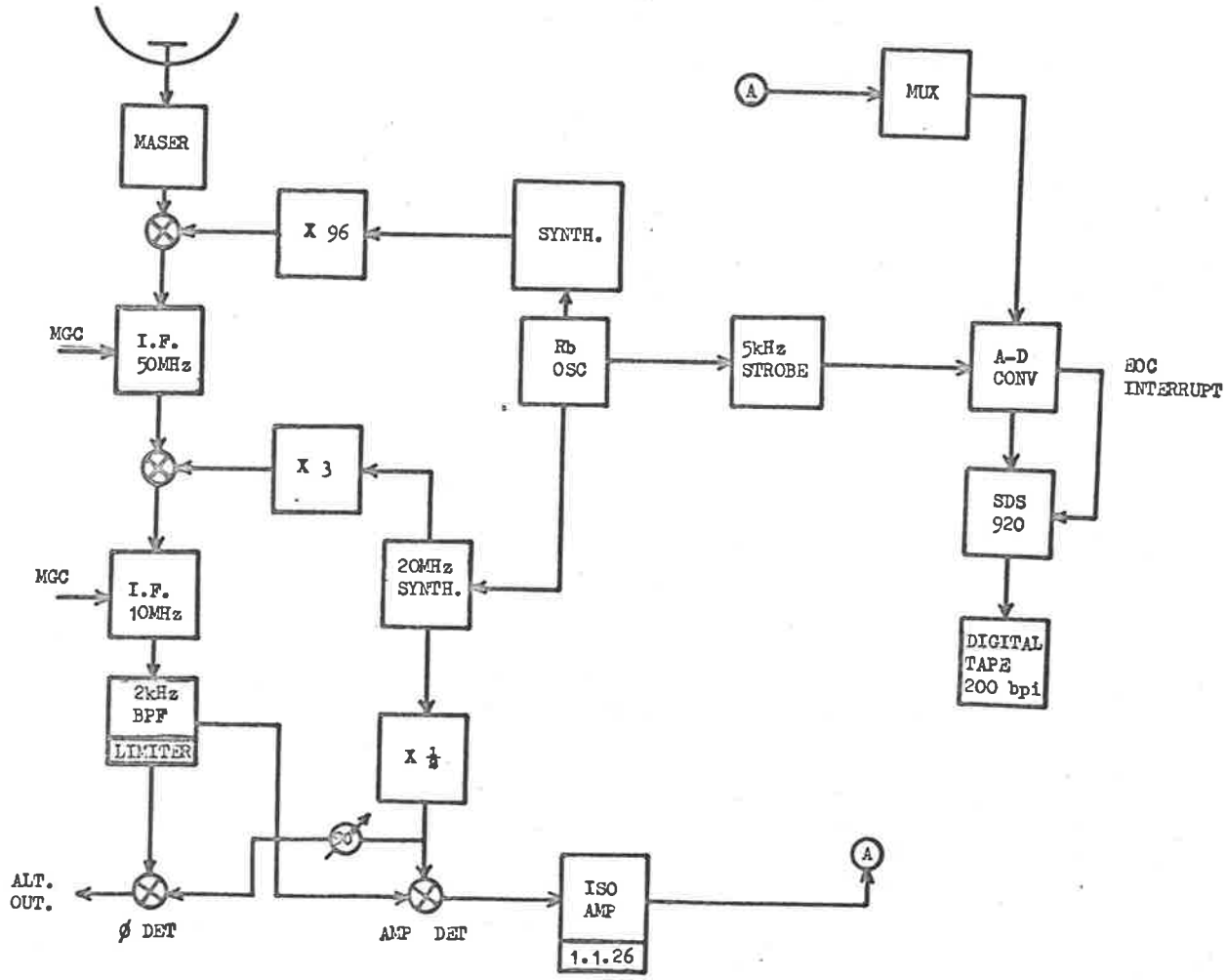

FIGURE 3.1 BLOCK DIAGRAM DEPICTING EQUIPMENT CONFIGURATION ADOPTED FOR DEEP SPACE STATIONS PARTICIPATING IN MICHELSON MODE INTERFEROMETER OBSERVATIONS.

FIGURE 3.1 BLOCK DIAGRAM DEPICTING EQUIPMENT CONFIGURATION ADOPTED FOR DEEP SPACE STATIONS PARTICIPATING IN MICHELSON MODE INTERFEROMETER OBSERVATIONS.

96 and fed to a mixer amplifier between the maser and the 50 MHz IF. A second synthesizer set at 20 MHz operated off the same Rubidium in the 1967 and 1968 experiments. The synthesized frequency was multiplied by 3 and mixed with the 50 MHz IF and the output of the mixer passed through a 2 KHz band pass filter centred at a frequency of 10 MHz. The output of the filter was mixed with 10 MHz from the same Rubidium, passed through an isolating amplifier and finally digitized at a sampling frequency of 5 kHz onto magnetic tape at 200 bits per inch. The 3db bandwidth of the data was 1 kHz (see Chapter 5 for noise equivalent bandwidth of the data).

The antenna pointing programme and antenna servo system were checked by pointing at a relatively strong source, i.e. above 10 flux units, which was easily visible on the noise temperature chart recorder. The data was viewed on an oscilloscope before it was digitized to check the AGC levels and the computer output was examined for mean level and symmetry of data distribution.

The configuration was altered for the 1969 experiment as concurrent observations were run by NRAO and by the W.R.E./University of Adelaide/C.I.T. team using separate back ends. The resulting data parameters were effectively unchanged except in that the NRAO rubidium which had a short term stability of 10^{-12} was used so that an improvement in phase stability in the data of about one order of magnitude was expected (see Chapter 4).

CHAPTER 4

DATA REDUCTION

At each of the observing stations the output of the 2 kHz centre frequency filter centred at 10 MHz, was sampled and digitized by an A-D converter at the rate of 5000 6 bit samples per second and written from buffers onto magnetic tape (see Section 3.4.5 and figure 3.1). The sampling programme for the Scientific Data Systems 920 computer at the stations was written by the system analyst at DSS 41, Mr. A. J. Legg.

The data from the stations were correlated on the CDC 6400 at the Adelaide University Computing Centre using programmes written by Dr. D. S. Robertson and Mr. J. S. Gubbay for the IBM 7090 at W.R.E. and recoded for the CDC 6400 with the assistance of Mr. J. Weadon and Dr. Barbara Kidman of the Computing Centre.

In general, the time of arrival of corresponding signals differ for the two stations, depending on the relative position of the stations with respect to the line of sight to the source. Furthermore, an apparent difference is introduced when the clocks at the respective stations are not synchronized. The relative motion of the stations along the line of sight results in a relative displacement of the spectrum of corresponding signals arriving at the respective stations. The calculation of the expected time lag and the expected

spectral displacement between stations pairs is shown in section 3.2. The relative displacements in the time and the frequency domain is illustrated in figure 4.1 for a source which is closer to the horizon viewed from the westernmost station than for the easternmost station.

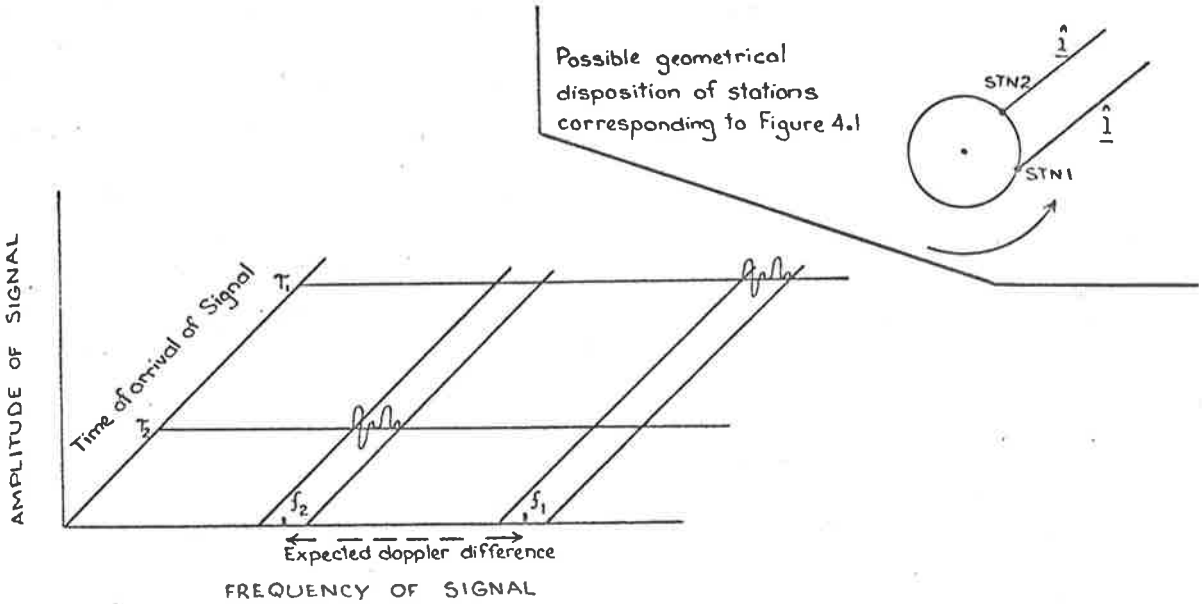

Fig. 4.1 Relative time and frequency displacements at interferometer stations.

Here τ_1 and τ_2 designate the time of arrival of corresponding signals at the two stations with reference to an arbitrary zero time, and ν_1 and ν_2 refer to the lower limits of the spectrum viewed at the two stations were the zero datum is arbitrarily defined and the index 1 corresponds to the western station while the index 2 refers to the eastern station.

The reduction programme corrects for the time displacement $\tau_1-\tau_2$ arising from the difference in the physical distance of the two stations from the source, by slipping the data stream from one of the stations with respect to U.T. before the two data streams are cross correlated. The time

displacement is recalculated and the correction made once each second.

If the same receiving frequency were selected at each station, the spectrum of the radiation from a celestial source appearing within the 2 kHz pass band would be relatively displaced for the two stations by the doppler difference frequency, ν, discussed in Chapter 3. As ν was greater than 1 kHz for the trans-Pacific observations, the source spectra contributing to the output of the audio filters at the two stations would not be common or overlapping bands of the emission spectrum. On the other hand, if different receiving frequencies f_1 and f_2 were selected to take account of the relative spectral displacement a correlation peak would appear at zero Hertz as a result of cross-correlating the two data streams, when the source contains a component which is not resolved at the effective baseline separation of the two stations. Although bias levels are set to obtain a closely symmetrical distribution of data values about zero, in general some small D.C. offset will remain and after cross-correlation the normalized product of the respective D.C. components would also contribute to the correlation at zero Hz.

This problem is simply overcome by choosing receiving frequencies at the respective stations so that the difference between them does not fully compensate for the doppler induced relative spectral displacement. Thus the operating frequencies were so chosen that the relative spectral displacement

appearing at the outputs of the respective audio filters lay in the range 10-60 Hz where possible. The upper limit was exceeded when the change in doppler difference frequency over the 18 minutes of recording was greater than 50 Hz. The receiving frequency at each station was selected by setting the frequency of a synthesizer before the X96 multiplier shown in figure 3.1. The synthesizer frequencies at the Californian stations were equal and were not changed throughout the period of the experiment as the doppler difference frequency was small but sufficient to provide a relative spectral displacement of between 1-6 Hz. As very little change occured in the value of ν during any recording period the lower limit was deemed quite safe even where the starting time for an observation had to be delayed by a few minutes. Compensation for the doppler displacement across the trans-Pacific baseline was effected at the Australian-based station.

When the waveforms represented by the data streams from the two stations are cross-correlated, the signal would appear at the sum and difference of the expected doppler difference frequency and the difference in the respective operating frequencies. The sum frequency is not accepted by the filter and in any case is not constant through the observed spectral band. The lower or difference frequency which is chosen to be much less than the extent of the data spectrum conveys information on the unresolved celestial components in the common viewing area of the sky.

The correlation of the data consists of correcting for the difference in time of arrival of the corresponding waveforms at the two stations and then cross correlating the data. The resulting data stream then goes through a process of numerical filtration as follows. A sub-routine generates the difference frequency, discussed above, at which the signal is expected to appear and two streams of data are generated by multiplying the correlated data with the sine and with the cosine of the phase derived from the generated frequency. The result of this is effectively to find the quadrature components of the generated frequency in the correlated data. The data streams are then separately summed over a given period of coherent integration and the square of the sums are added and the result is normalized so that unity represents the results of correlation of identical data streams from the respective stations. One of the reduction programmes repeats this procedure for a range of values of time displacements, $\tau_1-\tau_2$, for a given value of the expected frequency, the other assumes a given time displacement and searches over a range in the frequency domain about the expected frequency. In each case the difference between the separate values of the square of the correlation coefficient and the mean value of the correlation coefficient is calculated and displayed. The mean level and some statistical fluctuation about this mean derives from the random noise due to the receivers. The significance of the peak values of the deviation from the mean value, $\rho^2 - \langle\rho^2\rangle$ (where ρ^2 refers to the

peak values and $\langle\rho^2\rangle$ refers to the mean value of the array) is assesed in Chapter 5 in terms of fluctuations arising from noise originating in the equipment and uncorrelated background.

The peak values of $\rho^2 - \langle\rho^2\rangle$ are also interpreted in terms of signal strength by reading the corresponding value of flux density obtained using the results from the short baseline shown in figure 1 of Gubbay, Legg, Robertson, Moffet, Seidel, 1968. The phase history of the expected signal frequency depends on the geometrical configuration of source and station and upon the phase of the rubidium frequency standards at each station which is not known and which can vary stochastically over the recording period. It is therefore necessary to obtain the quadrature components of the signal.

The calculated values of ρ^2 for each coherent block are progressively calculated, added and normalized and the value of $\rho^2 - \langle\rho^2\rangle$ at each frequency in the search range is progressively displayed. This process is continued through the period of integration, T (i.e. 16 minutes). The period of coherent integration, t, is varied to determine its optimum value which is entirely dependent on the phase stability of the rubidium clocks driving the synthesizers.

4.1 Experimental Determination of Time Displacement

Errors in the predicted displacement of signals at any

two stations may arise from errors in the measured clock difference and from errors in station or source co-ordinates and from minor effects due to various second order terms discussed in section 3.2 which are ignored in the reduction programme in the interests of simple economy. To ascertain the divergence between the true and calculated values of time displacement the first programme is used to search for the position of the peak value of $\rho^2 - \langle\rho^2\rangle$ in the time domain using a source known to have a strong unresolved component. For all the experiments, the divergence has been shown to be less than 50 μs. A divergence below ~ 50 μs does not affect the results and is not discernable for the experimental parameters employed.

Various techniques were used to ascertain the relative clock displacements.

For the November 1967 experiment a time correlation between the clocks at DSS 41 and DSS 14 was achieved by comparing the arrival times of signals from a lunar orbiter space craft, for some days prior to the experiment and again after the experiment. The relative clock difference during the experiment was obtained by interpolation of these results and the relative frequency setting of the clocks was calculated. For the same experment, a Caesium clock was transported between the Californian stations DSS 14 and DSS 12 to provide a time correlation and the relative frequency setting of their clocks was also calculated. The correlation procedures confirmed the time and frequency determinations carried out by

Mr. F. Borncamp and Mr. F. Parker of JPL.

The relative time and frequency settings were determined for the May 1968 experiment by reflecting a signal off the moon. A coded signal was transmitted from DSS 13 in California and received at DSS 42 near Canberra. The received signal was compared with the local time standard. This procedure was repeated daily as part of the station time-keeping routine. A rough time correlation was also achieved by observing the pulsar, CP 1133. The period between pulses is about 1.187911171 9×10^{-9} secs and comparison of the arrival times of the pulses at the respective stations provided a time correlation during the experiment. The determination was carried out by Dr. D. G. Singleton of W.R.E. and the time correlation between the three stations agreed with that obtained using the "Moonbounce" technique to within about 800 μs. The extent of the clock displacement obtained from the signals reflected off the moon was found to be correct to within 50 μs. The pulsar determination was made in order to guard against accidental changes in clock settings as had occurred between the observations of the 2nd November and those on the following day. A ceasium clock was again transported between the Californian stations to make similar determinations.

The "Moonbounce" procedure was repeated to obtain the time correlation and relative frequency setting for the third experiment which took place on the 9th June, 1969. On this

occasion however the respective station receiving frequencies were synthesized from high performance rubidium frequency standards installed by the National Radio Astronomical Observatory for an experiment run concurrently.

The station rubidium timing standards are stated to have a short term frequency stability of 2 parts in 10^{11}, whereas the NRAO rubidium standard was stable to 1 part in 10^{12} and therefore comparable in performance to the ceasium clocks transported between the Californian stations.

4.2 Experimental Determination of Relative Doppler Difference

Although the adoption of the Michelson technique in November, 1967 had reduced the correlation noise threshold below that for the post-detection technique, no results were immediately obtained for the trans-Pacific interferometer. The reasons for the delay were as follows:-

(a) The unresolved components of the sources observed were all below or near the threshold.

(b) The baseline was the longest to that time and possible degradation of the correlation peak in the passage of the signal thrcugh an intervening medium, through errors in station position, time correlation between station, refraction etc. (see section 3.2) as well as the phase excursions of the rubidium had to be considered.

(c) The reduction programme was undergoing conversion

for CDC 6400 operation. Later when the computing costs were reduced by a factor of 4 it was possible to extend the trial runs over a period of 16 minutes of record time.

In order to prove that the system was operated correctly, the Pioneer VIII spacecraft was included in the source list for May, 1968. Pioneer VIII was at a distance of about 30 million kilometres in the direction within the scheduled right ascension viewing bracket. The crystal controlled 2292.1158089 MHz transmission was observed by the three stations DSS 42, DSS 14 and DSS 11. Both long baseline and short baseline pairs gave the same correlation peak height, i.e. the correlation peak value was 0.18 in each case. As the respective station system temperatures at that time were roughly estimated as 42° (DSS 42), 23° (DSS 14) and 42° (DSS 42) the equivalent noise temperature of the signal was about 5.6° (see Chapter 7 for station system temperatures). However the frequency at which the correlation peak appeared was about 0.45 Hz below the predicted frequency (see section 6). The quasar data were then processed with a correction to the predicted doppler difference frequency and the data from the May 1968 experiment were reduced. The procedure was immediately repeated for the November, 1967 data and the results from the two experiments were compared (see Chapter 7). It was evident that an unresolved component of 3C 279 < 0.001 second of arc had increased in intensity in the intervening period.

The calculations for the predicted doppler difference frequency for the case of a spacecraft was discussed in section 3.2. The position and velocity data for Pioneer VIII, based on orbit P8203, was kindly provided by the JPL Deep Space Network Manager for Future Projects, Mr. Justin R. Hall.

The correlation peak height for Pioneer VIII was well above noise after only 5 seconds of coherent integration of the long baseline data. It was thus possible to ascertain whether there was any variation in the correction to the predicted frequency through the 10 minute period of observation. No variation in the value of the correction was discernible and consequently the total period of integration of data from station pairs was extended to that order of time.

4.3 System Parameters

The viewing conditions imposed on a source under observation are determined by the station parameters, the geometrical configuration of the source and any two stations, and the integration parameters used in the reduction programme. The value of these parameters affect the detectable threshold of flux density, angular resolution, the orientation of the measured dimension of the source or its unresolved components and the frequency of the radiation received.

The factors which bear on these viewing conditions are assessed below.

4.3.1 Station Parameters

Table 4.1 lists the main characteristics of the equipment of the participating stations.

Location	ILS	Tidbinbilla ACT	Goldstone CALIF.	Goldstone CALIF.	Goldstone CALIF.
DSN Designation	DSS 41	DSS 42	DSS 14 (Mars)	DSS 11 (Pioneer)	DSS 12 (Echo)
Antenna diameter	85	85	210	85	85
Receiver noise Temp	------- See Chapter 7 -------				

All stations operated at a receiving frequency close to 2295 MHz. The polarization mode selected for interferometer observations was right hand circular. The 3db bandwidth of the filtered IF was effectively 1 kHz. The filter output was sampled to an accuracy of 6 bits at the rate of 5000 samples per second. The digitized data was written on to magnetic tape at 200 bpi. The capacity of the tape corresponded to an observation time of about 18 minutes and 20 seconds. At all stations the rubidium frequency standard is not worse that a few parts in 10^{11}.

4.3.2 Geometrical Configuration

The celestial position of each source was precessed for each experiment, using the 1950.0 positions supplied either by Dr. A. F. Moffet or the C.S.I.R.O. Radiophysics catalogue of sources. Station positions were obtained from the

geodetic latitude, longitude and height above sea level referenced to the NASA 1966 ellipsoid (see section 3.2). Calculations of the X, Y and Z coordinates were checked against values provided by Mr. A. Bomford of the Department of National Mapping.

Figure 7.2 is a chart depicting the elevation limits about the common sky, from stations DSS 42 and DSS 14. The tracks of sources observed in May 1968 are also displayed. Figure 7.5 shows the tracks of sources observed in June 1968. It will be seen that the common sky is limited in declination to $\pm 40^{\circ}$.

The resolution and the orientation of the measured source component for the station pair alters with declination and time. The value of these quantities are simply ascertained by following the course of the sub-source point on figures 7.3 and 7.4 respectively. Similar sets of charts are available for each station and were drawn from computer listings by Helen Fleming and Marjory King of the computing staff.

4.3.3 The Intermediate Type Interferometer for Correlation Measurement

The relative merits of the interferometer technique due to Michelson, sometimes called coherent or phase coherent interferometry, and that due to Hanbury Brown and Twiss have been discussed by Hanbury Brown and Twiss, 1954. In essence, the Michelson mode of operation acheives a lower correlation threshold but is much more sensitive to phase path length

variations in the medium and to erratic phase behaviour of the frequency standard at the stations.

During the November 1967 experiments, Dr. Moffet observed the phase behaviour of the fringes obtained at DSS 14 by mixing the output of the 2 kHz filter transmitted from DSS 12 via land line, with the output of the local filter. He observed that the fringe pattern suffered variations in phase of the order of 180° with a characteristic time between 50 seconds and 80 seconds. Dr. Robertson also noted that some sources were observed within a few degrees of the sun and that variations in the relative phase path due to the intervening solar plasma might occur. It was found that by dividing the data from each pair of tapes into blocks of 10 seconds, then treating each block of data as a separate Michelson experiment and adding corresponding values of ρ^2 from each block of data, the correlation peaks obtained were reproducible. About the same time Dr. Clark, 1968 described the characteristics of this technique designating it as an interferometer of intermediate type. The length of the coherent block must be optimised for each system, having regard to the total number of independent samples obtained, to provide the lowest correlation threshold consistent with reproducibility of the result. The optimum coherent period was experimentally determined to be about 10 seconds.

The square of the correlation coefficient ρ^2 is calculated in the fourier search programme through the formula

$$\rho^2 = \frac{(\Sigma\ X_t\ Y_{t+\tau}\ \mathrm{Cos}\omega t)^2 + (\Sigma\ X_t\ Y_{t+\tau}\ \mathrm{Sin}\omega t)^2}{\Sigma\ X_t^2\ \Sigma\ Y_{t+\tau}^2}$$

where X_t and $Y_{t+\tau}$ are the samples from respective data streams for times displaced by an interval τ representing the geometrical difference in arrival times of corresponding signals at the two stations,

and ω, the searching angular frequency, is varied in steps over a selected band.

The DC component of ρ^2 (see Chapter 5) was subtracted to obtain the component due to the signal $\rho^2 - \langle\rho^2\rangle$.

CHAPTER 5.

STATISTICS OF CORRELATION NOISE

As discussed in Chapter 4, the data are correlated and then integrated in a phase coherent manner in blocks of 10 seconds. For any given value of frequency over the range of the search in frequency, the values of ρ^2 (the square of the correlation coefficient) for each 10 second record are progressively added and averaged over the total number of blocks.

A mean value, $\langle\rho^2\rangle$, is calculated from all computed values of ρ^2 in a frequency range of 1 Hz. The values of $\rho^2 - \langle\rho^2\rangle$ are then listed for each of the 20 values of frequency in the range. The statistical distribution of $\rho^2 - \langle\rho^2\rangle$ resulting from noise will be derived in the following sections in order to assess the significance of the results presented in Chapter 7.

The length of the phase coherent block is determined by the stability of the rubidium frequency standard. The use of a hydrogen maser as the frequency standard however, would allow greater phase coherent integration times and an increase in sampling rate and bandwidth would improve the system correlation threshold. The problem is treated generally in order to assess the value of system modifications.

According to the expression for signal to noise ratio due to Clark, 1968, discussed in Chapter 4, the threshold of the system is unchanged if either 100 blocks of 10 seconds of phase coherent data are summed or a single block of 100 seconds of phase coherent data is taken alone. The latter mode of processing appeared to have the advantage of better defining the doppler difference frequency of a correlation peak so that a change of 0.02Hz in the difference between the observed and predicted values of the frequency over a period of 16 minutes could easily be detected. However it immediately became apparent that such treatment of the data caused unexpectedly high noise peaks to occur. The occurrence of the high noise peaks conforms with the statistical theory discussed in this chapter.

5.1 Coherent Integration - First Stage

The first stage of the integration process may be represented as a phase coherent integration of a predetermined number of independent samples, n, where

$$n = Bt$$

and B is the predetection equivalent bandwidth of the audio filter and t is the length of time over which phase coherent integration is sustained. The relationship between the predetection equivalent bandwidth of a centre frequency filter and its measured half power bandwidth has been

discussed by Kraus, 1966.

The probability distribution of the values of the correlation coefficient obtained by coherent integration of random noise was obtained by Lord Rayleigh and is presented by Deming in the form,

$$f\,dr = \frac{2}{n} r e^{-r^2/n}\,dr$$

where f dr is the probability that the correlation will have a value within the range $r \pm \frac{1}{2}$ dr after phase coherent integration of n independent noise samples. This probability curve does not fall off as rapidly as a normal curve centred at the mode, for values of r above the modal value. It will be shown that long coherent times can give rise to unexpectedly high peak values of correlation noise.

As the relative phase between the generated waveform correlated against the data and any fringe waveform in the data is unknown, the data is correlated in quadrature and the sum of the squares of the correlation with the sine and the cosine of the predicted angular frequency is obtained. When the generated frequency is equal to the actual fringe frequency the relative phase between the two waveforms is constant but unknown. Consequently values of r^2/n are obtained after normalization, corresponding to ρ^2, the square of the correlation coefficient. The probability distribution for t where $t = r^2/n$, is now

$$f_t dt = e^{-t}\, dt$$

We may however treat the quantity r^2 and normalize the results later. If we put

$$s = r^2$$

then
$$f_s ds = \frac{1}{n} e^{-s/n}\, ds$$

and
$$\langle s \rangle = n \,.$$

5.2 Non-coherent Integration - Second Stage

The second stage may be represented as a summation of the values of r^2 or r^2/n over a predetermined number of phase coherent records, each of time t, for each value of frequency in the search range. If T is the total number of samples, T/n is then the number of phase coherent records N, which are summed to obtain ρ^2. Let the value of s so obtained be s_T. The process of coherent integration is represented by the condition that N is unity.

Let us first consider the case where N = 2

The probability that the value of s will be equal to s_T after integration of two coherent records is the product of the probability that the value of s for the first record is some value s_1 where $0 \leq s_1 \leq s_T$ and the value of s for the

second record is s_2, where $s_2 = s_T - s_1$, and is expressed as

$$f(s_T)\,ds = \left(\frac{N}{T}\right)^2 \int_0^{s_T} e^{-\frac{s_1 N}{T}} e^{-\frac{(s_T - s_1)N}{T}} ds_1$$

Let us now take the case where $N = 3$.

If we consider first that s_1 is defined, then the problem becomes that for $N = 2$ where s_1 is substituted for the origin and s_2 is substituted for s_1. Thus

$$f(s_T)\,ds = \left(\frac{N}{T}\right)^3 e^{-\frac{s_1 N}{T}} \int_{s_1}^{s_T} e^{-\frac{s_2 N}{T}} e^{-\frac{(s_T - s_2)N}{T}} ds_2$$

However, s_1 can take any value $0 \leq s_1 \leq s_T$, therefore

$$f(s_T)ds = \left(\frac{N}{T}\right)^3 \int_0^{s_T} e^{-\frac{s_1 N}{T}} \int_{s_1}^{s_T} e^{-\frac{s_2 N}{T}} e^{-\frac{(s_T - s_2)N}{T}} ds_2\, ds_1$$

We can now express the probability distribution of s_T for any value of N as follows,

$$f(s_T)\,ds = \left(\frac{N}{T}\right)^N \int_0^{s_T} e^{-\frac{s_1 N}{T}} \int_0^{s_T - s_1} e^{-\frac{s_2 N}{T}} \int_0^{s_T - s_1 - s_2} e^{-\frac{s_3 N}{T}} \cdots$$

$$\cdots \int_0^{s_T - s_1 - s_2 \cdots - s_{N-3}} e^{-\frac{s_{N-2} N}{T}} \int_0^{s_T - s_1 - s_2 \cdots - s_{N-2}} e^{-\frac{s_{N-1} N}{T}}$$

$$e^{-\frac{(s_T - s_1 - s_2 \ldots - s_{N-1})N}{T}} \, ds_{N-1} \, ds_{N-2} ds_{N-3} \ldots ds_3 ds_2 ds_1$$

where $s_1, s_2, s_3 \ldots\ldots s_{N-1}$ are the respective values of s corresponding to the first N-1 phase coherent records. Integrating the above expression with respect to ds_{N-1} we obtain,

$$f(s_T)ds = \left(\frac{N}{T}\right)^N e^{-\frac{s_T^N}{T}} \int_o^{s_T} \int_o^{s_T - s_1} \int_o^{s_T - s_1 - s_2} \ldots\ldots \int_o^{s_T - s_1 - s_2 \ldots - s_{N-3}}$$

$$\left[s_{N-1}\right]_o^{S_T - s_1 - s_2 \ldots - s_{N-2}} ds_{N-2} ds_{N-3} \ldots ds_3 ds_2 ds_1$$

and after carrying out all stages of integration, the right hand side of the equation reduces to

$$\left(\frac{N}{T}\right)^N e^{-\frac{s_T^N}{T}} \frac{s_T^{N-1}}{(N-1)!}$$

If s_N is the normalized value of s_T,

$$f(s_N)ds_N = T^N e^{-s_N^T} \frac{s_N^{N-1}}{(N-1)!} \, ds_N$$

where $$s_N = s_T/n^2 N$$

The distribution of s_N, the square of the correlation coefficient, ρ, is thus represented by a gamma function of the variate $s_N T$. To obtain the probability that s_N will

exceed a lower limit, L, the function is integrated by parts.

$$\int_{L}^{\infty} f(s_N)\,ds_N = e^{-LT} \sum_{N=1}^{N} \frac{(LT)^{N-1}}{\Gamma(N)}$$

Thus the probability that s_N will exceed L can be expressed in terms of L and any two of the inter-related quantities T, N and n.

When N is unity, the probability falls exponentially and when L is zero, the probability is unity, as required. The expected value of s_N is N/T, or

$$\langle s_N \rangle = \frac{N}{T} = \frac{1}{n}$$

where

$$s_N - \langle s_N \rangle \equiv \rho^2 - \langle \rho^2 \rangle$$

This quantity is the end result of the data reduction process.

$$\text{If } l = L - \frac{N}{T}$$

The probability $\pi(l)$ that $\rho^2 - \langle \rho^2 \rangle$ will exceed some value l, is then

$$\pi(l) = e^{-(lT+N)} \sum_{N=1}^{N} \frac{(lT+N)^{N-1}}{\Gamma(N)}$$

5.3 Comparison against Experimental Results

The simple relationship between the probability that

$\rho^2 - \langle\rho^2\rangle$ will exceed a specified value and any two of the three quantities T, n or N was tested against experimental results. The values of the parameters of the statistical distribution function were:-

N = 96 phase coherent integrations

n = B * t = 1250 Hz * 10s = 12500 independent samples

The population of values of $\rho^2 - \langle\rho^2\rangle$ was obtained by including the results for all sources observed in November 1967 and May 1968 where a significant peak did not occur at the expected value of doppler difference frequency (after allowance was made for the offset in frequency indicated by observation of Pioneer VIII). Where a peak occurred within ± .05 Hz of the expected value, within the search range of 1 Hz, the results for that source were omitted. The population of 390 points accounted for roughly 75% of all results obtained before the experiment of June 1969. The results of the later experiment in June 1969 justified the exclusion of the remaining points (see Chapters 7 and 8).

The curve in figure 5.3.1 represents the theoretical probability that $\rho^2 - \langle\rho^2\rangle$ will exceed the corresponding value along the absisca. The points marked with a cross denote values obtained from the statistical population. The degree of agreement indicates that the noise equivalent bandwidth of the system was within ± 50 Hz of the estimated value. The scale along the right hand side refers to the curve on the right in the figure which is a continuation of the curve on

the left hand side.

The scale inside the left ordinate refers to a normal distribution. For N = 96, the distribution is near to normal and probabilities can be quoted in terms of σ values.

A similar graph for N = 1 phase coherent integration n = 1250 Hz * 100s = 125000 independent samples appears in figure 5.3.2.

The S/N power, discussed in Chapter 4, is not markedly different whether N = 1, n = 125000 or N = 96, n = 12500 as:-

$$S/N \propto \sqrt{Tt}\ B$$

where here T = total integration time in seconds,

t = length of coherent integration in seconds,

B = bandwidth of the data.

Thus

$$S/N \propto \sqrt{N\ n}$$

It is readily seen however, from a comparison of figure 5.3.1 and 5.3.2, that large values of $\rho^2 - \langle\rho^2\rangle$ arising from noise are more likely in the case of the longer coherence time of 100 seconds although the values of S/N in each case are sensibly equal, as observed at the beginning of this chapter.

The selection of the integration parameters t and T are of vital importance when the investigation concerns secular

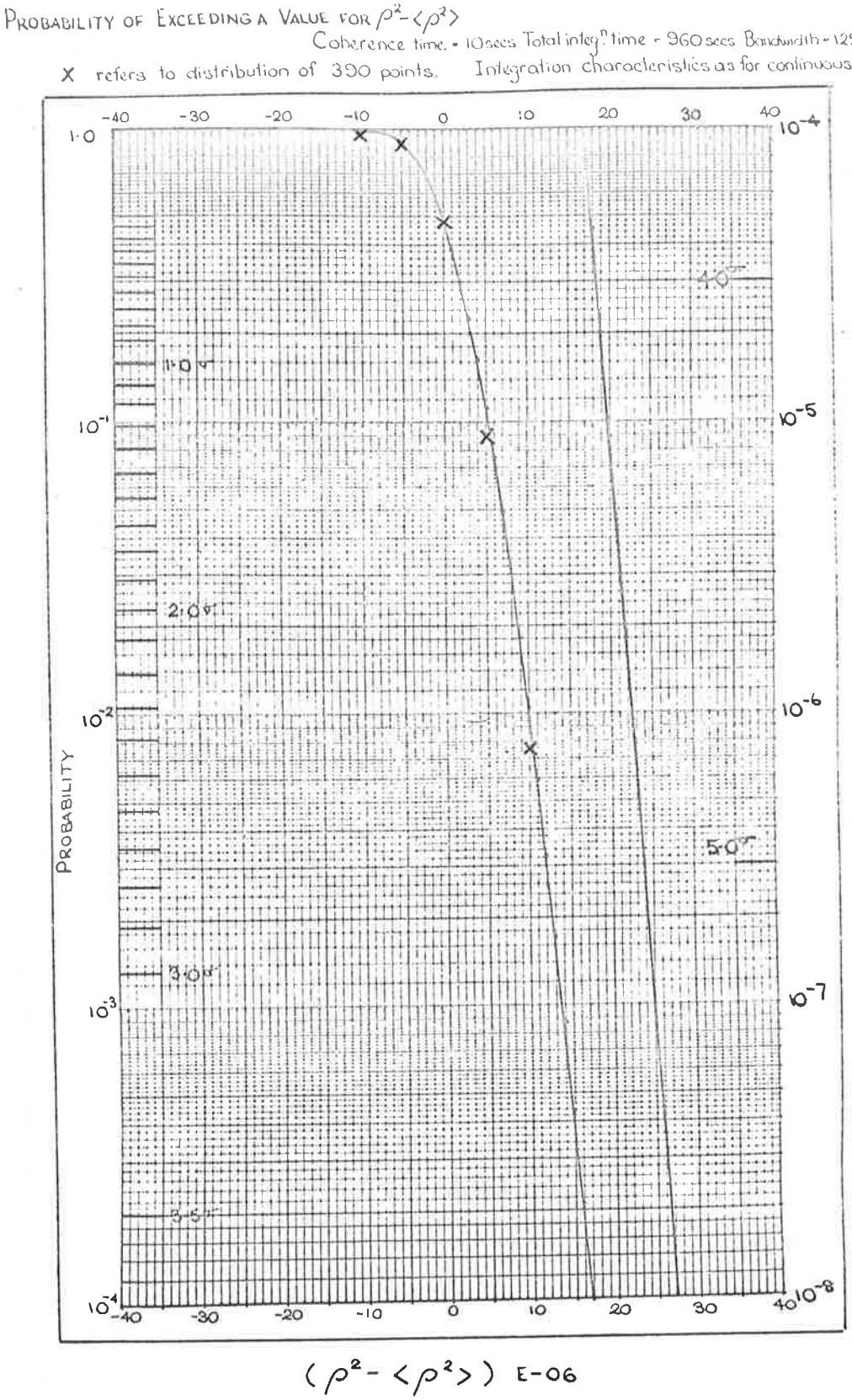

FIG. 5.3.1 PROBABILITIES THAT $\rho^2-\langle\rho^2\rangle$ WILL EXCEED VALUES ALONG ABCISSA. THE THEORETICAL CURVE IS SHOWN FOR SUMMATION OVER 96 10 SEC. RECORDS INTEGRATED COHERENTLY. X REFERS TO EXPERIMENTALLY DETERMINED VALUES.
N = 96 RECORDS
n = 12500 INDEPENDENT SAMPLES
NOISE EQUIVALENT BANDWIDTH = 1250 Hz.

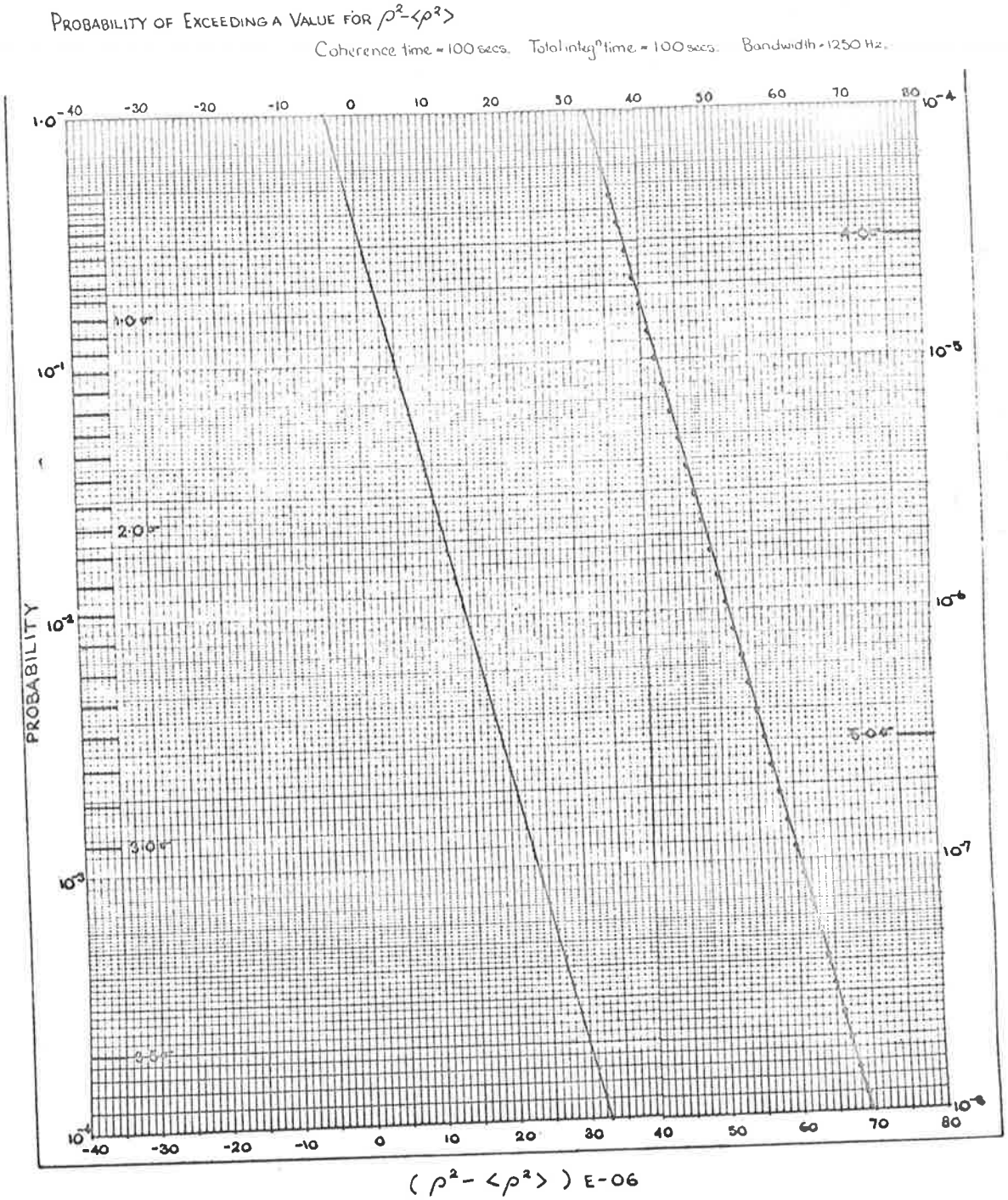

FIG. 5.3.2 PROBABILITIES THAT $\rho^2-\langle\rho^2\rangle$ WILL EXCEED VALUES ALONG ABCISSA. THE THEORETICAL CURVE IS SHOWN FOR A SINGLE 100 SEC. RECORD INTEGRATED COHERENTLY.
N = 1 RECORD
n = 125000 INDEPENDENT SAMPLES
NOISE EQUIVALENT BANDWIDTH = 1250 Hz.

variation in the correlation coefficient corresponding to the unresolved component in a celestial body. This will be evident when the results are discussed in Chapter 8. Basically, to improve the correlation threshold of an interferometer system, the total number of independent samples should be increased where possible.

In order to illustrate the above, the data from a pair of tapes were correlated using a coherence time t of 100 seconds and N = 1. This process was repeated eight times through the tape, so that a total of 800 seconds of data was used to produce the eight populations. Each population contained 20 values of $\rho^2 - \langle\rho^2\rangle$ corresponding to an array of generated frequency functions over a search range of 1 Hz. Correlation peaks of '4σ' and '5σ' appeared. The semblance of signal correlation was heightened by the correspondingly low values of $\rho^2 - \langle\rho^2\rangle$ over the rest of the spectrum. Apart from statistical considerations developed above these results might have provided strong evidence for rapid changes in the celestial source or in the intervening medium.

CHAPTER 6

GEODESY

Phase coherent radio interferometry requires an accurate knowledge of the position of the observing stations. The degree of accuracy necessary to predict the frequency at which the correlation peak will appear depends on the record time over which coherent integration takes place (see Chapter 4). Conversely, the discrepancy between the predicted doppler difference frequencies and the frequency at which the corresponding observed correlation peaks appear may determine the error in the assumed positions of the stations in terms of errors in station longitudes and errors in the distance of each station from the axis of the earth (see section 3.2). A determination of station position by this means is independent of the direction of the locally determined vertical in contrast with astronomical or satellite determinations of station position by that station alone. Furthermore, the accuracy of interferometer measurements of position is not affected by the distance between stations as is the case when geodetic determinations are made by extended triangulation from some baseline.

Thus the interferometer offers a technique for geodetic measurements directly related to the figure of the earth, which is independent of the vagaries of the earth's gravitational field.

6.1 Errors in Predicted Doppler Frequency

Using the symbols as defined in section 3.2.1 we can calculate the expected doppler difference frequency, ν_d, for two stations viewing a source, at a common receiving frequency, f,

$$\nu_d = \hat{\underline{l}} \times \underline{\omega} \cdot (\underline{R}_1 - \underline{R}_2) * \frac{f}{c}$$

The error in ν_d arising from errors in station location when represented by the vectors $\underline{R}_1$ and $\underline{R}_2$ respectively is given by

$$\Delta\nu_d = \hat{\underline{l}} \times \underline{\omega} \cdot (\underline{r}_1 - \underline{r}_2) * \frac{f}{c}$$

where the true value of $\underline{R}_1$ is equal to the vectorial sum of the assumed value of $\underline{R}_1$ and $\underline{r}_1$ and similarly the true value of $\underline{R}_2$ is the vectorial sum of the assumed value of $\underline{R}_2$ and $\underline{r}_2$. Thus if $\underline{r}_2 = \underline{r}_1$, then the true value of $\underline{R}_2 - \underline{R}_1$ is equal and parallel to its assumed value and $\Delta\nu_d = 0$. Components of $\underline{r}_2 - \underline{r}_1$ along the direction of $\underline{\omega}$ and $\hat{\underline{l}}$ do not contribute to $\Delta\nu_d$. The direction normal to $\underline{\omega}$ and $\hat{\underline{l}}$ lies in the equatorial plane and along the radius vector 90° west of the sub-source point, defined in Chapter 7, when the declination of the source is positive. Thus $\Delta\nu_d$ is independent of the quantities $\underline{R}_1$, $\underline{R}_2$ and of $\underline{R}_2 - \underline{R}_1$, the vectorial separation of the observing stations. The value of $\Delta\nu_d$ is determined by the vectorial difference in the components of the errors in $\underline{R}_1$ and $\underline{R}_2$ along the direction defined by $\hat{\underline{l}} \times \underline{\omega}$.

The doppler difference frequencies of the observed correlation peaks were found to differ from the corresponding predicted frequencies. The period of coherent integration, t, selected for data reduction was 10 seconds, and the observed doppler difference frequencies could be read to ±.03 Hz. Coherent integration of successive 100 sec blocks of data indicated that correlation peaks were generally spread over .04 Hz, due to short term instability in the rubidium frequency standards. The deviations from the predicted frequencies were significantly greater than the possible reading error.

Observations made in May 1968 were scheduled for a period when the doppler difference frequency for each source approached its maximum value, as the reduction process is simplified when the doppler differential frequency is close to its stationary value. As a result, observations were made when the ground track of each source was passing through or near the same fixed longitude (see figure 7.2), except for 3C 345, the northernmost source. In this latter case, the source did not attain a satisfactory elevation from DSS 42, the southern station, until the doppler difference frequency was well past its stationary value. The deviations of the observed doppler difference frequencies from the predicted values, which we shall call the offsets, were grouped about a value of -0.40 Hz, including the offset for Pioneer VIII. The offset for 3C 345 however was not clearly defined as two correlation peaks appeared, both of which had small offsets.

The experiment carried out in November 1967 was also scheduled so that the doppler difference frequency for each source was close to its maximum value and again the offsets were grouped about -0.40 Hz after correction for the difference between the clock rates at the two stations. On this occasion 3C 345 was not observed with the 210 ft. antenna at DSS 42. However, three separate observations were made on 3C 273, the first, as the doppler difference frequency was approaching its stationary value, the second at the stationary value and finally when the frequency was decreasing from its stationary value.

Had the offset arisen from a gross error in the time at both stations, the offset would have reversed in sign between the first and third observations. However, the offsets for the three observations agreed to within ± 0.03 Hz.

As the result for Pioneer VIII was in agreement with the quasar offsets, the cause of these offsets was unlikely to be outside the solar system or indeed any further than the Pioneer spacecraft itself. The offsets could not have been due to a differential propagation of the radiation from the source through the solar plasma as the order of relative proximity to the sun of the lines of sight from the source to the respective stations for November, 1967 was reversed in May, 1968.

For the experiment on June 1969, sources were observed when the source elevations from the interferometer stations

were about their optimum value (see figure 7.5). In consequence, the ground tracks of the sources spanned some 50 degrees in longitude. The offset for each source is plotted against longitude of its ground track in figure 6.1. When these results are considered with the results of the earlier experiments, it can be seen from figures 7.2 and 7.5 that source declination cannot be primarily responsible for the offsets observed.

Other possible causes of the offsets that were investigated include refraction, tracking movement of the antenna, movement of the axis of the earth obtained from listed secular independent day numbers, rotation of the earth about the moon and sun, aberration etc. which are dealt with in section 3.2. Mechanical effects such as possible variation in the length of feed as the antenna rotated about its axes were also assessed. The maximum offset arising from the effects enumerated above was less than 0.1 Hz. Comparison of station timing and frequency standards are dealt with in Chapter 4.

The offsets for the observations in June, 1969 are plotted against longitude of the ground track of the source in figure 6.1. The pattern of offset values was first considered to have arisen from an error in the assumed value of one or more of the astronomical or geodetic constants used in data reduction. The offsets for the observed correlation peaks lie between the values +0.3 Hz and -0.8 Hz.

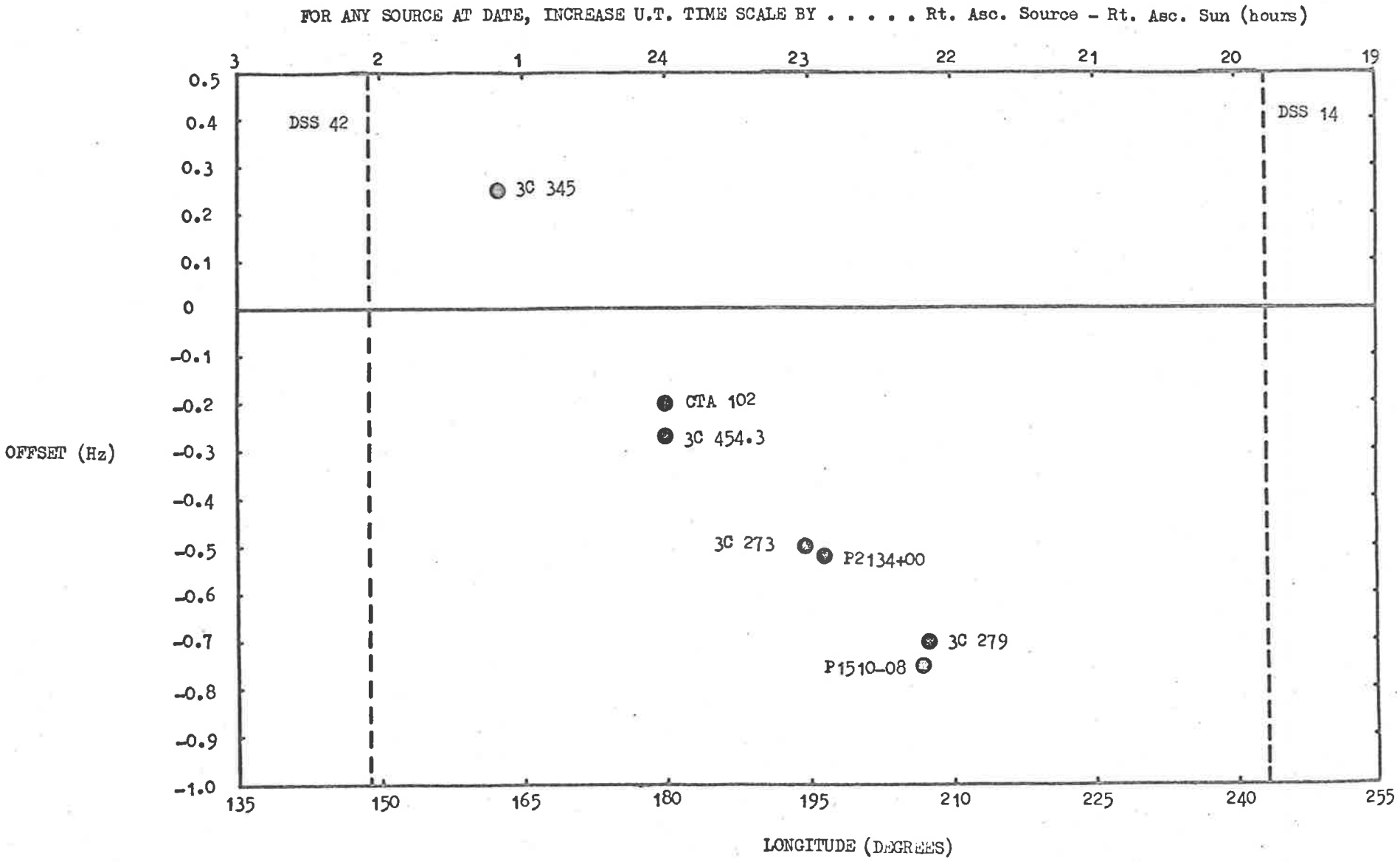

FIGURE 6.1. OFFSET PATTERN FOR SOURCES OBSERVED DAY 160, 1969 (SEE FIGURE 7.2).

FIGURE 6.1 OFFSET PATTERN FOR SOURCES OBSERVED DAY 160, 1969 (SEE FIGURE 7.2).

6.2 Effect of Errors in Common Parameters

The doppler difference frequencies for the observations made by DSS 42 and DSS 14 in May, 1968 were in general about 4200 Hz, whereas the corresponding frequencies for the observations made by DSS 41 and DSS 14 in November, 1967 lay about a value of 4700 Hz.

The order of magnitude of the fractional errors, $\Delta\nu/\nu$, in predicted doppler difference frequency displayed in figure 6.1 was therefore about 10^{-4}. The formula for the calculation of doppler difference frequency obtained in section 3.2.1 includes the quantities ω, the angular velocity of the earth about its axis, and c, the velocity of light. As these quantities are factors common to both stations the fractional error in the values chosen for ω and c would have been reflected in an equal fractional error in ν_D, the predicted doppler frequency. Neither the known secular variation in ω or the estimated error limit in the value of c (see Weast 1967-1968) exceeds a fractional variation of about 10^{-7} in order of magnitude. Short term variations in ω may however exceed this value.

Had the observed offsets been due primarily to either ω or c, the offsets for the observations on 3C 273 and 3C 279 made with the DSS 41/DSS 14 pair in November, 1967 would have exceeded those made with the DSS 42/DSS 14 pair in May, 1968 and June, 1969.

6.3 Geodetic Data

The reference frames for the geodetic coordinates of the stations were discussed in Chapter 3. The station longitudes, geodetic latitudes, and height above sea level with respect to the reference ellipsoid, were obtained from satellite observations and provided by the Jet Propulsion Laboratory of the California Institute of Technology. The coordinates were converted to the X, Y and Z frame of reference described in Chapter 3 and used to calculate the relative time displacement (see section 4.1), the local hour angle of the source from each station and the distance of the station from the axis of the earth. The axis of rotation of the earth was assumed to coincide with the Z axis of the reference ellipsoid.

The shape of the offset curve of figure 6.1 conforms with the offset pattern that would arise from an error either in local hour angle or in axial distance. As the two stations in the June 1969 experiment are close to 90 degrees apart in longitude, the affect of an error in the local hour angle from either station, appearing in the argument of the sine term is difficult to distinguish from the affect on ν_D of an error in the axial distance of the complementary station.

$$\text{If} \quad \nu_D = K*\cos(DECQ)(FREQ1*AX1*\sin(DLNG31) - FREQ2*AX2*\sin(DLNG32))$$

$$\frac{d\nu_D}{d(AX1)} = K*\cos(DECQ)*FREQ1*\sin(DLNG31) \propto \sin(DLNG31)$$

$$\frac{d\nu_D}{d\ (DLNG31)} = K*\cos(DECQ)*FREQ1*\cos(DLNG31) \propto \cos(DLNG31)$$

$$\frac{d\nu_D}{d(AX2)} \simeq \frac{d\nu_D}{d(DLNG31)}$$

as FREQ1 ≃ FREQ2

and SIN(DLNG32) ≃ cos(DLNG31).

Similarly,

$$\frac{d\nu_D}{d(AX1)} \simeq \frac{d\nu_D}{d(DLNG32)}$$

where the symbols retain the definitions of section 3.2.1.

Thus it is difficult to separate the errors in station positions related as above. However it may be seen from figure 6.1 that the offset is negative most of the time and has a value of about -0.40 when the doppler difference frequency reaches its maximum value. Such an offset pattern would arise if the primary source of error lay in the value assumed for the DSS 14 station longitude or for the DSS 42 axial distance. The offset curve rises to positive values which cannot be ascribed to the presence of either or both such errors. The positive or lesser effect could arise from an error in the assumed value for the DSS 42 station longitude or for the DSS 14 axial distance. Thereis however some

constraint on the possible combination of errors. If the offsets were due purely to errors in the longitudes of the two stations, the errors though differing in magnitude would be of the same sense. The effect on ν_D would be precisely that for a timing error equivalent to the lesser error in longitude plus an affect due to the difference between the two errors. The possibility of a timing error common to both stations, an error in the right ascension of the mean sum or the right ascension of all sources was considered in section 6.1 and ruled out as the primary source of error on the basis of three consecutive observations on 3C 273 in November, 1967. Further evidence is provided by the fact that the offset curve of figure 6.1 does not cross the zero line at or near the stationary value of ν_D. Consequently the error in one of the assumed station longitudes, that of DSS 42, is negligible in the present context.

A computer programme was written to calculate the effect of varying the station longitudes and axial distances on the pattern of offsets. The four quantities were made to vary in steps of 0.002° and 0.2 km respectively over a range of about $\pm\ 0.02^{\circ}$ and $\pm$ 2.0 km about their assumed value. It was found that for an offset curve lying between $\pm$ 0.10 Hz, at least one of the station coordinates was in error and that the maximum correction required was about 1 km in axial distance or an equivalent shift in longitude.

The investigation was not carried further because, for

a pair of stations separated in longitude by 94°, there is an essential difficulty in separating the errors in station coordinates for offsets that were only correct to ± 0.1 Hz. An experiment designed for geodetic purposes would have included an observation of 3C 345 west of DSS 42 as the effect of an error in the longitude of this station would have reversed as the source ground track crossed the longitude of the station.

A comparison between the geodetic systems of Australia and of the U.S.A. would be more easily obtained from observations made by the DSS 41/DSS 14 pair. These stations are 107 degrees apart in longitude and the affect of errors in the co-ordinates of the two stations are more readily separated than for the DSS 42/DSS 14 pair. The observations would be scheduled to cover the widest possible range in local hour angle including the local meridian at each station where possible. Offsets could be determined to within ± 0.01 Hz so that accuracies of ± 20 metres would be achieved. Observation of a spacecraft similar to the Pioneer VIII spacecraft in transmission power and in distance would be very suitable.

Determinations of accurate station positions would allow accurate redeterminations of source positions. An accuracy approaching 1 second of arc in local hour angle or in declination would be possible for an offset reading accuracy of ± 0.01 Hz. These accuracies would be easily achievable if hydrogen masers were substituted for the present rubidium frequency standards at the Deep Space Stations.

6.4 Residual Offsets After Correction

Station co-ordinates obtained by the application of doppler tracking techniques using individual stations were very recently supplied by the Jet Propulsion Laboratory following an enquiry based on the above considerations. This section has therefore been added in a posteriori fashion after the final draft of this work. The main correction was that for the longitude of DSS 14, amounting to ~0.011 degrees or some 700 metres, well outside the assumed uncertainty of the value previously supplied. The correction to the longitude of DSS 42 however was only ~0.001 and in the opposite sense. The estimated value of the axial distance for DSS 42 was substantially unchanged but that for DSS 14 was reduced by ~150 metres.

Curve A in figure 6.2 describes the offset pattern corresponding to the corrected co-ordinates for stations DSS 42 and DSS 14. The degree of symmetry of the curve about the line representing zero offset suggests a common timing error or a corresponding error in the right ascension of all sources. The value of the offset at the extremes where it is most sensitive to timing or right ascension error indicates an error of 2 seconds. As the extent of this error was too great to be ascribed to station timing or the right ascension of the mean sun, the 1950.0 position of the sources were precessed using a computer precession programme compiled earlier in the investigation for the purpose of correctly pointing the antennae during each observation, rather than

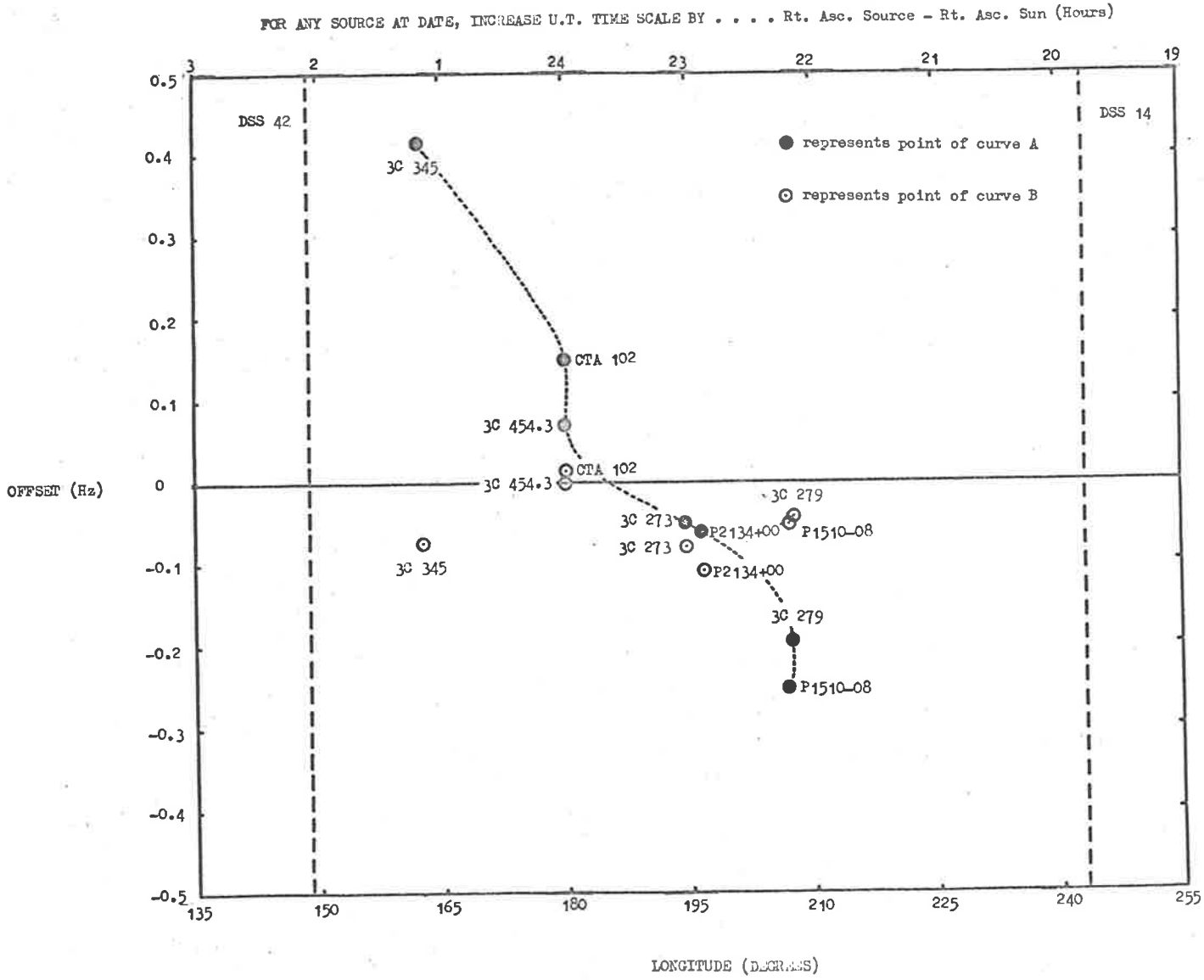

FIGURE 6.2 CURVE A REPRESENTS THE OFFSET PATTERN FOR SOURCES OBSERVED ON DAY 160 1969 AFTER CORRECTIONS FOR STATION LONGITUDES (SEE SECTION 6.4) HAVE BEEN APPLIED. CURVE B SHOWS THE EFFECT OF USING THE LOCAL PRECESSION COMPUTER PROGRAMME TO CALCULATE THE OFFSETS.

FIGURE 6.2 CURVE A REPRESENTS THE OFFSET PATTERN FOR SOURCES OBSERVED ON DAY 160 1969 AFTER CORRECTIONS FOR STATION LONGITUDES (SEE SECTION 6.4) HAVE BEEN APPLIED. CURVE B SHOWS THE EFFECT OF USING THE LOCAL PRECESSION COMPUTER PROGRAMME TO CALCULATE THE OFFSETS.

using precessed positions that had been supplied. The resulting offset pattern shown as curve B in figure 6.2 suggests that the precessed positions obtained using the local programme were the more accurate.

The source positions at 1950.0 were obtained from the Parkes Catalogue of Radio Sources for the declination zone + 20° to - 90°, and from "Positions for 3C Revised Radio Sources" published by Fomalont, Wyndham and Bartlett 1967, except that for P2134 + 004 which is given by Shimmins et al 1968.

The r.m.s. errors for positions from the Parkes Catalogue are typically ±10" and for the Owens Valley determinations by Formalont et al the estimated error in right ascension is given as ± 0.2^s/cosine (Declination) = 3"/Cosine (Declination), and ± 6"/Cosine (elevation) for measurement of source declination. These errors could account for the residual offsets of curve B in figure 6.2 but it is possible that the position of the object identified as 3C 345 by the 400 ft. interferometer of Fomalont et al does not correspond with the position of the unresolved component associated with 3C 345, seen by the trans-Pacific interferometer.

In the recorded discussion following a presentation of a technique for position determinations for radio astronomy by B. G. Clark 1967, Luyten remarked that Burbridge had found a change in the red shift in 3C 345 corresponding to a change

in radial velocity of 4000 km/sec and reported that Campbell had suggested that this might be due to increased emission from a different part of the quasar and that one might detect the shift in the centre of the optical emission. Similar considerations may well apply equally to any radio source and its component observed across a trans-Pacific baseline. If the offset were entirely due to this effect, the separation of the active component from the main source is roughly 8". The declination of 3C 345 places it outside the zone where source structure can be studied by occultation.

The estimated error for the right ascension of P2134 is $\pm$ 2^{s}.0 and 20" in declination. The relatively large uncertainties in source position easily account for the offset for P2134 shown in curve B.

The position for 3C 273 at 1950.0 obtained from the Parkes Catalogue corresponds to the optical object associated with the source, which is within 2" of the position of the B radio component obtained by occultation of the source. The separation between the A and B components is 19".5. These positions have been obtained to accuracies of better than 1". The established errors barely account for the observed offset shown on curve B. As the angular diameter of the A component is 2" and that of the B component is 0".5 they would be easily resolved across the trans-Pacific baseline. The correlations observed for this source are due to components of angular diameter $\leq$ 0°.001. These components are identified in Chapter 8. Some weak evidence is provided

here in support of our later finding that the unresolved component of 3C 273 does not correspond to the B component of the source.

These considerations on the sources for which the largest offsets were obtained are of a speculative nature and are presented here as an indication of the value of stable frequency standards such as the hydrogen maser and of accurate station positions, to astrophysical observations. The effect of a frequency standard of increased stability on the accuracy of geodetic measurements has already been discussed. When hydrogen maser frequency standards are available the higher order effects contributing to the predicted doppler difference frequency as discussed in section 3.2 must be included in calculating the offsets for each source.

There are three sources of error remaining, any one of which may be primarily responsible for or may contribute significantly to the offsets which determine curve B in figure 6.2. These are:

(1) Values for the 1950.0 position of the sources and and assumption that positions obtained for the source with apertures of no more than 400' correspond with the position of components which are unresolved across the trans-Pacific baseline.

(2) The precession programme.

(3) Station positions.

Statistical errors in the source position for 1950.0

will result in a random scatter of the source offsets about a value of zero. Systematic errors however will result in a pattern. To check the position of a source it should be tracked when its sub-source point is close to the longitude at which the doppler difference frequency is stationary and as long before and after reaching this point as possible. An error in the declination of a source can be easily distinguished from an error in right ascension. The affect of a declination error is to reduce the absolute value of the offset of the source as the sub-source point approaches a stationary value for the doppler difference frequency and thereafter the change in the value of the offset reverses in direction so that the sign of the offset does not alter. However, if the right ascension alone is in error, the scalar value of the offset reduces to zero about the time the sub-source point crosses the longitude at which the doppler difference frequency is a maximum. The offset will then reverse in sign. Thus a discrepancy between the position of the component and that of the main source observed at "zero baseline" can be recognised and measured provided all other errors have a significantly smaller effect on offset values.

6.4.1 Assessment of Station Position Accuracy

The offset values shown as curve B of figure 6.2 do not appear to have been derived from a random process. However, as the total population of offset values comprises only seven points, no conclusion can be drawn about the shape of

the curve.

The main sources of error which contribute to a scatter in the value of the apparent doppler difference frequencies are reading error and excrusions of the rubidium frequency standard. For the interferometer experiments the maximum composite error could be as high as ± 0.06 Hz.

The co-ordinates of DSS 42 and DSS 14 were varied about the values obtained from single station doppler observations, and station co-ordinates for which all offsets were less than ± 0.06 Hz were studied. The solution which most closely agreed with the assumed values, required no change to either co-ordinate of DSS 42 or to the longitude of DSS 14. The value thus obtained for the axial distance of DSS 14 however was ~ 150 metres less than the assumed values.

There were no solutions for the co-ordinates of the stations when the limit on the offset values was reduced to < 0.056 Hz. This means that at least one offset value is in error by ≥ 0.056 Hz or that there remains some residual effect due to one or more of the three sources of error listed in this section.

The substitution of a hydrogen maser for the present rubidium standard should reduce the composite random error in the apparent offset values to well within ± 0.01 Hz. Offsets outside this range would be due to errors in source co-ordinates and station co-ordinates. Errors in source co-ordinates may be isolated by viewing the source under various geometrical configurations as its sub-source point

travels across the doppler difference pattern shown in figure 7.5 and discussed in this section. An unambiguous solution for the co-ordinates of interferometer stations to an accuracy of better than 20 metres should then be possible.

CHAPTER 7.

EXPERIMENTAL RESULTS

The results of three interferometer experiments which took place on the 2nd/3rd November, 1967 the 30th May, 1968 and on the 9th June, 1969 are presented in this chapter. Sources selected for observation are each listed in table 6.1 against their total intensities measured at 2650 MHz, and their angular diameters derived from scintillation measurements as discussed in section 3.4. The values of red shift listed in table 7.1 are taken from Burbridge and Burbridge, 1969, the value of source intensity at 2650 MHz, and the class of the source are those appearing in the Parkes Catalogue of Radio Sources and the angular size determinations were made by Gardner, Morris and Whiteoak, 1969.

The observing stations and their system temperatures at zenith are listed in table 7.2 against each epoch.

The value of the correlated flux density from each source observed by DSS 14 and DSS 11 on day 151, 1968 across a Californian baseline of ~4.8 km is listed in table 7.6. The relationship between source intensity and $\rho^2 - \langle\rho^2\rangle$ (see Chapter 5) for this baseline is plotted in figure 7.1. The relationship thus provided a calibration curve which was used to interpret the results of all values of $\rho^2 - \langle\rho^2\rangle$ obtained from the trans-Pacific pair of stations, DSS 41/DSS 14 on day 306/307, 1967 or DSS 42/DSS 14 at the second and third epoch

(see table 7.2), in terms of the intensity of the unresolved component after a scale factor for that epoch had been applied.

$$I(\text{unresolved}) = I(y) \text{ as given by figure 7.1}$$

$$\text{where} \qquad y = \left\{ \rho^2 - \langle \rho^2 \rangle \right\} * S$$

and the scale factor S is given by

$$\left(\frac{T_{SYS}(A)_E * T_{SYS}(14)_E}{T_{SYS}(11) * T_{SYS}(14)} \right)$$

where

$T_{SYS}(A)_E$ is the system temperature at the Australian station at epoch

$T_{SYS}(14)_E$ is the system temperature at DSS 14 at epoch

$T_{SYS}(11)$ is the system temperature at DSS 11 on day 151, 1968

and $T_{SYS}(14)$ is the system temperature at DSS 14 on day 151, 1968,

relates the values of $\rho^2 - \langle \rho^2 \rangle$ obtained using a trans-Pacific pair to the values of $\rho^2 - \langle \rho^2 \rangle$ obtained across the Californian baseline on day 151, 1968. As sources were in general observed at elevations between 20° and 40°, the system temperatures at zenith listed in table 7.2 are incremented by 5°K in calculating the scale factor.

The techniques employed in the measurement of difference between the time standards at each station as well as the experimental controls used to check the proper functioning of the interferometer system have been dealt with in Chapter 4. The epoch code listed against the corresponding date is

used in the discussion that follows in Chapter 8 to denote the respective epoch.

Tables 7.3 through to 7.6 list the results of all observations for the three experiments against the geometrical parameters defining the conditions of observation. The intensities of source components listed in tables 7.3, 7.4 and 7.5 will be reconsidered in Chapter 8, where evidence for secular variation in the strength of the unresolved component of several sources will be presented. The orientation of the dimension of the source observed is measured from the projection of the earth's spin vector in the plane normal to the line-of-sight to the source. The sense in which the angle is measured from the projection of the earth's spin vector is anti-clockwise about the direction to the source.

The angle between the baseline and the line-of-sight to the source determines the effective resolving power of that baseline and appears in the tables of results. Resolving power, RP, is here defined as

$$RP = \left\{ \pi \, B(\lambda) \right\}^{-1}$$

where $B(\lambda)$ is the effective baseline distance in wavelength units and appears in the fifth column of tables 7.3 through to 7.6. The error quoted against each calculated component intensity corresponds to 1 standard deviation of statistical noise. An account of statistical noise appears in Chapter 5.

The elevation contours in these figures define the common sky for the trans-Pacific pair of stations after correction is made to the Universal Time scale across the top of the figures for each source and each epoch. The correction is made by subtracting the right ascension of the sun from the right ascension of the source and then incrementing the time scale by the result. Source latitude is plotted vertically and longitude east of Greenwich appears across the bottom of the figures.

The intersection of the line-of-sight from the centre of the earth to the source and the surface of the earth describes a "ground track" as the earth rotates. The ground tracks of sources observed during the second experiment, which took place on day 151, 1968, are shown against contours of doppler difference frequency in figure 7.2, against contours of resolving power in figure 7.3, and against contours of orientation of the measured dimension in figure 7.4. The orientation of the measured dimension is shown to lie between about 35° to about 50° for all sources observed with the DSS 42/DSS 14 station pair. However, the NASA-JPL Deep Space Network includes DSS 51, a station near Johannesburg in South Africa and another, DSS 61, near Madrid in Spain. The common sky defined by the elevation contours for the DSS 51/DSS 41 station pair would allow roughly two hours of observing time at elevations above 20° from both stations for sources south of the celestial equator. The orientation of the measured dimension for the DSS 51/DSS 41 station pair is around 80° to 120°.

It is expected that the trans-Pacific interferometer experiments will be complemented shortly with experiments using the DSS 51/DSS 41 station pair and the source list will include several of these observed by the DSS 42/DSS 14 station pair. The South Africa-Australia observations will follow the Australia-California observations within a space of about two months in order to obtain information on the structure of the respective sources. Figure 7.5 shows the ground tracks of sources observed in the third experiment on day 160, 1969, for which correlation peaks were observed, against contours of doppler difference frequency. Formulae for the calculation of doppler difference frequency, resolution and orientation of the measured dimension are presented in section 3.2.9.

The doppler difference frequency at which the tabulated correlation peaks, for the trans-Pacific experiment appeared, differed from the predicted value between the limits of -0.75 Hz for P1510-08 and +0.25 Hz for 3C 345. The pattern of these differences between the predicted and actual frequencies and the primary cause is discussed in Chapter 6.

The results of the first and second interferometer experiments suggested that sources for which spectral variations had been observed by Dent, 1965, 1968, Epstein 1965, Low 1965, Pauliny-Toth and Kellermann 1966, Kellermann and Pauliny-Toth 1968a, 1968b were most likely to have unresolved components and the source list for the third experiment was revised to include this class of sources as well as a number of others

satisfying the selection criteria of section 3.4.1 but which had been outside the restrictions of our previous right ascension window.

The interpretation of the several data in tables 7.3 through 7.5 will be discussed in the following chapter.

Source	Z_{em}	Z_{abs}	Total Intensity at 2650 MHz (f.u.)	Scintillation (min. of arc)	Class	Estimated Magnitude
P1055+01			3.5	< 0.0008	QSO	18
P1116+12	2.118	1.947	1.8	< 0.002	QSO	19.3
P1148-00	1.982		2.7	< 0.0008	QSO	17.6
3C273	0.158		26 (2) (B component)	< 0.0003	QSO	13
3C279	0.538		11.8	≤ 0.0003	QSO	17.8
P1345+12			3.6	< 0.003	SO	17.0
3C298	1.439	1.419	2.7	0.6I<0.003	QSO	16.8
P1453-10	0.938 (1.)		2.6	< 0.3	QSO	17.5
P1510-08	0.361	0.351	3.1	< 0.0008	QSO	17.8
P1603+00			1.4	< 0.3	E4	16.5
3C345	0.595		5.7 (3) (2841 MHz)		QSO	
NRAO 530			4.9	< 0.3	III	
P2134+00	1.94		7.6 (4)		QSO	
CTA 102	1.037		5.6		QSO	17.3
3C454.3	0.859		10.5	< 0.0004	QSO	

TABLE 7.1

REFS:- (1) Moffet A.T., Schmidt M., Slater C.H., and Thompson A.R. - Astrophysical J. 148 p283 1967.
(2) Hazard C., Gulkis S., Bray A.D., - Nature 212 pp 461-463, October 29, 1966.
(3) Howard W.E., and Maran S.P. - Astrophysical Journal, Supplement Series, No. 93 Vol. X p 132 March 1965.
(4) Shimmins A.J., Searle L., Andrew B.H., Brandie G.W. - Astrophysical Letters 1 pp 167-169 1968.

Epoch Day/Year	Epoch Code	Australian Station 85' Antenna		Californian Station 210' Antenna		Californian Station 85' Antenna	
		Station	System Temp. at Zenith (^{o}K)	Station	System Temp. at Zenith (^{o}K)	Station	System Temp. at Zenith (^{o}K)
306/1967 307/1967	1	DSS 41	45	DSS 14	28	DSS 12	45
151/1968	2	DSS 42	42	DSS 14	18	DSS 11	42
160/1969	3	DSS 42	40	DSS 14	22		

TABLE 7.2 SYSTEM TEMPERATURES AT ZENITH

Source	$\rho^2 - \langle\rho^2\rangle$ (10^{-6})	I (f.u.)	Baseline (km)	Baseline ($10^6 \lambda$)	Orientation (deg.)	Elevation of line of sight (deg.)	Angle between Line of Sight & Baseline (deg.)	Resolution (10^3sec. of arc)
3C273	12.47	$1.96 \pm .41$	11009	84.4	50.7	29/32	88.5	.778
3C279	10.82	$1.83 \pm .38$	10994	84.3	50.8	33/26	86.6	.779
P1055+01	6.088	$1.37 \pm .84$	11012	84.4	50.7	31/29	89.2	.778
P1148-00	4.846	$1.22 \pm .78$	10990	84.3	50.6	26/34	86.3	.780
3C273	15.38	$2.18 \pm .32$	10940	83.9	50.7	23/37	83.4	.783
3C273	10.48	$1.82 \pm .40$	11003	84.4	50.7	28/33	87.5	.778
3C273	10.15	$1.78 \pm .40$	11009	84.4	50.6	32/29	88.4	.778
3C279	6.724	$1.43 \pm .86$	10929	83.8	51.0	37/23	83.9	.784
P1345+12	7.042	$1.48 \pm .87$	10894	83.5	51.5	22/38	81.6	.786
3C298	6.850	$1.45 \pm .84$	10980	84.2	50.9	26/35	85.5	.780
P1453-10	5.888	$1.34 \pm .82$	10953	84.0	51.1	35/23	84.0	.782
P1510-08	6.090	$1.37 \pm .83$	10907	83.6	51.3	38/22	82.0	.785

TABLE 7.3 CORRELATED FLUX INTENSITIES OF SOURCES OBSERVED ACROSS THE PACIFIC FROM DSS 41 AND DSS 14, ON DAY 306/307 1967.

TABLE 7.3 CORRELATED FLUX INTENSITIES OF SOURCES OBSERVED ACROSS THE PACIFIC FROM DSS 41 AND DSS 14, ON DAY 306/307 1967.

Source	$\rho^2 - \langle\rho\rangle^2$ (10^{-6})	I (f.u.)	Baseline (km)	Baseline ($10^6 \lambda$)	Orientation (deg.)	Elevation of Line of Sight (deg.)	Angle between Line of Sight and Baseline (deg.)	Resolution (10^{-3} sec. of arc)
P1116+12	6.900	$1.31 \pm .40$	10220	78.3	47.5	19/49	75	.838
3C273 B component	10.49	$1.63 \pm .32$	10540	80.8	46	28/39	85	.813
3C273 B component	11.21	$1.67 \pm .32$	10580	81.1	46.1	32/36	88	.809
3C279	30.12	$2.78 \pm .18$	10530	80.7	46.3	40/28	84	.813
P1345+12	7.091	$1.33 \pm .84$	10500	80.5	46.5	26/40	82	.815
3C298	7.179	$1.35 \pm .84$	10570	81.0	46.1	30/37	87	.810
P1453-10	3.795	< mean error	10500	80.5	46.6	41/26	82	.816
P1510-08	11.00	$1.68 \pm .32$	10550	80.4	46.6	43/25	81	.819
P1603+00	9.191	$1.52 \pm .34$	10590	81.2	46.0	33/35	89	.809
NRAO 530	8.497	$1.45 \pm .99$	10490	80.4	46.6	41/25	82	.816
3C345	11.14 to 13.68	$1.68 \pm .30$ to $1.86 \pm .26$	10260	78.7	43.8	11/37	76	.834

TABLE 7.4 CORRELATED FLUX INTENSITIES OF SOURCES OBSERVED ACROSS THE PACIFIC FROM DSS 42 AND DSS 14, ON DAY 151, 1968.

TABLE 7.4 CORRELATED FLUX INTENSITIES OF SOURCES OBSERVED ACROSS THE PACIFIC FROM DSS 42 AND DSS 14, ON DAY 151, 1968.

Source	$\rho^2 - \langle\rho\rangle^2$ (10^{-6})	I (f.u.)	Baseline (km)	Baseline ($10^6 \lambda$)	Orientation (deg.)	Elevation of Line of Sight (deg.)	Angle between Line of Sight and Baseline (deg.)	Resolution (10^{-3} sec. of arc)
3C279	60.62	$4.02 \pm .12$	10563	81.0	45.1	29/37	86.1	.811
3C273	10.14	$1.64 \pm .34$	10587	81.2	46.0	34/34	89.5	.809
P1510-08	18.51	$2.21 \pm .25$	10585	81.2	45.1	32/34	89.3	.809
P1510-08	24.18	$2.54 \pm .22$	10581	81.1	45.7	35/31	88.0	.810
NRAO 530	8.730	$1.52 \pm .38$	10528	80.7	46.2	39/27	83.9	.813
3C345	17.12	$2.14 \pm .26$	10487	80.4	37.2	14/28	82.1	.817
P2134+00	21.20	$2.37 \pm .23$	10588	81.2	46.0	34/34	89.5	.809
P2134+00	27.3	$2.69 \pm .20$	10572	81.0	45.9	37/31	86.9	.810
CTA 102	11.23	$1.73 \pm .32$	10568	81.0	43.8	35/28	86.6	.811
3C454.3	194.2	$7.21 \pm .15$	10588	81.2	43.7	31/31	89.8	.809
P0237-23	8.717	$1.52 \pm .38$	10571	81.0	42.9	32/26	86.7	.810

TABLE 7.5 CORRELATED FLUX INTENSITIES OF SOURCES OBSERVED ACROSS THE PACIFIC FROM DSS 42 AND DSS 14, ON DAY 160, 1969.

TABLE 7.5 CORRELATED FLUX INTENSITIES OF SOURCES OBSERVED ACROSS THE PACIFIC FROM DSS 42 AND DSS 14, ON DAY 160, 1969.

Source	$\rho^2 - \langle\rho\rangle^2$ (10^{-6})	I (f.u.)	Baseline (km)	Baseline ($10^6\lambda$)	Orientation (deg.)	Elevation of line of Sight (deg.)	Angle between Line of sight & Baseline (deg.)	Resolution (10^3sec. of arc)
P1116+12	19.3	2.20±.23	4.76	36.5	132.2	49/49	83	1.80
3C273 B comp.	2500	25.5±.05	4.79	36.7	132.6	39/39	88	1.79
3C273 B comp.	2500	25.5±.05	4.77	36.6	132.6	36/36	84	1.80
3C279	462	10.8±.10	4.78	36.7	133.3	28/28	87	1.79
P1345+12	19.4	2.22±.23	4.64	35.6	131.2	40/40	75	1.85
3C298	40.8	3.21±.17	4.71	36.1	132.2	37/37	80	1.82
P1453-10	17.8	2.13±.14	4.79	36.7	132.9	26/26	87	1.79
P1510-08	48.6	3.51±.14	4.79	36.7	133.4	25/25	90	1.79
P1603+00	5.9	1.22±.78	4.78	36.6	132.7	35/35	86	1.79
NRAO 530	103	5.12±.12	4.77	36.6	132.6	25/25	85	1.80
3C345	137	5.82±.14	3.44	26.3	114.7	37/37	46	2.49

TABLE 7.6 CORRELATED FLUX INTENSITIES OF SOURCES OBSERVED ACROSS THE CALIFORNIAN BASELINE FROM DSS 14 AND DSS 11, ON DAY 151, 1968.

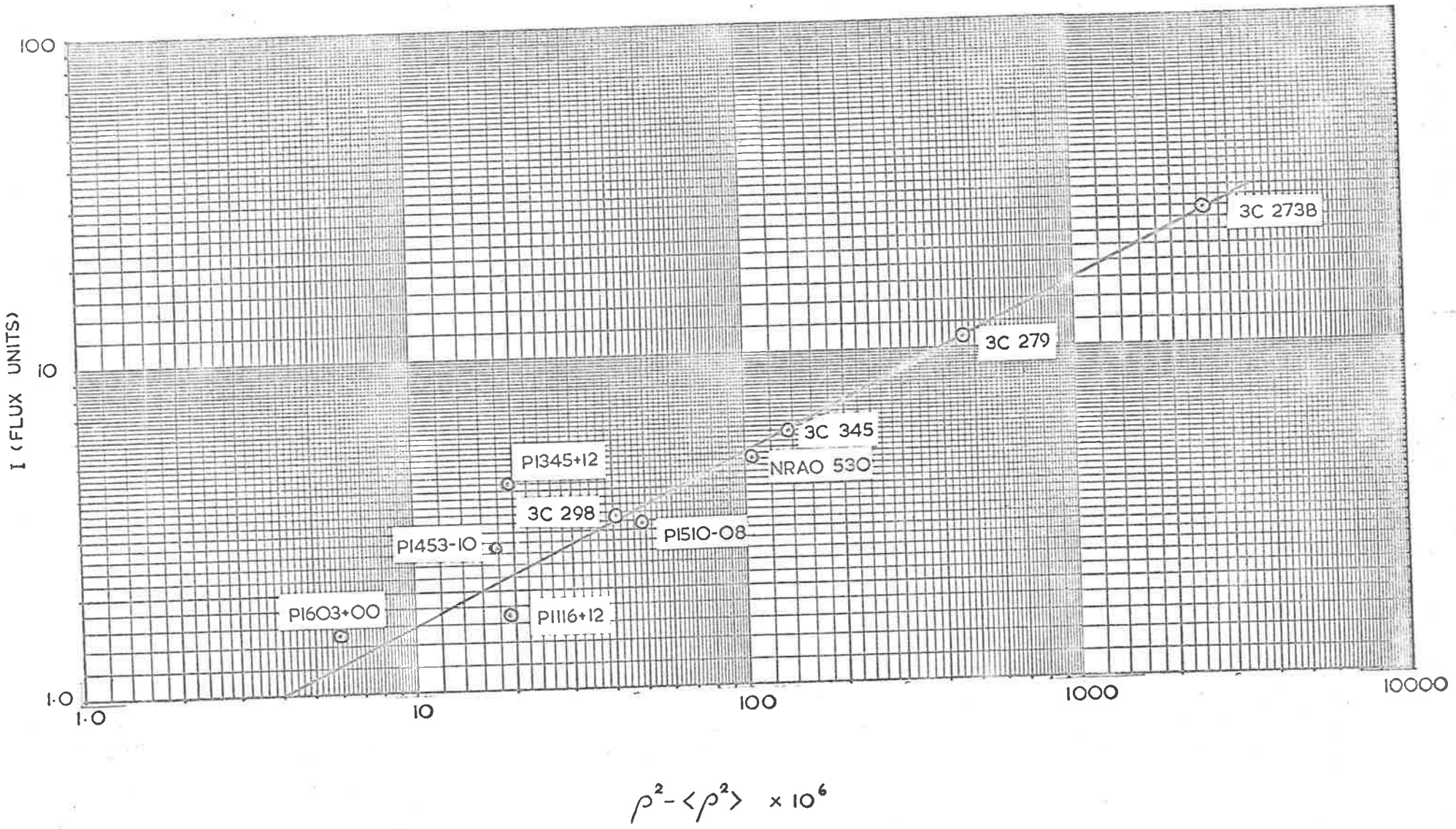

FIGURE 7.1 SHORT BASELINE CALIBRATION OBSERVATIONS WERE MADE ACROSS A CALIFORNIAN BASELINE USING DSS 14 AND DSS 11.

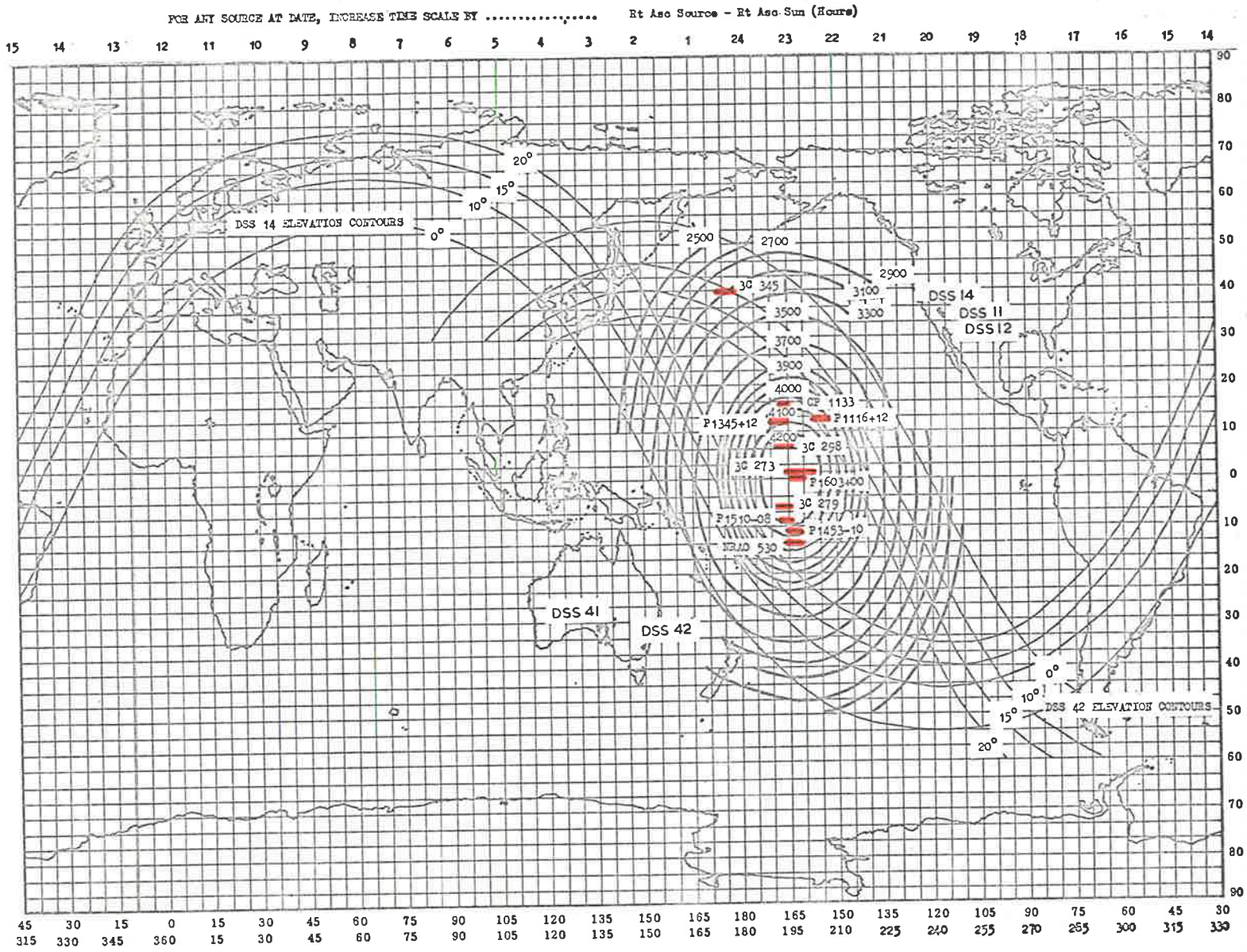

FIGURE 7.2 GROUND TRACKS OF SOURCES OBSERVED ACROSS THE TRANS-PACIFIC BASELINE ON DAY 151 1968 AGAINST CONTOURS OF DOPPLER DIFFERENCE FREQUENCY FOR DSS 42 AND DSS 14. THE FINE LINES REPRESENT ELEVATION CONTOURS.

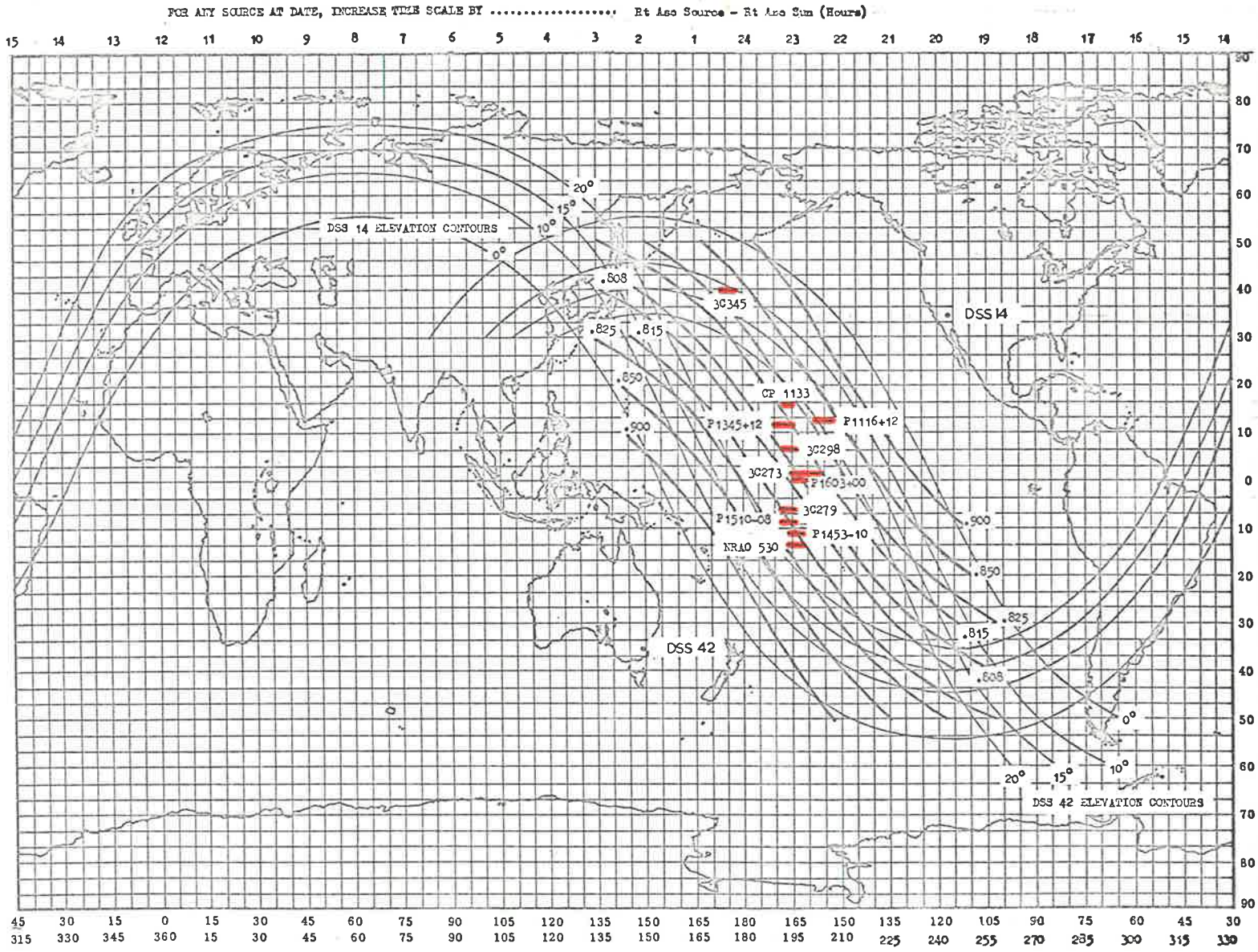

FIGURE 7.3 GROUND TRACKS OF SOURCES OBSERVED ACROSS THE TRANS-PACIFIC BASELINE ON DAY 151, 1968 AGAINST CONTOURS OF RESOLUTION FOR DSS 42 AND DSS 14. THE FINE LINES REPRESENT ELEVATION CONTOURS.

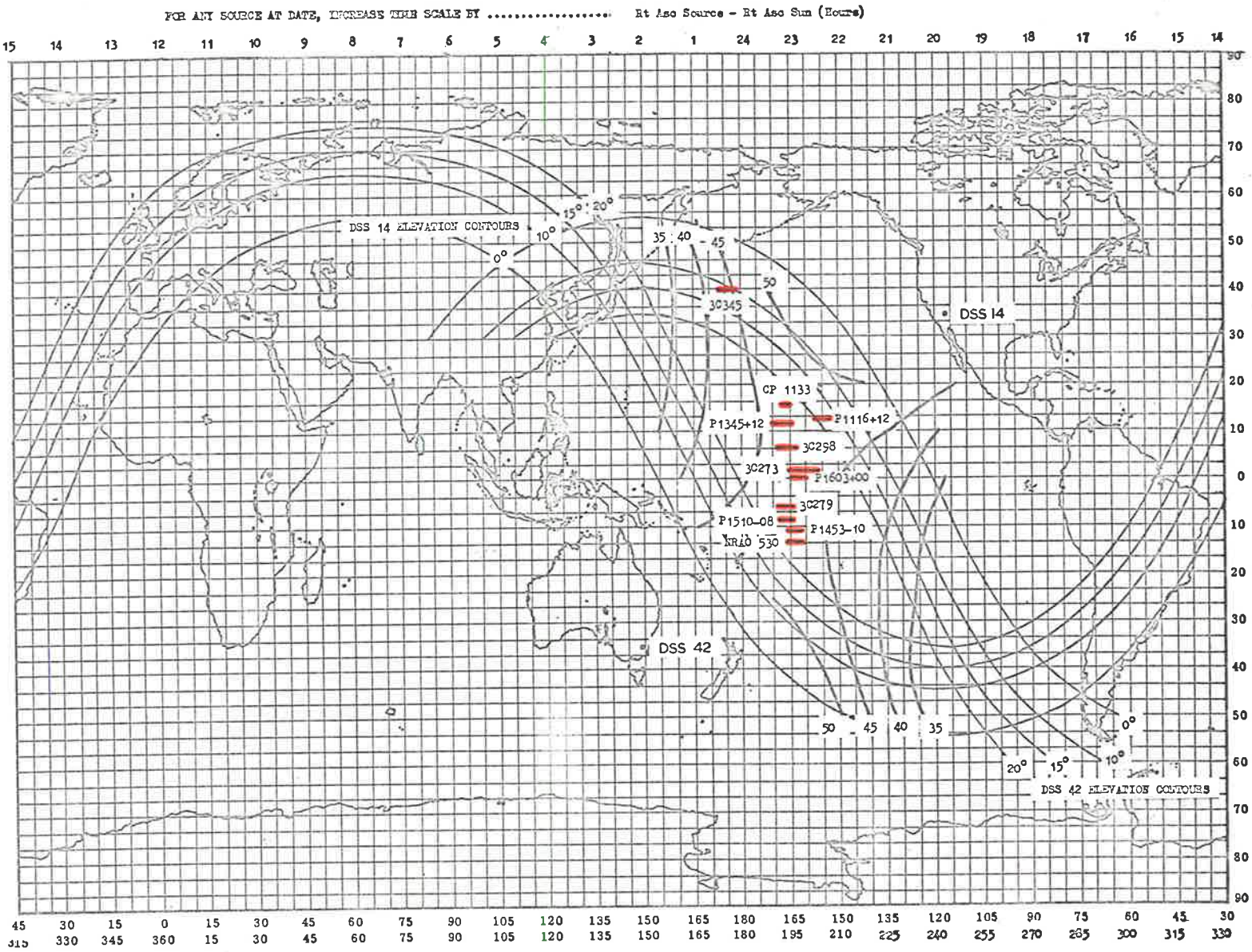

FIGURE 7.4 GROUND TRACKS OF SOURCES OBSERVED ACROSS THE TRANS-PACIFIC BASELINE ON DAY 151, 1968 AGAINST CONTOURS OF ORIENTATION OF THE MEASURED DIMENSION OF THE SOURCE WITH RESPECT TO THE AXIS OF THE EARTH. THE FINE LINES REPRESENT ELEVATION CONTOURS.

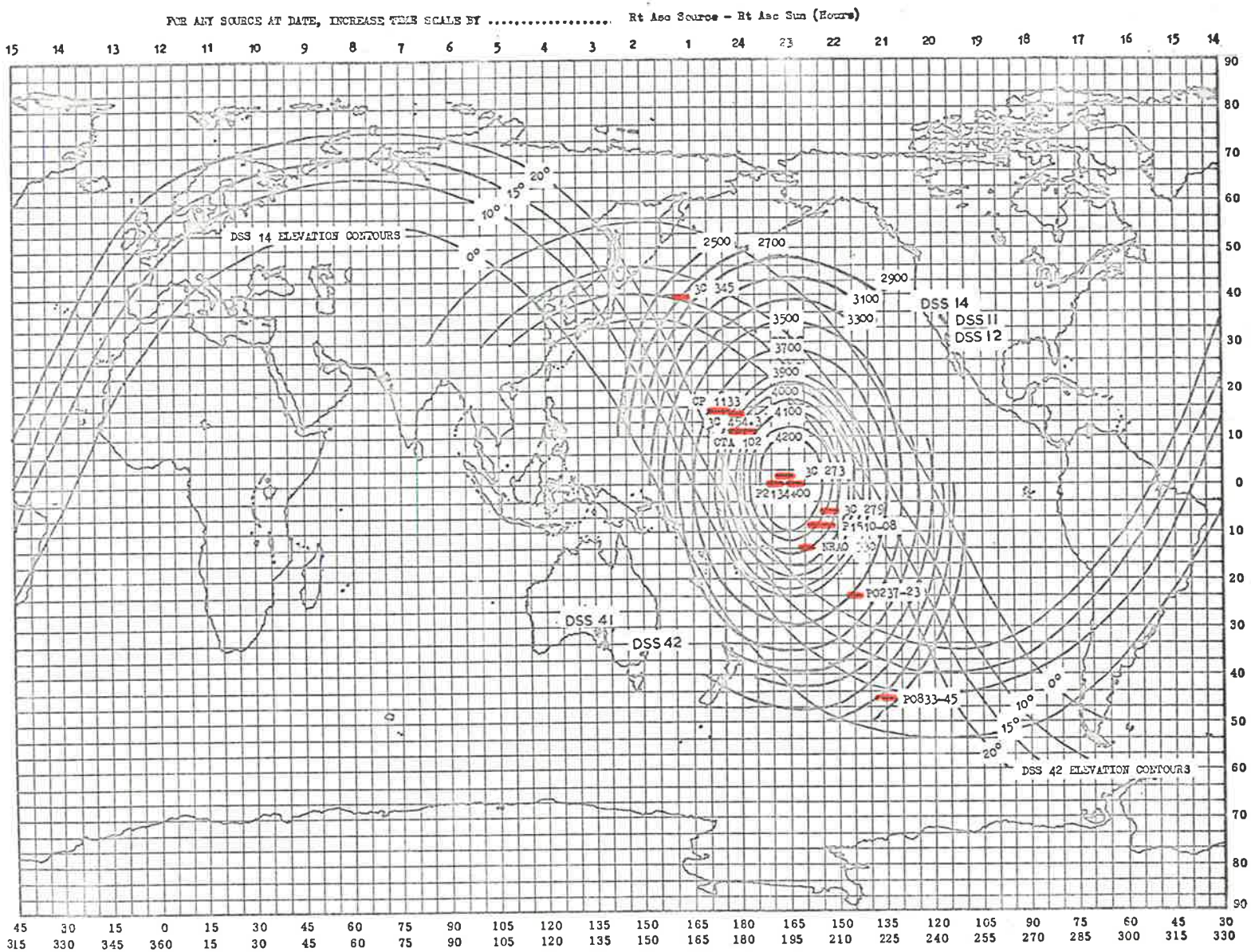

FIGURE 7.5 GROUND TRACKS OF SOURCES OBSERVED ACROSS THE TRANS-PACIFIC BASELINE ON DAY 160, 1969 AGAINST CONTOURS OF DOPPLER DIFFERENCE FREQUENCY FOR DSS 42 AND DSS 14. THE FINE LINES REPRESENT ELEVATION CONTOURS.

CHAPTER 8.

DISCUSSION OF RESULTS

Comparison of the results of the 1967 experiment with those of the 1968 experiment presented in tables 7.3 and 7.4 respectively, strengthened the view that there was a greater likelihood of finding unresolved components in those sources for which Kellermann and Pauliny-Toth 1965b, had reported some spectral variations. It was also apparent that the unresolved component in 3C 279 had increased markedly in intensity between November 1967 (see table 7.3) and May 1968, whereas the unresolved component in 3C 273 had probably decreased slightly over the same period. The intensity of the unresolved component in P1510-08 was weak at both epochs and the probable slight increase over that time was hidden in the relatively large statistical errors.

These sources, among others, were observed again in June 1969. 3C 279, 3C 273, P1510-08, P2134-+00, 3C 454.3 and CTA 102 were found to contain unresolved components whereas no significant correlation coefficients were obtained for NRAO 530 or for P 0237-23. NRAO 530 is a Type III source but P 0237-23 is a quasi-stellar object with an emission red shift of 2.228 and is listed in the Parkes catalogue as having an intensity of 5.3 flux units at 2650 MHz. Spectral variations have not been reported as yet for this source.

The results from the experiment of May 1968 were more

easily obtained than those for the previous epoch because the search for the correlation peak about the predicted doppler difference frequency was simplified by the appearance of a highly significant correlation peak for 3C 279, (about 7σ), at this second epoch, and by the observation of a Pioneer spacecraft as described in Chapter 4. Correlation peaks for other sources observed in 1968 and in 1967 were subsequently found at closely similar offsets from the predicted frequency by reducing 16 minutes of recorded data. There is some inherent selectivity in sources known as variables in that these were in fact sources seen in the previous few years to vary at frequencies higher than 2300 MHz and consequently at the first epoch, self-absorption of 13 cm radiation in those variable components was possibly still too great to allow highly significant correlation coefficients in November 1967 from their unresolved components. This did not apply to the variable component in 3C 273 which,however, was already almost completely resolved (see figure 8.2). The consequences of this finding are of prime importance and are discussed in section 8.3.

The observation of a Pioneer spacecraft during the 1968 experiment also greatly facilitated the reduction of data (see Chapter 4). The offset from the predicted doppler frequency at which the correlation peaks for Pioneer and for the unresolved celestial objects appear, indicated that the location of the observing stations with respect to the axis of the earth, determined from interferometer observations

differed from station locations obtained by single station optical observations on satellites and celestial sources and requiring a knowledge of the local vertical at each station. As the interferometer pair DSS 42 and DSS 14 for which calculations were made are separated by just over 90° and the offset frequency only determined to an accuracy of ~ ± 0.06 Hz it was not possible to avoid multiple solutions for the four position coordinates but results indicated minimum errors of some hundreds of metres in at least one of the stations (see Chapter 6). It was later found that the assumed position of DSS 14 was incorrect by several hundreds of meters. The use of DSS 41 and DSS 14 and the substitution of hydrogen masers for the rubidium frequency standard in an experiment designed primarily for geodetic purposes would yield important data of a geodetic nature as well as information on the degree of correspondence of the position of a nominal source and any unresolved component associated with that source.

The trans-Pacific baseline seems ideally suited to 13 cm observations on the secular variations of the unresolved components of quasi stellar sources. Statistical errors of the order of the observed variations would greatly reduce the value of any results and care has been taken to minimize statistical errors though this has marginally increased the intensity threshold of the system (see Chapter 4 and Chapter 5).

At each epoch multiple observations were taken on some of the sources where possible of tables 7.3, 7.4, 7.5 and 8.1. Four observations were made on 3C 273 during the first experiment and the degree of variation among the four results of the set was found to be consistent with the statistical errors quoted in the tables.

8.1 Secular Variations of the Components

In figure 8.2, the fringe amplitudes of the unresolved components of the sources 3C 279, 3C 273, P 1510-08 are compared against their total flux densities measured by G. D. Nicholson, for the three epochs of observation. Dr. Nicolson's observations were made at the NASA-JPL Deep Space Station 51 near Johannesburg in South Africa, at the same observing frequency, i.e. 2300 MHz. These results are discussed by Gubbay, Legg, Robertson, Ekers, Moffet, Seidel, 1969b (Appendix 3). The following discussion is an amplification of this earlier work.

8.1.1 3C 279

The trend towards increasing values of fringe amplitude of the unresolved component and of total flux density of the source, as shown in figure 8.2, are closely similar. The variation in the total flux density of the source may therefore be ascribed primarily to the unresolved component. Thus, the fringe amplitude has increased $2\frac{1}{2}$ times over a period of nineteen months, and the changes in fringe amplitude and in

		Day 306/307 1967	Day 151 1968	Day 160 1969
3C 279	Total	11.4	12.1	13.3
	Comp^{t}	1.64±0.29(2)	2.78±0.18	4.02±0.12
3C 273	Total	42.0	40.5	37.6
	Comp^{t}	1.94±0.18(4)	1.65±0.22(2)	1.64±0.34
P1510-08	Total	3.65	3.55	3.45
	Comp^{t}	1.37±.83	1.68±0.32	2.38±0.16(2)

TABLE 8.1

TABLES COMPARING HISTORIES OF FLUX DENSITIES OF UNRESOLVED COMPONENTS OF 3C 279, 3C 273 AND P1510-08 AGAINST TOTAL FLUX DENSITY FROM THE SOURCE FOR THE CORRESPONDING EPOCHS.

NO. IN BRACKETS ( ) REFER TO NO. OF RECORDINGS USED TO OBTAIN READINGS. FLUX DENSITIES ARE IN FLUX UNITS. ERROR LIMITS ON FLUX DENSITIES CORRESPONDING TO FRINGE AMPLITUDES ARE FOR 1 σ .
INFORMATION ON TOTAL FLUX DENSITIES RECEIVED FROM DR. G.D. NICOLSON. TOTAL FLUX DENSITIES ARE ON KELLERMANN SCALE AND ARE GOOD TO ±2% OR 0.1 FLUX UNIT (CONFUSION LIMIT FOR 85 FOOT DISH).

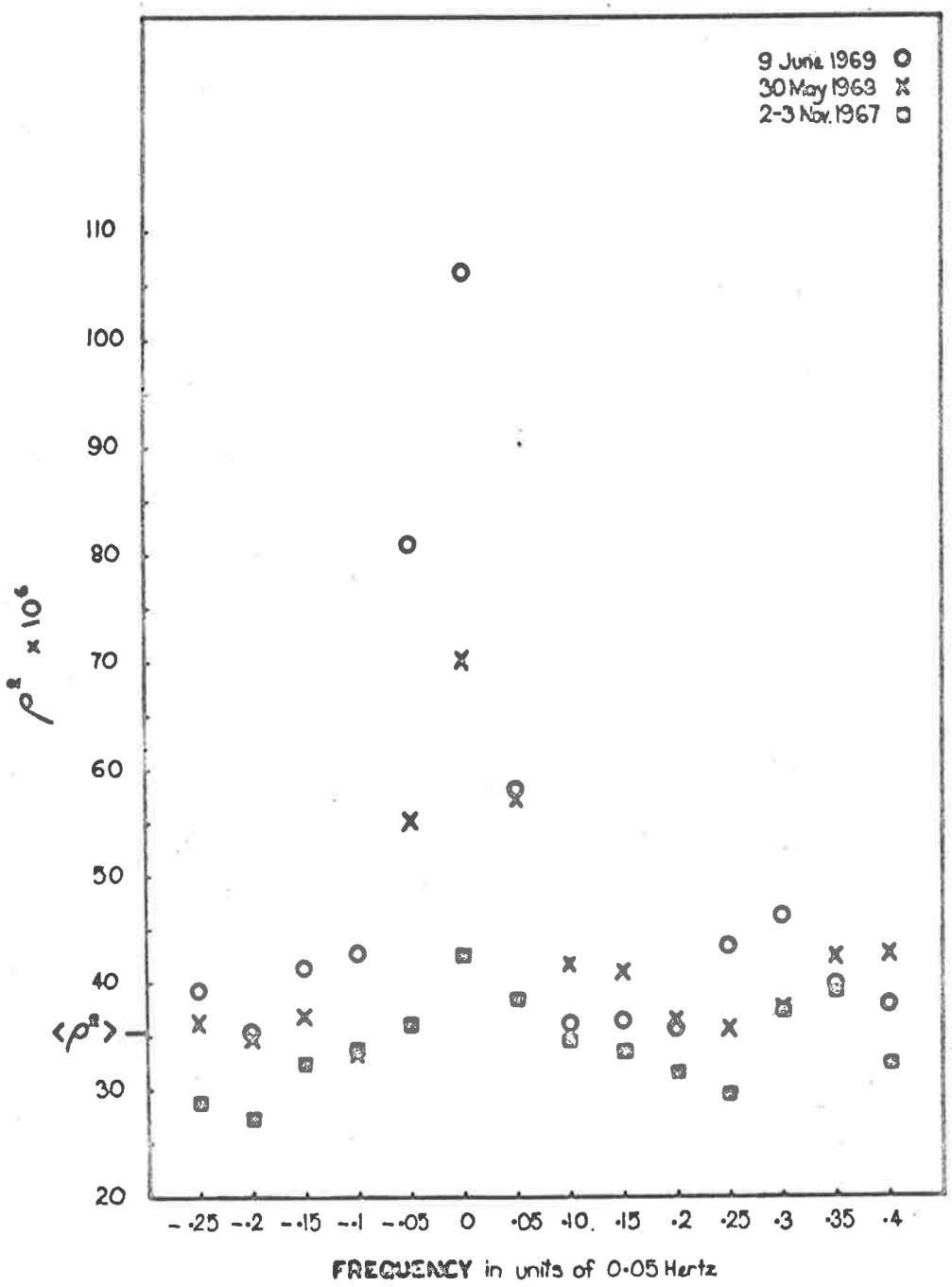

FIGURE 8.1 CURVES SHOWING THE VALUE OF THE SQUARE OF THE CORRELATION COEFFICIENT, ρ^2, AGAINST FRINGE FREQUENCY FOR 3C 279 AT THE THREE EPOCHS OF OBSERVATION. THE MEAN VALUE OF ρ^2 INDICATED ALONG THE ORDINATE WAS OBTAINED FROM A LARGE NUMBER OF RECORDS.

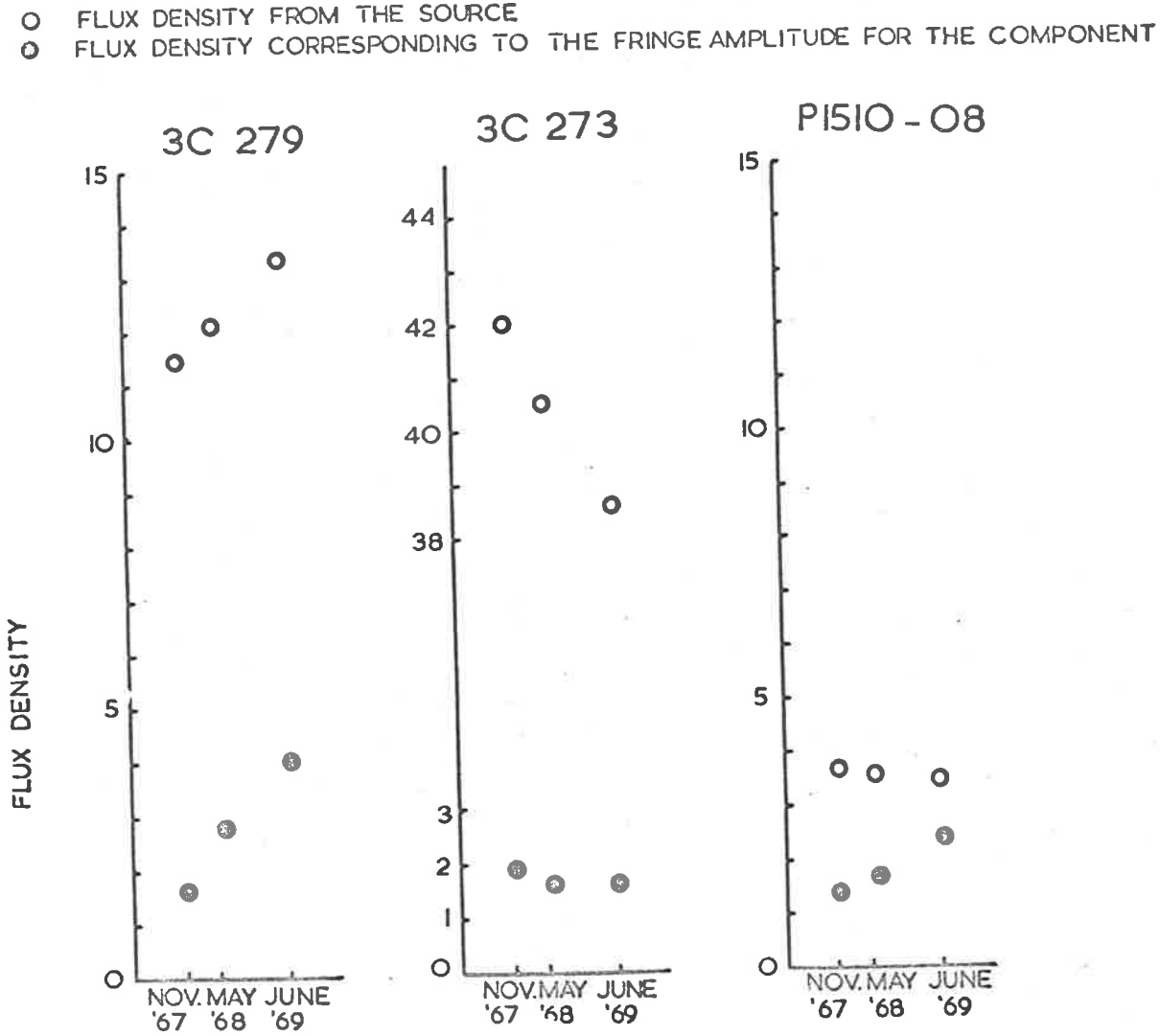

FIGURE 8.2 COMPARISON OF THE HISTORIES OF THE FLUX DENSITY FROM THREE SOURCES WITH THAT OF THEIR UNRESOLVED COMPONENTS AT 80 X 10^6 WAVELENGTHS.

FIGURE 8.2 COMPARISON OF THE HISTORIES OF THE FLUX DENSITY FROM THREE SOURCES WITH THAT OF THEIR UNRESOLVED COMPONENTS AT 80 X 10^6

flux density between the second and third epochs are equal. Note, however, that the rate of increase in fringe amplitude over the first 6 - 7 months is significantly greater than the rate of increase in flux density of the source over this period. Spectral observations on 3C 279 by Kellermann and Pauliny-Toth, 1968a indicate the existence of a component which decreased from 1964 to 1967. This decrease was followed by an increase at 11 cm corresponding to a sharp increase in flux density at shorter wavelengths. Pauliny-Toth and Kellermann, 1966 calculated the time of inception of the decreasing component, t_o, to be about 1956.0 and for the younger event seen as a sharp increase in 1966 at 2 cm, t_o ~ 1965.0. Interferometric observations by Kellermann et al. September 1968, at 6 cm and 18 cm across a trans-Atlantic baseline of 6319 km in January-February 1968 indicate that the angular diameter of the decreasing component was ~0".002 while the younger component was ~0".001. The decreasing component which is component C of Kellermann et al. September 1968, was thus fully resolved by the trans-Pacific baseline at the first epoch so that its reducing contribution to the flux density of the source between November, 1967 and May, 1968 did not affect the fringe amplitude for the unresolved component, the unresolved components seen with the Deep Space Network trans-Pacific interferometer being about 0.001 arcsec. The close correspondence between the increase in flux density and the fringe amplitude between the second and third epochs indicatesthat the change in flux density over this period is

due solely to variation in the young component, i.e. component D of Kellermann et al. September 1968 and that this component was less than 0.001 arcsec in June 1969, at which date the apparent age of the source was $4\frac{1}{2}$ years. At the red-shift distance of 3C 279 the source would be partially resolved if its apparent metric dimensions extended beyond 20 l.y. Rees 1967 demonstrated that if v is the velocity of expansion of a spherically symmetrical shell as seen by an observer at its centre, the source will appear to a remote observer to expand with an apparent transverse velocity βv, where $\beta = \left(1 - \frac{v^2}{c^2}\right)^{-\frac{1}{2}}$. Thus for component D of 3C 279, a value of the Lorentz factor, $\beta \leq 2$ is consistent with the observations. A value of β as distinct from a limit will be established once component D becomes resolved.

For a universe where $q_0 = 1$, the observed apparent angular diameter θ' is given by

$$\theta' = \theta (1 + z)^2$$

where θ is the apparent angular diameter of the source if the velocity of recession were zero and z is the red-shift of the source. For 3C 279, z=0.538 so that the metric diameter of the source in the reference frame of the source is reduced to 8.45 l.y. and hence the apparent extension of the source does not then exceed its equivalent light travel time of 9 l.y. Thus, the inferred age, the known red shift and the results of the observations reported here relating to the completely unresolved nature of component D of Kellermann

et al, in June 1969 are self consistent and explicable in terms of the source model in which an electron gas expands with its magnetic field as described by Van der Laan 1966.

8.1.2 3C 273

As shown in figure 8.2, the flux density from 3C 273 has reduced by 4.4 flux units over nineteen months so that the component primarily responsible for the variation must be optically thin at 13. cm. Furthermore the component was almost completely resolved as the degree of concurrent variation in fringe amplitude is very small, even between the first and second epoch when Kellermann et al. September 1968 found a component $\lesssim$ 0.0006 arcsec, i.e. component D. Component D is associated with variations at mm and short cm wavelengths but which as yet have no counterpart at our observing frequency. The variations at 13 cm must be due to component C for which the apparent angular diameter θ at epoch January/February 1968 is given as 0.0025 $\pm$ 0.001 arcsec by Kellermann et al. September 1968. This component first appeared as a sudden increase in flux density in 1966 at 2 cm and subsequently peaks appeared at lower frequencies, as shown in figure 2 of Kellermann and Pauliny-Toth, 1968a who derived a value of t_o = 1965.7. At the red-shift distance of 3C 273, the angular diameter of component C represents a metric radius of ~9.5 l.y. so that the Lorentz factor $\beta = 4 \pm 1$. Kellermann and Pauliny-Toth, 1968a did not identify component C of Kellermann et al. September 1968 with the variations for which Kellermann and Pauliny-Toth, 1968a calculated

$t_o \sim 1965.7$ and consequently they believed that the radii of the variable components of the sources they had observed were all less than the light travel time corresponding to the apparent age of the source. Assuming the interpretation of the red shift as due to a recession velocity following the Hubble expansion law, results from the trans-Pacific observations reported here provide the first direct evidence of highly relativistic expansion velocities in variable sources.

Rees 1967 has suggested that one of the components of 3C 273 may be expanding at a highly relativistic velocity and chose a Lorentz factor of 4 to illustrate his model. He showed that the minimum limits for the total energy of the particles in a variable component was thus reduced and consequently the strength of the magnetic field could exceed 10^{-4} gauss. The illustration he has chosen can therefore be taken as a close representation of 3C 273C, as established herein. For his model Rees, 1967 assumed a magnetic field strength of 50 gauss when the age of the component, t, is 1 year. As the source expands adiabatically the field strength decreases to 0.1 gauss when t = 3 years. The 1966 outburst in 3C 273 was observed by Aller and Haddock, 1967 to be associated with a marked increase in polarization at 8 GHz which would indicate the influence of a well ordered magnetic field.

If the electron energy distribution in the source has the form

$$N(E)\,dE = KE^{-\gamma}\,dE$$

and radio emission is the result of synchrotron action, then radiation at any frequency, ν, for which the source is optically thin is given by

$$S(\nu) \propto \nu^{\alpha}$$

where $\alpha = (1-\gamma)/2$. For 3C 273C Kellermann and Pauliny-Toth 1968a derive a value of γ between 1 and 1.5 from the way peak flux decreases with increasing wavelength so that $0 \leq \alpha \leq -0.25$. The predicted secular variation in intensity at any frequency, for $\alpha = 0$ and a Lorentz factor of 4 is compared in figures 3 and 4 of Rees 1967 to variations for other values of β and α, assuming the same given values for the field strength and electron density after unit time. The decreasing phase steepens as the Lorentz factor increases and as α reduces. Rees and Simon 1968 deduced values for the Lorentz factor, the magnetic field and the total electron energy from the flux density history of the 1966 outburst shown in figure 2 of Kellermann and Pauliny-Toth, 1968a. The findings of Rees and Simon and the contrary views expressed by Pauliny-Toth and Kellermann 1968, Kellermann et al. 1968 and Kellermann and Pauliny-Toth 1968a, are discussed in section 8.3. The results reported here are used to adjudicate between respective arguments presented.

As the rate of expansion is now determined, repetition of the trans-Atlantic observations of Kellermann et al.

September 1968 at 18 cm should provide a value for the deceleration coefficient, p, which is defined by the proportionality

$$r \propto t^{p}$$

where r is the radius of a spherically isotropic expanding electron gas. As p increases, the ratio of fractional increase and subsequent decrease in flux density, steepen. A knowledge of p will provide information on the strength of the associated magnetic field. The trans-Pacific interferometer distinguished between component C which it resolved and component D which was n ot resolved. The variations in 3C 273 must be due to the resolved component as shown in figure 8.2 and not to the unre solved component which shows very little variation over the interval November 1967 to June, 1969. The unresolved component appears therefore to be still opaque at 13 cm in June 1969. The rate of expansion of component C is inferred from the age of the component given by the movement of the spectral peak in 3C 273 by Kellermann and Pauliny-Toth 1968a, which is responsible for the rise in flux density at 13 cm during the period of our experiment, and from the diameter of component C determined by Kellermann et al. September 1968, and identified as the cause of the variations at 13 cm by us. The rate of expansion is calculated here to be ultra relativistic and to validate the predictions of Rees 1967, Rees and Simon 1968 in a spectular manner.

8.1.3 P1510-08

In figure 8.2, the flux density of P 1510 is shown to have decreased over the period November 1967 to June 1969, whereas the fringe amplitude for the trans-Pacific baseline, increased significantly.

The resolved part of the source therefore decreased in flux density faster than the unresolved component had increased. Over the interval of observation the unresolved component was optically thick whereas the resolved variable component was optically thin.

Let us designate the resolved variable component, the A component and the unresolved variable component will be referred to here as the B component. The result suggests that when viewed with the NASA-JPL trans-Pacific interferometer, a variable component of this source may become resolved as it passes from the optically thick phase to the optically thin phase. We appear to have seen a single variable component in 3C 279 and 3C 273, which were optically thick and unresolved in the first instance and optically thin and almost completely resolved in the second. The red shift distance to 3C 279 is about three times greater than that to 3C 273 and the resolution of the variable component of the nearer source might have been ascribed largely to its closer distance. The two variables seen in P 1510 however appear concurrently at 13 cm as an increasing unresolved component and as a decreasing resolved component, as shown in figure 8.3.

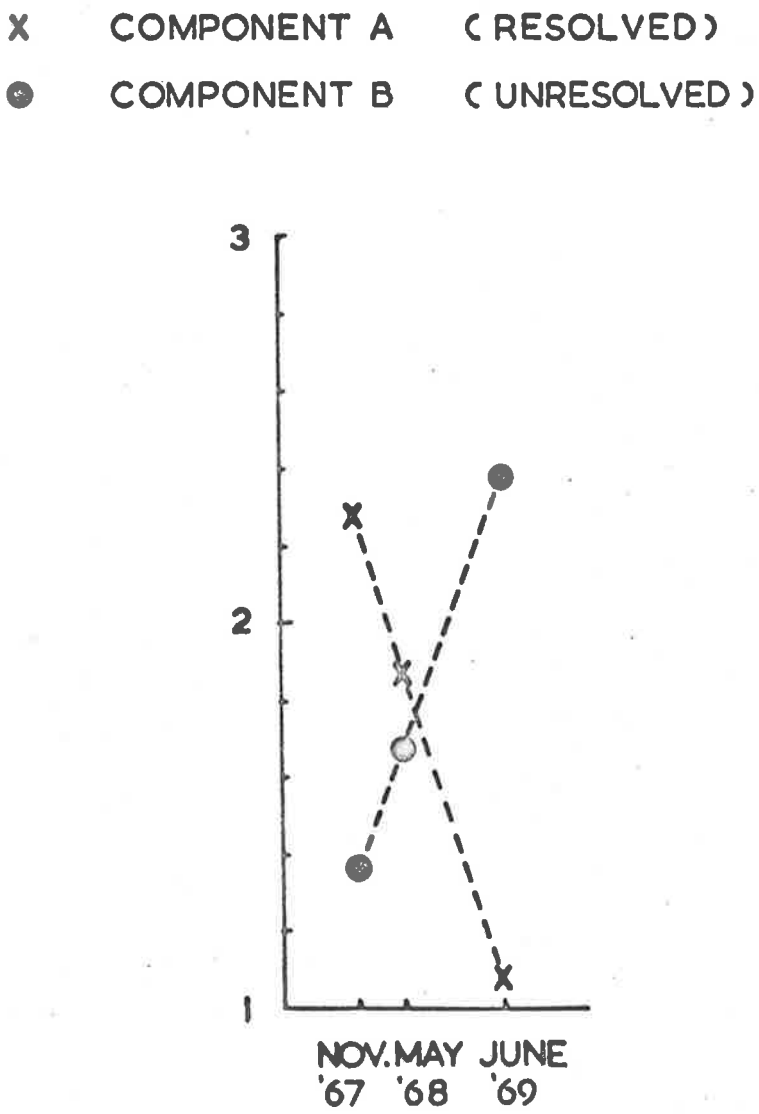

FIGURE 8.3

SECULAR VARIATIONS IN TWO COMPONENTS OF P1510-08.

The comparative rates of change of the two components need to be explained. Figure 2 of Andrew, Locke and Medd 1969 shows the time variation characteristic of a variable radio component expanding adiabatically and radiating through synchrotron action in the manner proposed by Van der Laan 1966. The fractional rate of increase in flux density during the optically thick phase exceeds the fractional rate of decrease during the ensuing optically thin phase, provided that $\gamma < 1.5$, a condition which normally pertains for variable components. As our results (figure 8.3) show, the fractional rate of decrease in the A component to exceed the fractional rate of increase in the B component, the A component would appear to be the stronger component. However, this conclusion should be treated with some caution since the observations of Locke et al. 1969 at 2.8 cm and 4.6 cm show that at least one of the two bursts which appeared at 2.8 cm in 1967 is anomalous in that the flux density of the source decreased more rapidly than it had increased and that the amplitude of the rise at the two frequencies were equal instead of reducing with increasing wavelength as predicted for a typical burst. This burst appeared in the latter half of 1967. The secular changes in the flux density of P 1510 at 2.8 cm and 4.6 cm are shown in figure 1 of Locke et al. 1969.

If the component which gave rise to the late 1967 burst were always optically thin at 4.6 cm, then the corresponding peak amplitude at 2.8 cm should be equal to or less than

the peak due to the variable component at 4.6 cm, for a value of $\gamma = 1$ or > 1 respectively. A similar explanation was offered by Kellermann and Pauliny-Toth 1968, for the 1964 burst on 11 cm in the source 3C 345. The rise in flux density would then follow the process of injection of relativistic particles, with $\gamma = 1$, prior to adiabatic expansion of the cloud of particles.

Whatever the reason for the anomalous profile of flux density at 2.8 cm, it is evident that the fall in flux density through April/May, 1967, was markedly steeper than the rise from May through November, 1967. The burst of early 1967 therefore may correspond to the A component and the burst in the latter half of that year may correspond to the appearance of the B component at 2.8 cm. The delay between the occurrence of these bursts in the low centimetre spectral region and their appearance at 13 cm by about a year is typical of several such events. The interferometer measurements provide the strengths of the components individually which cannot be seen from the flux density history of P 1510. The burst of 1968 at 2.8 cm is well behaved in all respects but cannot correspond to either the A or B component through the whole period of observation. It could not have contributed significantly to the B component at 13 cm even at the 3rd epoch.

Even if the unresolved component included a part of the component associated with the first burst or if the resolved

component included a part of the component which gave rise to the second burst in 1967 at 2.8 cm it is obvious from a comparison between the flux density history of the total source and the fringe amplitude that there are at least two variable components and that the secular change in the flux density of the resolved component demands that the larger component suffered a very rapid fractional decrease (figure 8.3). The explanation of the anomalies of the burst associated with component B offered here agrees with one of three alternative suggestions put forward by Andrew et al. 1969, who stated that if the red shift distance were correct, the corresponding variable component has the form of a jet and is expanding at a highly relativistic velocity.

The other alternatives suggested by Andrew et al. 1968 do not explain the equal burst strengths at the two observing frequencies or the simultaneity of the maxima as noted by the authors.

If, for component B, $t_o \sim 1967.9$, then at the third epoch, the age of the source, t, ~ 1.5 years and at its red shift distance the source would still have been substantially unresolved, provided the Lorentz factor for the expansion of the source $\gamma \sim 5$. The contribution from the A component will vary slowly after the third epoch and it will be possible to recognise the time at which the B component becomes resolved at 13 cm provided the source is observed with the trans-Pacific interferometer at intervals of no longer than six

months.

There is a time lag between the appearance of a component at any frequency and the time at which it manifests itself at a lower frequency provided that initially the source was optically thick at the lower frequency. Variations at the lower frequency are slower according to the equations

$$\dot{S}_\nu/S_\nu = \frac{3p}{t}$$

for the optically thick phase and

$$\dot{S}_\nu/S_\nu = \frac{-2\gamma p}{t}$$

for the subsequent optically thin phase, as t, the age of the source increases for increasing wavelength. Here $\dot{S}_\nu/S_\nu$ is the fractional rate of change in flux density, and p is the deceleration parameter of the expanding electron gas of radius $r \propto t^p$. It is thus possible for the contributions of the components which gave rise to the two bursts seen at 2.8 cm in 1967 to merge at 13 cm so that the B component in fact consists of two variable components. It is not possible to predict the time lag between the appearance of the latter burst at 4.6 cm and at 13 cm, as it is not known at which frequency this component became optically thick in October, 1967.

In this section we have discussed the activity of two

distinct components which have been distinguished for the first time by the trans-Pacific interferometer and which cannot be recognised from observation of the total flux density of P 1510 at 13 cm. Continued observation of the source with the trans-Pacific interferometer will provide information on the expansion rate of the as yet unresolved variable component. We deduce that these components are probably responsible for the anomalous spectral behaviour of the source at 2.8 cm and 4.6 cm reported by Locke et al. 1969. The unresolved younger component is of particular interest as it has not evinced spectral behaviour consistent with the model of Van der Laan 1966 but instead appears to expand before the protracted particle injection phase is complete.

8.1.4 3C 345

Fringes were obtained from trans-Pacific interferometer data on 3C 345 for the second and third epoch. It was not possible to observe the source at the first epoch, within the available observation time as either DSS 41 or DSS 14 returned to other duties on the two days 306/307, 1967 before the source had risen. Tables 7.4 and 7.5 show that the fringe amplitude increased between the second and third epoch.

The variable component must be the C component observed by Kellermann et al. September 1968, during their trans-Atlantic experiment at 6 cm and 18 cm in January/February,

1968. The delay between the increase in flux density at 2 cm, 3.75 cm and 6 cm in the interval 1966.0 - 1968.0 as shown in figure 6 of Kellermann and Pauliny-Totha, indicate that an increase could be expected to occur at 13 cm between our second and third epochs. Our observation of the increase in fringe amplitude over this period therefore indicates that component C is responsible for the increase in flux density at 2 cm and at 3.75 cm between 1966.0 and 1968.0. From the limited data available, it appears that t_o = 1964.0 if p, the acceleration parameter = 1, i.e. the component is expanding linearly with time. At its red shift distance a source $\gtrsim$ 50 light years would be completely resolved.

No Californian baseline observations were obtained for the third epoch so that it is not possible to compare the total flux densities in this manner. As the declination of this source is outside the limits chosen by G.D. Nicolson for his survey of secular variations at 13 cm, the change in fringe amplitude cannot be compared against the change in flux density and it is therefore not certain whether the source is wholly unresolved at the third epoch, in which case the Lorentz factor β would be ≤ 1.5, or partially resolved, for which case the value of β is given by $1.5 \leq \beta \lesssim 5$. We therefore adopt the value $\beta \lesssim 5$, pending further observations. In a universe for which $q_o = 1$, the corrected value of $\beta \lesssim 2$.

8.2 Source Model

The experimental observations of secular changes in

flux density over the centimetre region of the spectrum of the source and in fringe amplitude of their components support the expanding synchrotron model put forward by Sklovsky 1960, 1965 and developed by Pauliny-Toth and Kellermann 1966, Ozernoy and Sazonov 1968, Van der Laan 1966, Rees 1967, Rees and Simon 1968. Andrew et al. 1969 have found that of 50 variable sources, only three showed fluctuations that were not simply explained by the model. The development of the relativistic model represents an important extension of the theory as proven by our results.

Pauliny-Toth and Kellermann 1966 considered that the large and nearly simultaneous outbursts of 1966 in 3C 273 and 3C 279, which are separated by only 10 degrees at the earth, may have been caused by a local disturbance in the line of sight to distant sources of constant intensity. Figures 2 and 3 of Kellermann and Pauliny-Toth 1968a show that the outburst in 3C 273 was more intense than that for 3C 279.

It is shown in section 8.1 that the variable component in 3C 273 has an apparent angular diameter which is larger than that of the variable component in 3C 279. This would seem to rule against an explanation that the closely similar variations were caused by common refraction or absorption effects in a region local to the sun, unless the irregularity which caused changes in both sources changed its refractive properties significantly during the northern spring of 1966

when the outburst in both sources were seen.

8.3 Relativistic Expansion of the Variable Component in 3C 273

Variation in the flux density of 3C 273 was first reported by Dent, 1965 who had monitored its emissions at 8 GHz from July, 1962. He deduced the distance to the source from the requirement that the time scale for a significant change in flux density must be greater than the light travel time across the source and from occultation measurements of the angular size of 3C 273B, and found the source to be within 2 megaparsecs across. Lunar occultation observations by Hazard et al. 1963 has isolated a flat spectrum from a bright core about 0.5 arcsec in diameter and this spectrum was ascribed to the component seen to vary at 8 GHz so that if the source were at its red shift distance and its angular diameter about 0.002 arcsec, the emission was not due to synchrotron action as the synchrotron self absorption expected from a source of that angular diameter was not evident. These conclusions were shown by Field 1965 to be incorrect if 3C 273B is a complex source.

The multiplicity of components listed by Kellermann et al September, 1968 which had been observed to early 1968, and the calculations by Rees 1967 of the effect of relativistic expansion velocities on the time scale of source fluctuations seen by a remote observer, alters the significance of Dent's early observations and the expanding synchrotron source

located at its red shift distance is accepted as a viable model on the basis of observations on the spectral variations of numerous sources. An estimate of the distance to the source may be obtained from the spectral characteristics of the source provided the strength of the magnetic field is known. The non-relativistic treatment of the expansion process usually requires a field strength in the vicinity of 10^{-4} gauss if observations are to conform with the hypothesis for the cosmological location of quasi-stellar sources. Fields several orders higher are accommodated by the relativistic treatment of cosmological sources. However, the lack of absorption on the short wavelength side of Lyman alpha in the spectrum of their associated optical objects argues for the view that quasi-stellar objects are much closer than their red shift distances.

A more cogent argument for their cosmological location would come from evidence for an evolutionary sequence which linked the quasi-stellar source to the N-galaxy, which stage was thenfollowed by the Seyfert galaxy. The red shift of these galaxies are generally intermediate between those of the closer galaxies and the range of values characteristic of a quasi-stellar object. One could reason that if the red shifts of the Seyfert galaxies and the N-galaxies were due to Hubble expansion and that if the quasi-stellar source manifested other similar characteristics, differing in degree through overlapping in part, then though such a process of induction, the cosmological view would be strengthened. One

such characteristic is the variation in the optical region of the spectrum as observed for the N-galaxies 3C 371, by Oke 1967 and 3C 390.3 by Cannon, Penston and Penston, 1968 who suggested that quasi-stellar objects are in fact the more distant N-galaxies. If the galaxy is placed at its red shift distance the resulting attenuation through increased distance may thus reduce the brightness of the galactic halo to a level below visibility so that the relatively bright core will appear as a stellar source. This proposal is attractive. However the galactic halo may be the consequence of explosions in variable quasi-stellar sources at the rate of say .01 to 1 explosionper year over an alleged quasi-stellar phase of ~ 10^9 years, each of which projects, on the average, the equivalent of one solar mass into the neighbourhood of the source.

Variations in the radio spectrum of the Seyfert galaxies 3C 84 (NRC 1275) and 3C 120 have been observed by Kellermann and Pauliny-Toth 1968a, b. The trans-Atlantic interferometer observations at 6 cm and 18 cm by Kellermann et al. September, 1968 revealed components down to ~ .001 arcsec in diameter in 3C 84 and multiple components in 3C 120, the smallest of which was less than .0008 arcsec. The authors reported that the varying components in the two Seyfert galaxies did not expand with extreme relativistic velocities in the manner suggested by Rees and Simon, 1968. Pauliny-Toth and Kellermann, 1968 had found excellent agreement between observed variations in the radio spectrum and the model of an electron cloud expanding at a

rate $\leq$ 0.6c corresponding to a Lorentz factor $\beta \leq 1.25$ and a field strength of 0.01 gauss when the apparent age was 0.7 years. In their analysis Rees and Simon found that when the relative strengths of the emissions in the radio, optical and X-ray regions were taken into account, $\beta \sim 1.5$. The interferometer observations of Kellermann et al. September, 1968 seem to indicate however that the expansion velocity of the variable component in 3C 120 $\leq$ 0.7c, corresponding to $\beta \lesssim 1.4$. The disagreement between this result and that of Rees and Simon does not appear to be serious so that the energy requirements of the model and the optical and X-ray emissions may be reduced by adopting their relativistic treatment.

In the same paper Rees and Simon find that the 1966 burst in 3C 273 originated in a highly relativistic explosion for which $\beta \sim 3$. They suggested that an interferometer with a baseline of 100 million wavelengths would resolve the variable component in 3C 273. The trans-Pacific observations on this source had commenced in 1967 and later observations proved that the variable component was even then substantially resolved with an interferometer baseline of 80 million wavelengths. The value of the Lorentz factor $\beta \gtrsim 3$ given by Gubbay et al. 1969b is somewhat conservative as shown in section 8.1.2.

In the discussion following their review, Kellermann and Pauliny-Toth, 1968a state that it is generally accepted

that significant variations in emission from components cannot occur in a time much shorter than the light travel time across the component. The trans-Pacific observations of 3C 273 thus provide the first direct evidence for highly relativistic expansion velocities, vindicating the contentions of Rees 1967 and Rees and Simon 1968.

Whereas the magnetic field was limited to $\sim 10^{-4}$ gauss to account for the rate of spectral variations, in the non-relativistic treatment of Rees and Simon 1968, fields of up to 10^{-1} gauss were possible for $\beta = 3$, reducing the role of the inverse Compton effect and thus reducing the required flux densities in the optical and X-ray regions and consequently reducing the expenditure of energy of the event from $>> 10^{58}$ergs to $\sim 10^{54}$ergs. According to Colgate, 1967 the maximum amount of energy which can be released in a supernova is $\sim 10^{54}$ergs. This led Rees and Simon, 1968 to propose that relativistic particles in strong radio sources are generated by a succession of supernovae within a dense star cluster. Thus the case for evolution from quasi-stellar source to radio galaxy is strengthened, and it seems reasonable to suggest that the earlier phases in the evolutionary sequence of the universe have indeed been seen to have the greater values of red shift.

The trans-Pacific experiments reported here have led us to conclude (section 8.1.2) that the variable component in 3C 273 has undergone ultra-relativistic expansion. It

seems reasonable to assume that repeated explosive processes in active sources will result in the formation of a surrounding shell of ejected material. As the explosions continue, the particle density in the shell will increase until it is dense enough to scatter sufficient light from the nucleus to be seen as a halo around the nucleus. The characteristic expansion rates for associated explosive events during the subsequent evolutionary phase gradually reduces due to the resistive effect of the halo on the newly ejected material. So far there appears to be no evidence that the expansion velocity corresponding to the value of the Lorentz factor β calculated for component C in 3C 273 in section 8.1.2 has been exceeded in an N-galaxy or Seyfert galaxy. The probability for ultra-relativistic expansion rates of galactic components should be very low. It may be suggested on the basis of our results that the value of β associated with a class of objects serves as a degradation index in an evolutionary sequence.

APPENDIX 1

"Nine Million Wavelength Baseline Interferometer Measurements of 3C 273B"

J.S. Gubbay and D.S. Robertson, 1967.

Gubbay, J. S. & Robertson, D. S. (1967). Nine million wavelength baseline interferometer measurements of 3C 273B. *Nature, 215*(5106), 1157-1158.

APPENDIX 2

"Trans-Pacific Interferometer Measurements at 2,300 MHz"

J.S. Gubbay, A.J. Legg, D.S. Robertson, A.T. Moffet and B. Seidel, 1969a.

Gubbay, J., Legg, A. J., Robertson, D. S., Moffet, A. T. & Seidel, B. (1969). Trans-Pacific interferometer measurements at 2,300 MHz. *Nature, 222*(5195), 730-733.

APPENDIX 3

"Variations of Small Quasar Components at 2300 MHz"

J.S. Gubbay, A.J. Legg, D.S. Robertson, A.T. Moffet, R.D. Ekers and B. Seidel, 1969b.

VARIATIONS OF SMALL QUASAR COMPONENTS AT 2300 MHz

Received _____

In a previous communication[1] we have reported long-baseline interferometer measurements of several quasi-stellar radio sources using stations of the NASA/JPL Deep Space Network in Australia and California. Comparison of three sets of similar observations now shows evidence for secular variations in the apparent intensities of small-diameter components in several of these objects. The results are compatible with the theory of expanding synchrotron sources, but an apparent expansion velocity greater than that of light seems to be required for the recent outburst in 3C273.

In our earlier paper[1] we described our instrumental techniques and discussed a set of observations made in May 1968, using stations DSS 42 at Tidbinbilla, A.C.T., and DSS 14 at Goldstone, California, when we first found fringes over the trans-Pacific baseline of about 8×10^7 wavelengths. The observing frequency is 2298 MHz, or a wavelength of 13.1 cm. We mentioned that a previous set of observations, made in November 1967, between DSS 41 at Island Lagoon, South Australia, and DSS 14 showed fringes of different amplitude for several sources. Since then we have obtained a third set of observations, in June 1969, using DSS 42 and DSS 14. This last set confirms the observation of fringe amplitude changes in several sources, and in this letter we discuss the history of these changes in three sources, 3C273, 3C279 and P1510-08.

The total source intensities and apparent fringe amplitudes of the three sources are shown in Figure 1. The source intensities were measured at this frequency by Dr. G. D. Nicolson at DSS 51

in Johannesburg, as part of a continuing program of monitoring radio intensity variations. It is evident that the fringe amplitudes of 3C279 and P1510-08 have increased while that of 3C273 has remained nearly constant. At the same time the flux density of each source has changed, 3C279 increasing and 3C273 and P1510-08 decreasing.

The interpretation seems most clear in the case of 3C279. The increase in fringe intensity of 3.3 flux units is somewhat greater than the increase in the flux density from the source over the same interval in time. Observations of the intensity variations in this source at various wavelengths (reviewed by Kellermann and Pauliny-Toth[2]) show at 11 cm wavelength a slow decrease from 1964 to 1967, followed by a rise beginning about 1967.0. This rise seems to be the first appearance at this wavelength of an expanding component which was initially seen in a sharp outburst at 2 cm in early 1966. On the basis of these spectral changes and interferometry at shorter baselines, Kellermann et al.[3] have proposed that 3C279 has four components, three of size $\gtrsim 0.002$ arcsec and one, component D, of smaller size. This last component they associate with the 1966 outburst at 2 cm, and it must be this component which contributes almost all our observed fringe intensity at 8×10^7 wavelengths spacing. The increase in the total intensity at 13 cm is somewhat less than the increase in the fringe intensity because the 13 cm emission from components B and C is still decreasing.

These results are completely in accord with the generally-accepted theory of expanding synchrotron sources. It will be interesting to follow the subsequent changes in the fringe amplitude at this spacing, since the component we are observing should soon become optically thin at 13 cm, after which its intensity should drop. The calculated angular size of the source when it first becomes optically thin at this wavelength will depend on the magnetic field in the source, but for fields $\sim 10^{-4}$ gauss, as found in other objects[3], the angular size should be ≈ 0.001 arcsec. Thus after the intensity starts to decrease we might also expect to see the effects of resolution.

In the case of 3C273 the change in the total intensity is not reflected in the fringe amplitude. In this source there was also an outburst at short wavelengths in early 1966 (ref. 2), and the decrease in the 13 cm flux density probably means that this expanding component is now optically thin at this wavelength. It must also be fully resolved by our interferometer, indicating that its angular size, even in November 1967, was >0.002 arcsec. This would be component C of Kellermann *et al.*[3], for which they calculated an angular size in early 1968 of 0.0025 ± 0.001 arcsec. If we suppose that 3C273 is at the cosmological distance indicated by its redshift, then the radius of this component in November 1967 must have been >2.5 pc. Since the outburst was then about two years old[2] the apparent rate of expansion would have been at least three times the velocity of light. Rees[4] has shown that apparent expansion velocities

greater than $\underline{c}$ are the consequence of relativistic expansion, and we conclude that this outburst in 3C273 probably has a Lorentz factor $\gamma \geq 3$. This is the first direct evidence that the expansion in variable sources takes place at relativistic velocities.

For P1510-08 we cannot make a simple interpretation because intensity variations have been observed in this source with very short characteristic times and with a wavelength dependence which does not fit the expanding source model[5]. The nature of these variations is still uncertain, and frequent observations with long interferometer baselines would be of considerable help in deciding among several possible explanations.

We thank the staffs of all the stations for their help. The use of the Deep Space Network facilities was by kind permission of NASA and the Jet Propulsion Laboratory; Messrs. J. R. Hall, S. Anastos, T. Sato, D. Spitzmesser and F. Borncamp of JPL were very helpful in making arrangements for us. It is with much pleasure that we acknowledge helpful discussions with Professor K. G. McCracken of the University of Adelaide and thank G. D. Nicolson for permission to use his unpublished intensity measurements.

Work in radio astronomy at the Owens Valley Radio Observatory is sponsored by the U.S. Office of Naval Research. This report represents one phase of research carried out at JPL under contract with NASA.

J. Gubbay

University of Adelaide

A. J. Legg

D. S. Robertson

Australian Defence Scientific Service

Department of Supply

Weapons Research Establishment

Salisbury, South Australia 5108

A. T. Moffet

R. D. Ekers

Owens Valley Radio Observatory

California Institute of Technology

B. Seidel

Jet Propulsion Laboratory

California Institute of Technology

Pasadena, California

REFERENCES

1. Gubbay, J., Legg, A. J., Robertson, D. S., Moffet, A. T., and Seidel, B., Nature, 222, 730 (1969).
2. Kellermann, K. I., and Pauliny-Toth, I. I. K., Ann. Revs. Astron. Astrophys., 6, 417 (1966).
3. Kellermann, K. I., Clark, B. G., Bare, C. C., Rydbeck, O., Ellder, J., Hansson, B., Kollberg, E., Hoglund, B., Cohen, M., and Jauncey, D. L., Astrophys. J. Lett., 153, L209 (1968).
4. Rees, M., Monthly Notices Roy. Astron. Soc., 135, 345 (1967).
5. Locke, J. L., Andrew, B. H., and Medd, W. J., Astrophys. J. Lett., 157, L81 (1969).

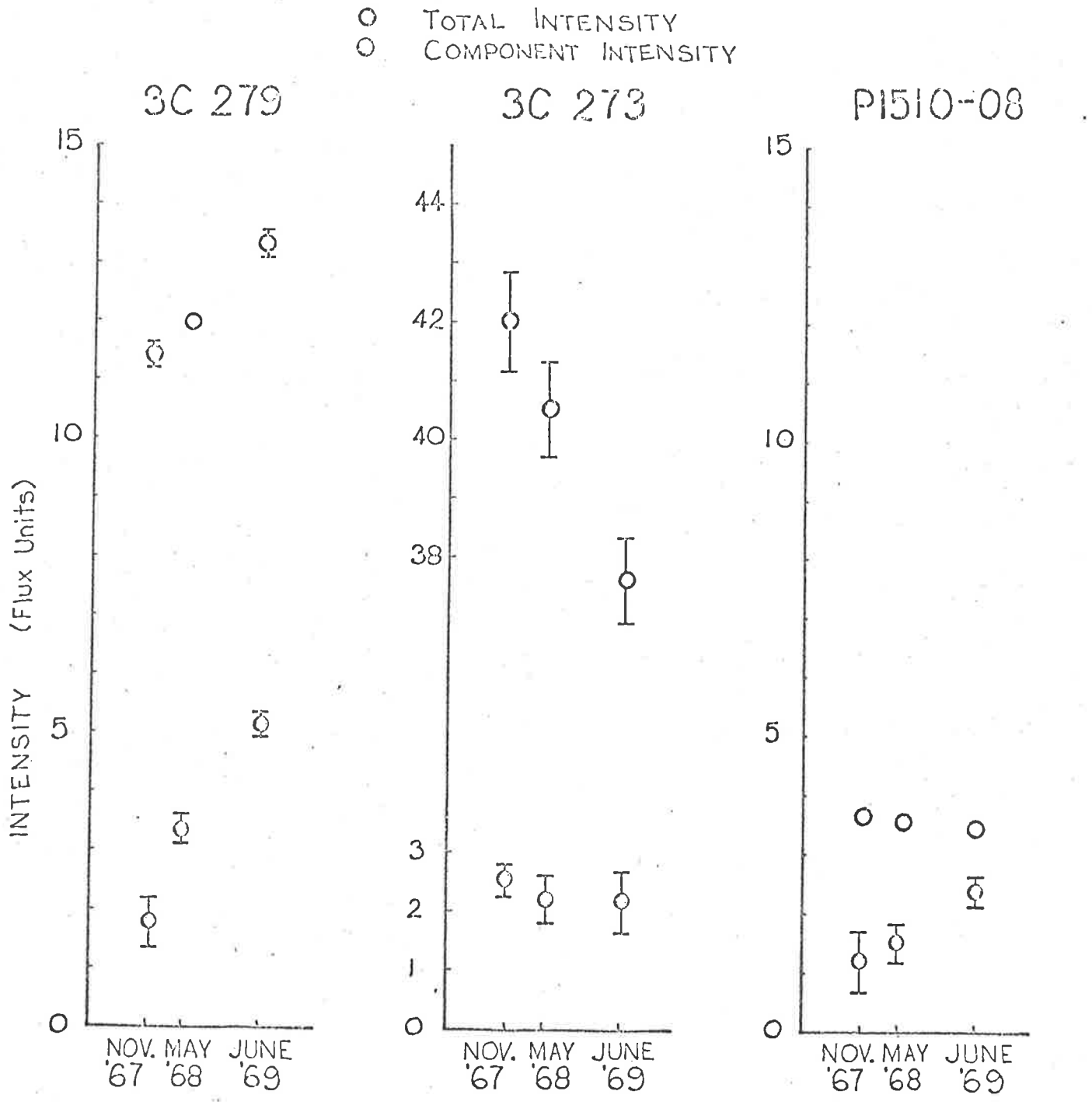

Figure 1 Comparison of the histories of the total intensities of three sources and the intensity of their unresolved components at 80×10^6 wavelength.

APPENDIX 4

"Quasars - a Review, and Proposals for the Measurement of their Small Scale Microwave Structure"

J. S. Gubbay, 1967.

Technical note APD 6, Gubbay, J. S. (1967). *Quasars - a review and proposals for the measurement of their small scale microwave structure*, Department of Supply, Australian Defence Scientific Service, weapons research establishment.

REFERENCES

Aller, H.D. and Haddock, F.T., 1967 - Astrophys. J., 147, pp833-837, 1967.

Andrew, B.H., Locke, J.L. and Medd, W.J., 1968 - Bulletin of Radio and Electrical Engineering Division, NRC Canada, 18, No. 3, pp45-51, July-September, 1968.

Appenzeller, I. and Hiltner, W.A., 1967 - Astrophys. J. Letters, 149, pp17-18, July, 1967.

Bare, C., Clark, B.G., Kellermann, K.I., Cohen, M.H. and Jauncey, D.L., 1967 - Science, 157, pp189-191, 14 July, 1967.

Bell, M.B., 1969 - Nature, 224, pp229-234, October 19, 1969.

Broten, N.W., Locke, J.L., Legg, T.H., McLeish, C.W., Richards, R.S., Chisholm, R.M., Gush, H.P., Yen, J.L. and Galt, J.A. 1867a - Nature, 215, p38, July 1, 1967.

Broten, N.W., Clarke, R.W., Legg, T.H., Locke, J.L., McLeish, C.W., Richards, R.S., Yen, J.L., Chisholm, R.M. and Galt, J.A., 1967b - Nature, 216, pp44-45, October 7, 1967.

Broten, N.W., Legg, T.H., Locke, J.L., McLeish, C.W., Richards, R.S., Chisholm, R.M., Gush, H.P., Yen, J.L. and Galt, J.A., 1967c - Science, 156, p1592, 1967.

Burbridge, G.R. and Burbridge, E.M., 1969 - Nature, 222, pp735-741, May 24, 1969.

Burke, B., 1969 - Physics Today, pp54-63, July, 1969.

Cannon, R.D., Penston, M.V. and Penston, Margaret J., 1968 - Nature 217, pp340-341, January, 1968.

Chisholm, R.M., Gush, H.P., Yen, J.L. and Galt, J.A., 1967 - Science, 156, p1592, 1967.

Clark, B.G., 1967 - Astronom.J. 72, No. 5, pp601-604, June, 1967.

Clark, B.G., Cohen, M.H. and Jauncey, D.L., 1967 - Astrophys. J., 149, ppL151-L152, September, 1967.

Clark, B.G., 1968 - PGAP of IEEE, January, 1968.

Clark, B.G., Kellermann, K.I. and Bare, C.C., 1968 - Astrophys. J., 153, ppL67-L68, July, 1968.

Cohen, M.H., Gundermann, E.J. and Harris, D.E., 1967 - Astrophys. J., 150, pp767-782, December, 1967.

Cohen, M.H., Jauncey, D.L., Kellermann, K.I. and Clark, B.G., 1968 - Science 162, pp88-94, October 4, 1968.

Colgate, S.A., 1967 - Astrophys. J., 150, p163, 1967.

C.S.I.R.O., Division of Radiophysics, 1967 - Aust. J. Phys., Astrophys. Supp., No. 7, April, 1967.

Deming, W.E., 1950 - "Some Theory of Sampling" pp461-462, Published in New York, Wiley, 1950.

Dent, W.A., 1965 - Science, 148, pp1458-1460, June 11, 1965.

Dent, W.A., 1966 - Astrophys. J., 144, No. 2, pp843-847, 1966.

Epstein, E.E., 1965a - Astrophys. J., 142, No. 3, pp1282 - 1285, 1965.

Epstein, E.E., 1965b - Astrophys. J., 142, No. 3, pp1285 - 1287, 1965.

Explanatory Supplement to the Astronomical Ephemeris - Issued by H.M. Nautical Almanac Office.

Field, G.B., 1965 - Science, 150, pp78-79, October, 1, 1965.

Fomalont, E.B., Wyndham, J.D. and Bartlett, J.F., 1967 - Astronom. J., 72, No. 3, pp445-452, April, 1967.

Gardner, S.S., Morris, D. and Whiteoak, J.B., 1969 - Aust. J. Phys., 22, pp79-106, 1969.

Gubbay, J.S. and Robertson, D.S., 1967 - Nature, 215, pp1157-1158, September 9, 1967.

Gubbay, J.S., Legg, A.J., Robertson, D.S., Moffet, A.T. and Seidel, B. 1969a - Nature, 222, pp730-733, May 24, 1969.

Gubbay, J.S., Legg, A.J., Robertson, D.S., Ekers, R. and Moffet, A.T., 1969b - Nature, 224, pp1094-1095, December 13, 1969.

Hanbury Brown, R. and Twiss, R.Q., 1954 - Phil. Mag. 45, pp663-681, July, 1954.

Hazard, C., Mackey, M.B. and Shimmins, A.J., 1963 - Nature, 197, pp1037-1039, March 16, 1963.

Hunter, J.H., Jun., Sabatino Sofia and Fletcher, E., 1966 - Nature, 210, pp346-348, April 23, 1966.

Jennison, R.C. and Das Gupta, M.K., 1956a - Phil. Mag. 1, pp55-64, 1956.

Jennison, R.C. and Das Gupta, M.K., 1956b - Phil. Mag. 1, pp65-75, 1956.

Kellermann, K.I. and Pauliny-Toth, I.I.K., 1968a - Ann. Review Astron. Astrophys., 6, pp417-448, 1968.

Kellermann, K.I., and Pauliny-Toth, I.I.K., 1968b - Astrophys. J., 152, pp639-646, May, 1968.

Kellermann, K.I., Clark, B.G., Bare, C.C., Rydbeck, O., Elder, J., Hanson, B., Kollberg, E. Hoglund, B., Cohen, M.H. and Jauncey, D.L., September 1968 - Astrophys. J., 153, ppL209-L215, September, 1968.

Kinman, T.D., 1967 - Astrophys. J., Letters, 148, pL53, 1967.

Kinman, T.D., Lamla, E., Ciura, T., Harlan, E. and Wirtanen, C.A., 1968 - Astrophys. J., 152, pp357-374, May, 1968.

Kraus, J.D., 1966 - "Radio Astronomy" p245, Published in New York, McGraw Hill, 1966.

Le Roux, E., 1961 - Annales D'astrophysique, 24, No. 1, pp71-85, 1961.

Locke, J.L., Andrew, B.H. and Medd, W.J., 1969 - Astrophys. J., 157, ppL81-L86, August, 1969.

Longair, M.S., 1967 - Contemp. Phys., 8, No. 4, pp357-372, 1967.

Low, F.J., 1965 - Astrophys. J., 142, No. 3, pp1287-1289, 1965.

Maran, S.P. and Cameron, A.G.W., 1967 - Science, 157, No. 3796, pp1517-1524, September 29, 1967.

McCrea, W.H., 1967 - Science, 157, pp400-402, July, 1967.

Moran, J.M., Burne, B.F., Barrett, A.H., Rogers, A.E.E., Carter, J.C., Ball, J.A. and Cudabeck, D.D., 1968 - Astrophys. J., 151, ppL99-L101, February 1968.

Morrison, P. and Sartori, L., 1968 - Astrophys. J., 152, ppL139-L143, June, 1968.

Oke, J.B., 1967 - Astrophys., J., 150, ppL5-L8, October, 1967.

Ozernoy, L.M. and Sazonov, V.N., 1968 - Nature, 219, pp467-469, August 3, 1968.

Parkes Catalogue of Radio Sources: Declination Zone +20° to -90° - Aust. J. Phys., Astrophys. Supp. No. 7, April, 1969.

Pauliny-Toth, I.I.K. and Kellermann, K.I., 1966 - Astrophys. J., 146, pp643-645, 1966.

Pauliny-Toth, I.I.K., and Kellermann, K.I., 1968 - Astrophys. J., 152, ppL169-L175, June, 1968.

Rees, M.J., 1967 - Mon. Not. R. Astr. Soc., 135, pp345-360, 1967.

Rees, M.J. and Simon, M., 1968 - Astrophys. J., 152, ppL145-148, June, 1968.

Schmidt, M., 1963 - Nature, 197, p1040, 1963.

Sciama, D.W., 1967 - Observational Cosmology, J. Brit. astr. Ass. 77, No. 3, pp157-175, 1967.

Shimmins, A.J., Searle, L., Andrew, B.H. and Brandie, G.W., 1968 - Astrophys. Letters 1, pp167-169, 1968.

Sklovsky, I.S., 1960 - Astron. Zhur, 37, p256, 1960, Doklady, 1961.

Sklovsky, I.S., 1965 - Nature, 206, 176-177, April 10, 1965.

Slish, V.I., 1963 - Nature, 199, p682, August 17, 1963.

Terrell, J., 1966 - Science, 154, No. 3754, pp1281-1288,

Van Der Laan, H., 1966 - Nature, 211, pp1131-1133, September 10, 1966.

Visvanathan, N., 1968 - Astrophys. J., 153, Letters pp19-22, July, 1968.

Weast, R.C., 1967-1968 - "Handbook of Chemistry and Physics", pF158, 48th Edition, Published in Cleveland Ohio, The Chemical Rubber Co. 1967-1968.

Williams, P.J.S., 1963 - Nature 200, pp56-57, October 5, 1963.